M-AM-Sym1 **AN HISTORICAL NOTE ON BIOMEDICAL APPLICATIONS OF NUCLEAR MAGNETIC RESONANCE**

Paula T. Beall, Department of Physiology, Baylor College of Medicine, Houston, TX, 77030

In 1946, Purcell and Bloch independently demonstrated the nuclear magnetic resonance effect in water and hydrocarbons, Since water, with abundant hydrogen protons, makes up 70-90 % of the mass of cells, it is not surprising that the technique was applied to biological tissues and fluids by Erik Odeblad of the Karolinska Institute in Sweden in 1956 on red blood cells. His series of papers on NMR of a range of tissues and fluids were pioneering work pointing out the diagnostic potential of NMR. In the late 1960's numerous investigators rediscovered the potential of proton NMR to monitor the behavior of water in tissues. In 1966 Rybak *et al* published a correlation between line width and contraction of ventricular tissue. Koga *et al* (1967) and Sussman *et al* (1967) opened up the field of NMR in food science. In 1968, J.A. Jackson published two papers on the possibility of a whole body NMR spectrometer. Methods were developed for measuring blood flow by NMR in living human arms (Morse, *et al* 1970). Damadian's 1971 paper describing a discernible NMR difference between normal and cancerous tissues was followed by his patent application on *in vivo* NMR diagnosis in 1972. In 1973, Lauterbur and Mansfield and Grannell independently published theoretical papers on the possibility of *in vivo* NMR imaging. In 1976, Damadian published the first NMR image of a human thorax, and Mansfield and Maudsley presented pictures of a human finger. Within this decade NMR imaging has gone from a theoretical possibility to a practical clinical tool. Other atomic nuclei of sufficient sensitivity and abundance may also have use in clinical NMR applications. Certainly ^{31}P, after the original demonstration by Hoult *et al* , has gone on to be applied to metabolic biochemistry and to measurements of intracellular pH. *In vivo* applications of ^{31}P NMr with a surface coil are called topical NMR and serve a useful purpose in the detection of metabolic disease. Other nuclei, such as ^{23}Na, ^{39}K, ^{17}O, ^{19}F, Ca and Cd may also have biomedical applications.

M-AM-Sym2 **MEASUREMENT OF FLUX THROUGH THE CREATINE KINASE REACTION IN THE INTACT RAT HEART: ^{31}P NMR STUDIES**

J.S. Ingwall, K. Kobayashi, and J.A. Bittl Department of Medicine, Brigham and Women's Hospital and Harvard Medical School, Boston, MA.

A ^{31}P NMR spectrum of muscle provides information about the composition and concentrations of phosphorus-containing metabolites present in relatively high concentration (>0.6mM), namely ATP, creatine phosphate (CrP), and inorganic phosphate. Using saturation NMR transfer techniques, reaction rates and fluxes of enzymes including creatine kinase, adenylate kinase and ATPases have been directly measured in the intact beating heart. Using a Nicolet wide bore NT 360 spectrometer operating at 145.75 MHz, the forward (CrP ->γATP) and reverse (γATP->CrP) creatine kinase fluxes were measured for working and isovolumic perfused rat heart preparations under a variety of substrate conditions. For the working heart perfused with either glucose (15 mM) or pyruvate (10 mM) at 37 C, the flux in the forward direction increased from 22 μmoles/gram dry weight (gdw/s) in the potassium-arrested heart performing no external work to 43 μmoles/gdw/s for hearts working at 150 mm Hg peak systolic pressure. The relationship between flux and cardiac work calculated as the product of heart rate and peak systolic pressure was linear. For each condition studied, flux for the forward reaction was larger than apparent flux for the reverse reaction; however, the difference can be accounted for by ATPase activity. These results show that the creatine kinase reaction is at equilibrium under normal conditions. Further, they show that over the range of work loads possible to achieve *in vitro*, flux changes by a factor of two. This may constitute an "energy reserve".

Flux through the creatine kinase reaction has also been measured in several pathophysiological states. For both working hearts with reduced flow (*i.e.* ischemia) and for hypoxic hearts, flux was lower than for control hearts working at the same load. This result was unexpected, since increased utilization of CrP to maintain normal ATP levels has previously been thought to be characteristic of myocardial injury. Flux in the hypertrophied heart of the spontaneously hypertensive rat is also lower than in control heart, consistent with decreased CrP pool and decreased pump performance.

M-AM-Sym3 **PHOSPHORUS NMR OF METABOLIC DISEASES**

J.S. Leigh Dept. of Biochemistry, University of Pennsylvania, Philadelphia, PA

M-AM-Sym4 **NMR IMAGING - AN INTRODUCTION.**

D. I. Hoult Biomedical Engineering and Instrumentation Branch, Division of Research Services, National Institutes of Health, Bethesda, Maryland 20205

The principle underlying most methods of NMR imaging is that a linear field gradient produces a linear dependence of resonant frequency upon distance, and thus the NMR "spectrum" becomes a graph of nuclear concentration versus distance. However, this graph only contains one dimensional information, and therefore some other variable is required in order to obtain two or three dimensional maps of, say, hydrogen concentration in a human. Many methods now exist for producing such maps, which are viewed as high quality images akin to those obtained by X-ray computed tomography. The principles underlying two of the most commonly used methods will be examined, and the importance of producing signal dependency upon relaxation times (T_1 and T_2) highlighted.

M-AM-Sym5 **NMR PROTON IMAGING – *IN VIVO* STUDIES**

Margaret A. Foster Department of Bio-Medical Physics and Bio-Engineering, University of Aberdeen, Foresterhill, Aberdeen, Scotland.

NMR imaging is a new field of study. The earliest *in vivo* human images date back to the late ninteen seventies, but these were of poor quality. Only during the last two or three years have potentially useful NMR proton images been available. The great impetus to develop NMR imaging systems have arisen from a combination of factors – the ubiquity of water in living material and the related fact that almost everything which brings about a change in state of a living system affects the amount and/or the distribution of water in that system.

In the normal, relaxed body the various tissues can be distinguished by their water proton relaxation times. Examined at 1.7 MHz the T_1 values can range from 300 ms for grey brain, through 250 ms for liver. Adipose tissue has an even shorter T_1 value (110-140 ms) but in this case the lipid chain hydrogens are giving a substantial contribution to the signal. Suggestions have been made that the differences between T_1 values of muscle and adipose tissue, along with possible small changes in fatty muscle, may be used for monitoring fat levels in certain human diseases or in animals for meat production. This is currently being investigated at Aberdeen. We are also looking at a variety of normal changes in tissue NMR relaxation behaviour associated with exercise levels, dietary factors and changes in mammary tissue during pregnancy and lactation.

The majority of pathological conditions are associated with an increase in tissue water content and in T_1 relaxation time. Such conditions include tumors, inflammation (*e.g.* in arthritis or transplant rejection), all œdematous conditions, abscesses, etc. A very few disease states are associated with reduced T_1 values, *e.g.* cirrhosis of the liver can cause reduced T_1 values of the tissue and hæmolytic anæmia can bring about large reductions in the T_1 relaxation time of the spleen. A variety of clinical and normal physiological studies employing NMR imaging will be discussed and illustrated.

M-AM-Sym6 **MULTINUCLEAR NMR STUDIES OF CALCIUM AND MAGNESIUM BINDING PROTEINS**

Sture Forsén Physical Chemistry 2, Chemical Center POB 740, Lund University, S–220 07, LUND, Sweden

NMR spectroscopy offers many alternative ways of studying the properties of calcium and magnesium-binding proteins. One obvious way is to observe the spectra of spin $I = \frac{1}{2}$ nuclei like ^{1}H, ^{13}C, and ^{15}N under various conditions as regards ion concentration, pH, temperature, etc. Information pertaining to structure and dynamics of the protein may be gained in this way. As a result of recent developments in methodology and instumentation, NMR of quadrupolar ions ^{25}Mg and ^{43}Ca has also developed into a useful tool in the study of calciproteins. Through the combined use of isotopically enriched ^{43}Ca and ^{25}Mg, FT NMR techniques, high magnetic fields and a solenoid type of probe design, NMR studies of these cations are now feasible at millimolar, or even submillimolar concentrations. The general types of information that can be obtained from ^{25}Mg and ^{43}Ca NMR are:

(i) association constants in the range $1 - 10^4$ M^{-1};
(ii) the competition of other cations for the Ca^{++} and/or Mg^{++} binding site(s);
(iii) the effects of other protein ligands (drugs, etc) on the ion binding;
(iv) the apparent pK values of the groups involved in Ca^{++} and Mg^{++} binding;
(v) dynamic parameters, *i.e.* chemical exchange rates and activation parameters or correlation times characterising the ion binding site(s);

Finally one can make profitable use of the fact that the ionic radii of Ca^{++} and Cd^{++} are very similar and substitute the spin $I = \frac{1}{2}$ nucleus ^{113}Cd for Ca^{++}. NMR spectra of ^{113}Cd bound to proteins – in many cases showing one or more fairly narrow signals – give valuable complementary information on such phenomena as cooperativity of ion binding, the nature of protein ligands and structural changes of the protein.

Some recent applications of ^{25}Mg, ^{43}Ca, and ^{113}Cd NMR in the study of skeletal muscle and heart muscle troponin C, bovine testis calmodulin and trypsin/trypsinogen will be presented.

M-AM-A1 MEMBRANOUS CYTOCHROME c OXIDASE: HYDROPHILIC FRACTURE PLANES SEEN IN COMPLEMENTARY REPLICAS. M.J. Costello, R. Fetter and T.G. Frey, Department of Anatomy, Duke University Medical Center, Durham, N.C. 27710 and Department of Biochemistry and Biophysics, University of Pennsylvania, Philadelphia, PA. 19104.
Crystalline vesicles of membranous cytochrome c oxidase isolated from beef heart mitochondria by Triton extraction have been examined in freeze-fracture, complementary replicas. These crystalline membranes preferentially fracture along hydrophilic surfaces, not within hydrophobic membrane interiors, (Costello and Frey, J. Mol. Biol. 161, 1982). These results are further substantiated using complementary replicas. The most commonly observed fracture surface follows the plane of interdigitation of the large tails of the y-shaped molecules within the center of the collapsed vesicles. The exposed low-relief crystalline surfaces contain complementary rectangular lattices (about 100 x 125Å). In each complementary replica the fracture plane at the center of the vesicle is separated from the surrounding ice by steps equal in height to the thickness of a single membrane (about 100Å). The hydrophilic fracture planes at the vesicle surfaces show the appropriate crystalline arrangement of protein, but the complementary impression of this pattern in the ice is perturbed, probably during the fracturing or shadowing steps. Other small regions of non-complementarity also indicate that deformations occur during fracturing and shadowing (at -150°C). These deformations can probably be minimized at lower specimen temperatures. Complementary fracture surfaces appear to be free of contamination at a vacuum of 10^{-7} torr. This work was supported in part by NIH Grants GM 27914 (to M.J.C.) and GM 28750 (to T.G.F.).

M-AM-A2 MITOCHONDRIAL DEFECT IN COMPLEX III OF HUMAN SKELETAL MITOCHONDRIA. Victor M. Darley-Usmar. Institute of Molecular Biology, University of Oregon, Eugene, Oregon 97403
Defects in mitochondrial metabolism have been described previously in human patients, and are called mitochondrial myopathies. I have isolated mitochondria from a patient with this disease. Spectral analysis revealed that the patient had low levels of reducible cytochrome b (< 15% of control values). The content of cytochrome c oxidase was also decreased by approximately 50%. Activity measurements showed that
1) ATPase activity (DCCD sensitive) was 60% greater than control, 2) Cytochrome c oxidase was 75% of control, 3) Succinic dehydrogenase activity was 60% of control, and 4) Succinate cytochrome c reductase activity was 2% of control.
These experiments localise the lesion to complex III, or the cytochrome bc_1 section of the inner mitochondrial membrane. The polypeptide composition of this protein is complex consisting of at least ten different polypeptides. I have examined the polypeptide composition of complex III in the patient and control samples by employing antibody binding techniques. The banding pattern for complex III of the patient is altered with most of the polypeptides not detectable. In contrast the subunits of cytochrome c oxidase and succinic dehydrogenase are present. Cytochrome b is the only mitochondrially synthesized component of complex III and as such is a primary candidate for the locus of this lesion.
Acknowledgments. I would like to thank Dr. Buist and Dr. Kennaway of University of Oregon Health Sciences Center for making tissue available for the experiments described above and Professor R.A. Capaldi for his comments.

M-AM-A3 THE DESIGN OF PHOTOACTIVATED MOLECULES: CHEMICAL AND STRUCTURAL CONTROL OF REACTION RATES AND EFFICIENCIES. Jeanne M. Nerbonne and Henry A. Lester. California Institute of Technology, Pasadena, California 91125.
Light-sensitive moieties have been widely used as protecting groups in organic synthesis. In an extension of this approach, the o-nitrobenzyl functional group in particular has been exploited by several groups for the preparation of biologically useful photoactivatable molecules. Little is known, however, about how the rates and efficiencies of these reactions are controlled by the nature of either the chromophore or the leaving group. During our work with photoactivated proton donors and cyclic nucleotides, we have begun to probe these questions. We have prepared a series of 12 photolabile proton donors with various protecting groups, chromophores, and leaving groups. We have measured the rate of H^+ release from these compounds by three independent methods. We find that the quantum yields for H^+ production are not highly sensitive to any of the structural modifications made. Although the reaction rates depend slightly (twofold) on the nature of the acid leaving group, the rates are highly dependent on the structure of the chromophore: simple substitution on the aromatic ring or the benzylic carbon increases the reaction rate 10-100 fold. All reactions show a pH dependence, increasing 2-3 fold for a unit decrease in pH. We also have prepared analogous photoactivated o-nitrobenzyl cyclic AMP analogues with various chromophores. Again, the rate of release of cAMP changes 10-100 fold by simple substitution on the aromatic nucleus.
Each of these factors sheds light on the problem of designing photoactivated protecting groups that are fast, efficient, insensitive to the nature of the leaving group, and therefore, generally useful. (Work supported by NIH grants GM-29836 and RCDA NS-272.)

M-AM-A4 RED CELL NA PUMP $E_1P \rightarrow E_2P$ CONVERSION IS BLOCKED AT 0°. J.H. KAPLAN & L.J. KENNEY, Department of Physiology, University of Pennsylvania, Philadelphia, Pa. 19104.

When [Na] > 5mM, at temperatures > 0°, phosphorylation of the red cell Na pump with ATP^{32} yields a phosphoenzyme which is predominantly K-sensitive (E_2P) with only a small fraction ADP-sensitive (E_1P). As previously observed (Blostein, J. Biol. Chem. 243:1957, 1968) at 0° EP obtained using ATP^{32} is K-insensitive. We have found that at 0° all the red cell Na pump phosphoenzyme is ADP-sensitive (E_1P). At temperatures > 0° the triphasic dependence of ATP:ADP exchange rate on [Na] is observed, at 0° the curve shows only simple saturation, the rate of ATP:ADP exchange is maximal by 1mM Na. The K inhibition of ATP:ADP exchange due to K_o (Kaplan, J. Gen. Physiol, in press 1982) observed at temperatures > 0° is not observed at 0°. The dependence of E_1P:E_2P on [Na] is not greatly altered in renal enzyme when the temperature is lowered from 25° to 0° in contrast with the present studies on red cell Na pump. Our data suggest that (i) $E_1P \rightarrow E_2P$ is blocked at 0° in red cell Na pump (ii) Na_o and K_o inhibitory effects on ATP:ADP exchange occur on E_2P (iii) the $K_{0.5}$ for Na in supporting phosphorylation is less than 1mM at 0° (iv) the different temperature dependence of E_1P:E_2P and [Na] may be due to differences in membrane composition or protein structure between red cell and kidney preparations. JHK is supported by RCDA K04 HL 01092.

M-AM-A5 THE STRUCTURAL ORGANIZATION OF THE ISOLATED, MEMBRANE-BOUND $(Na^+ + K^+)$-ATPase. G. Zampighi, J.W. Freytag and J. Kyte. Department of Anatomy, UCLA School of Medicine, Los Angeles CA 90024; E.I. Dupont de Nemours, Photo Product Department, Experimental Station, Wilmington DE 19898; Department of Chemistry, UCSD, La Jolla CA 92093.

We have studied the structural organization of purified, membrane-bound $(Na^+ + K^+)$-ATPase isolated from mammalian kidney by using conventional electron microscopy and computer image processing. Thin sectioning of the enzyme fractions bathed in ionic conditions favoring the E_2-P conformational state indicated the formation of a unique membrane-membrane complex. The complex was characterized by two plasma membranes having an overall thickness of 22-25 nm. The two membranes are separated by a gap about 12 nm wide which displays repeating densities connecting the surfaces of the apposing membranes. Ricin agglutinin, a lectin which binds to the carbohydrate moiety of the β-subunit of the enzyme, was observed covering the free surfaces of the membrane pairs. Therefore, the membrane-pair complex, formed when the enzyme was bathed in conditions favoring the E_2-P conformation, was the result of the interaction of the cytoplasmic surfaces of the $(Na^+ + K^+)$-ATPase molecules. Negative staining of the isolated enzyme fractions showed the presence of small two-dimensional arrays of molecules. Some arrays (6.0 nm and 5.0 nm) seemed to contain one α-β monomer per unit cell, whereas others (13.5 nm and 5.5 nm) were consistent with the presence of $(\alpha\text{-}\beta)_2$ asymmetric units. Our studies support a model of the enzyme where each α-β monomer is a cylindrically-shaped unit about 13 nm thick spanning the membrane asymmetrically. There is a large (about 6 nm) domain protruding from the cytoplasmic surface and a smaller one (about 3 nm) on the external surface of the membranes. (Supported by MDA CC811112, AHS Award 81-1003, and NSF PCM-8118108.)

M-AM-A6 FUNCTIONAL AND STRUCTURAL PROPERTIES OF THE RECONSTITUTED Ca^{2+}-ATPase. Javier Navarro, Brenda Smith, Aaron Lewis and Efraim Racker. Department of Applied Physics and Section of Biochemistry, Molecular and Cell Biology, Cornell University, Ithaca, New York 14853.

Ca^{2+}-ATPase from sarcoplasmic reticulum was delipidated and depleted of proteolipids by solubilization in Triton X-100 and ion-exchange chromatography on a DEAE cellulose column (Green,N.M., 1975, In: Calcium Transport in Contraction and Secretion, E. Carafoli et al., ed., pp. 339-348 North Holland, Amsterdam). Ca^{2+}-ATPase was reconstituted by the deoxycholate-cholate dialysis method (Knowles, A.F. and Racker, E., 1975, J. Biol. Chem. 250, 3538-3544) in the presence of synthetic phospholipids and glycolipids at various lipid to protein ratios. Depending upon the nature of the head group of lipids high Ca^{2+}/ATP ratios were obtained. Furthermore, the passive permeability of these vesicles was time-dependent and influenced by the lipid composition of the reconstituted vesicles. The conformational analysis of the Ca^{2+}-ATPase was carried out by applying Raman, Infrared and Circular dichroism spectroscopy in fully active preparations of reconstituted vesicles at low lipid to protein ratios.

(Supported by MDA fellowship (J.N.), Army and Navy (A.L.)

M-AM-A7 ASYMMETRIC MASS DISTRIBUTION OF Na^+-K^+-ATPase IN MEMBRANES STUDIED BY FREEZE-ETCHING. H.P. Ting-Beall, V.F. Holland, J.W. Freytag and D.F. Hastings. Depts. Anatomy and Physiology, Duke Univ. Med. Ctr., Durham, NC, 27710 and Dept. Physiology, Univ. South Dakota Sch. Med., Vermillion, SD 57069.

Freeze-fractured specimens from SDS purified porcine kidney Na^+-K^+-ATPase show no differences in the distribution of intramembrane particles (IMP) of 90-100 Å diameter between convex and concave fracture faces. However, there are 2 types of convex face: F_A, which shows a rather smooth background with many IMP, and F_B, which shows textured background with very few or no IMP. Etching the fractured samples further reveals that the F_B faces are covered with distinct pits of 90 Å or larger, as if the protein had been pulled out, leaving pits. The texture of the unetched F_B face may be due to closely spaced unresolved pits. The etched external surface (E_B) is covered with many particles of IMP size. F_A faces are covered with many IMP, while the etched external surface (E_A) is either smooth or reveals many particles half the size of IMP. There appears to be 2 types of vesicle in our resealed purified preparation: right-side-out, as in vivo, and inside-out. These results suggest that the major mass of the protein is distributed on one side of the membrane only. The specific saccharide marker, ferritin-con A, is being used to identify the true outer surface by EM. Two populations of resealed native membrane vesicles are also being separated by con A column chromatography in which the right-side-out vesicles are retained by virtue of glycoprotein-saccharide-Con A interaction. (Supported by NIH grants GM-27804 and NS-16063).

M-AM-A8 VANADATE BINDING TO THE GASTRIC H,K-ATPase: L. D. Faller, E. Rabon, and G. Sachs. CURE, Wadsworth Veterans Administration Hospital and the Department of Medicine, University of California, Los Angeles, CA 90073.

Vanadate binding to the gastric H,K-ATPase has been measured and correlated with earlier measurements of vanadate inhibition of ATPase activity and the variation of the hydrolytic rate with ATP concentration. 3 nmol/mg of vanadate bind specifically per mg of Lowry protein. The real and apparent dissociation constants found for vanadate binding to the K^+-enzyme are compatible with competitive binding of 1.5 nmol/mg of the inhibitor to each of the kinetically defined nucleotide sites with both ATP and vanadate binding tighter to the same site. Inhibition of 60% of the K^+-stimulated ATPase activity at 37 °C correlated with 1.5 nmol/mg of vanadate bound, and complete loss of activity correlated with 3 nmol/mg of vanadate bound. In contrast to the stoichiometry of vanadate binding, a maximum of 1.5 nmol/mg of acid precipitable phosphoenzyme is formed. Only the higher affinity ATP site had to be saturated for maximum phosphoenzyme formation. The simplest interpretation of the data is that vanadate ions inhibit the gastric H,K-ATPase by binding competitively with ATP at two catalytic sites. The difference between the stoichiometry of vanadate binding required for complete inhibition of ATPase activity and the stoichiometry of phosphoenzyme formation could mean that hydrolysis of ATP is catalyzed by different mechanisms at the two sites (supported by NIH).

M-AM-A9 STOICHIOMETRY OF THE NA/K PUMP IN ISOLATED EPITHELIA OF FROG SKIN. Thomas C. Cox and Sandy I. Helman. Dept. of Physiology and Biophysics, University of Illinois, Urbana, IL 61801

Unidirectional ^{42}K influx (J_K^{32}) at the basolateral membrane of R. pipiens was measured in a Cl-free (SO_4) Ringer. FJ_K^{32} averaged 6.6 ± 0.5 (N = 30) μA/cm². Since greater than 95% of the J_K^{32} was inhibited by 1 mM ouabain, the J_K^{32} could be used as an estimate of the K influx via the pump. By use of variable amiloride concentration and Na-free apical solutions, the I_{sc} was varied from 0 to 60 μA/cm². Between 5 and 60 μA/cm² FJ_K^{32} increased from 5 to 10 μA/cm². For I_{sc} < 5 μA/cm², ouabain inhibitable J_K^{32} remained nonzero even at I_{sc} = 0. Defining pump coupling ratio as I_{sc}/FJ_K^{32}, the apparent stoichiometry varied between about 1:1 at low I_{sc} to about 6:1 at the higher I_{sc}, indicating a relationship between transepithelial Na transport and pump coupling ratio. Net charge transfer through the pump (I_p) was measured electrically as described previously (Fed. Proc. 40:358, 1981). Between I_{sc} of 10 - 25 μA/cm², I_p ranged from 5 to 15 μA/cm². At I_{sc} > 5 μA/cm², the I_p agreed will with the charge transfer calculated above from the difference between I_{sc} and FJ_K^{32}. However, at low I_{sc} < 5 μA/cm², I_{sc} - FJ_K^{32} became negative while the pump remained electrogenic. Thus, at the usual I_{sc} > 5 μA/cm², the Na/K pump behaves somewhat classically with an apparent stoichiometry in the vicinity of 3:2, albeit variable. However, at low I_{sc}, and in the absence of a significant basolateral Na recycling, the pump appears capable of electrogenic, ouabain-inhibitable K extrusion. (Supported by USPHS AM 16663 and GM 07357.)

M-AM-A10 LATERAL MOBILITY OF MITOCHONDRIAL MEMBRANE COMPONENTS: IMPLICATIONS FOR THE MECHANISM OF ELECTRON TRANSPORT. J. Hochman, S. Ferguson-Miller, S. Foxall, and M. Schindler. Biochemistry Department, Michigan State University, East Lansing, MI 48824.

The mobility of lipid, cytochrome c, and cytochrome aa_3 were measured in giant mitochondria from cuprizone fed mice using the technique of fluorescence redistribution after photobleaching (FRAP). Rabbit anti-cytochrome aa_3 antibodies were labeled with the lipophobic fluorescent dye, morpholinorhodamine isothiocyanate, and were purified by gel filtration and chromatography on a cytochrome aa_3 affinity column. FRAP measurements on inner mitochondrial membranes labeled with the antibodies showed complete monophasic recovery with a diffusion coefficient of 1.0×10^{-10} cm^2/sec. Morpholinorhodamine and tetramethylrhodamine labeled derivatives of cytochrome c, demonstrating native activity, diffused on mitochondrial membranes at a rate of 1.7×10^{-10} cm^2/sec at low ionic strengths (42 mM mannitol, 8 mM hepes, pH 7.2). Under these conditons succinate oxidase had a turnover of 20 electrons/sec. N-4-nitrobenzo-2-oxa-1,3-diazole (NBD) phosphatidylethanolamine gave monophasic recovery at a rate of 2.4×10^{-8} cm^2/sec in inner membranes prepared by sonication. Inner mitochondrial membranes prepared by treatment of mitochondria with digitonin had slower lipid mobilities and biphasic recovery, but increased succinate oxidase activity. The results are explained in terms of a dynamic aggregate model of electron transport, in which freely diffusing components are in equilibrium with aggregated forms. This work was supported by NIH Grant GM 26916 (SFM) and GM 30158 (MS).

M-AM-A11 VOLTAGE INDUCED MEMBRANE CHANNELS AND Rb^+ PUMPING ACTIVITY OF (Na,K)ATPase IN HUMAN ERYTHROCYTES. Tian Yow Tsong & Engin E. Serpersu, Department of Physiological Chemistry, The Johns Hopkins University School of Medicine, Baltimore, Maryland 21205

A low magnitude AC field (10-25 V/cm, 0.1-100 kHz) that generates a transmembrane potential of 6-15 mV has been found to activate membrane channels, and stimulate Rb^+ uptake by erythrocytes in isotonic suspension against a concentration gradient. The reversible opening and closing of membrane channels was monitored by the appearence of membrane conductance after the voltage stimulation, and Rb^+ uptake was measured by the radioactive tracer assay. Roughly, 30% of the voltage induced membrane conductance was suppressed by ouabain, and 100% of the voltage stimulated Rb^+ uptake was inhibited by this specific inhibitor to the (Na,K)ATPase. The stimulated Rb^+ uptake was both voltage and frequency dependent, excluding Joule heating as a cause of the observed effect. At 3°C, the maximum stimulation (22 Rb^+/pump-s) occurred at 20 V/cm and at 1 kHz. Contrast to the Rb^+ uptake, no efflux of Rb^+ was stimulated by the AC field. Neither was the movement of Na^+ ion in either direction stimulated by the AC field. These results indicate that whereas the extrusion of Na+ by the enzyme requires consumption of ATP, the uptake of Rb^+ is likely driven by the electrochemical potential. This would imply that the pump is electrogenic under physiological conditions. Thus, the enzyme may, in effect, function as a rectifier for the influx of Rb^+ (or K^+) ion. A simple consideration of energetics further suggests that the electric field may have induced a conformational change of the enzyme, and the release of this conformational energy is linked to the pumping of Rb^+ ion into the erythrocytes. (Supported by NIH Grant GM 28795).

M-AM-B1 CONFORMATIONAL CHANGE RATES FOR HEMOGLOBIN IN VISCOUS SOLVENTS. C. A. Sawicki and M. Khaleque* Physics Department, North Dakota State University, Fargo, North Dakota 58105.

Laser photolysis experiments were carried out on carboxyhemoglobin in twelve viscous solutions at pH 8.3 and 20°C. Solutions were prepared from mixtures of sodium borate buffer with various amounts of sucrose, glycerol or ethylene glycol. All experimental results were consistent with a simple two-state model which included tetramer-dimer dissociation. Values for the R and T state association rate constants and the tetramer-dimer dissociation constants were determined experimentally for each solution. These parameter values were used with the two state model to produce least square fits to the biphasic CO recombination kinetics observed at 437 nm by varying K, the rate of the R→T conformational change of the R state deoxyhemoglobin present after photolysis. K is found to decrease with increasing viscosity (η) for all three mixed solvent systems studied. In the case of sucrose/borate solutions, fair agreement is seen between our data and an adaptation of Kramers' model (B. Gavish (1978) Biophys. Struct. Mechanism 4, 37-52) which predicts a $1/\eta$ dependence for K. For glycerol/borate and ethylene glycol/borate solutions K decreases much more rapidly than $1/\eta$ with increasing viscosity. For example, in the case of ethylene glycol/borate solutions K decreased by a factor of 20 for an increase in η from 1 to 4 cP.

Supported mainly by a Northwest Area Foundation Grant of Research Corporation (#9287) and in part by NSF Grant # PCM-8206920.

M-AM-B2 RESONANCE RAMAN DETECTION OF Fe-CO STRETCHING AND Fe-C-O BENDING VIBRATIONS IN STERICALLY HINDERED CARBONMONOXY "STRAPPED HEMES". Ellen A. Kerr and Nai-Teng Yu, School of Chemistry, Georgia Institute of Technology, Atlanta, GA. 30332; Brian Ward and C.K. Chang, Department of Chemistry, Michigan State University, East Lansing, MI 48824.

Resonance Raman spectroscopy is ideally suited for investigating the nature of the Fe-C-O distortion in hemoproteins; the Fe-C stretching, Fe-C-O bending and C-O stretching vibrations in carbonmonoxy Hb and Mb have been detected with Soret excitation. Here we report a study of CO binding to sterically hindered hemes equipped with a hydrocarbon chain strapped across one face of the porphyrin to provide a side-way shearing strain to CO ligand. Increasing the steric hindrance (by decreasing the chain length) was found to decrease the CO binding affinity,but to increase the Fe-C stretching frequencies: heme-5 (unstrapped), 495 cm^{-1}; SP-15, 509 cm^{-1}; SP-14, 512 cm^{-1}; SP-13, 514 cm^{-1}. The axial base used in these complexes is N-methylimidazole. We interpret this increase in Fe-C stretching frequency in terms of increased interactions between the C-atom of CO and the N-atom(s) of pyrrole ring(s).

More interesting is the finding that the degree of steric hindrance in these "strapped" hemes is correlated with the intensity of the Fe-C-O bending mode relative to the Fe-C stretching vibration. Its intensity decreases to undetectable level upon removal of the strap. In addition, we have estimated the Fe-C-O angles from isotope data in various heme-CO complexes, which will be discussed.

M-AM-B3 RESONANCE RAMAN STUDIES OF Co-O_2 AND O-O STRETCHING VIBRATIONS IN OXY COBALT-HEMES.* Helen C. Mackin, Motonari Tsubaki and Nai-Teng Yu, School of Chemistry, Georgia Institute of Technology, Atlanta, Georgia 30332

Strong evidence is presented that the stretching vibration of the bound oxygen can be perturbed by an accidentally degenerate porphyrin ring mode, resulting in two split frequencies. A decrease in O_2 binding affinity, caused by the proximal base tension, corresponds to an increase in the Co-O_2 stretching frequency. The ν(Co-O_2) at 527 cm^{-1} for the low affinity Co(II)(TpivPP) (1,2-Me_2Im) O_2 complex is 11 cm^{-1} higher than the 516 cm^{-1} value for the high affinity complex (with N-MeIm replacing 1,2-Me_2Im). There is a 24 cm^{-1} difference in the Co-O_2 stretching frequencies between Co(II)(TpivPP)(N-MeIm)O_2 (at 516 cm^{-1}) and oxy meso CoMb (at 540 cm^{-1}), suggesting a protein induced distortion of the Co-O-O linkage.

Evidence is presented that suggests the presence of two dioxygen stretching frequencies due to two different conformers in each of the N-MeIm and 1,2-Me_2Im complex of oxy Co(II)(TpivPP).

*Supported by a grant from NIH (GM 18894)

M-AM-B4 CONTRIBUTION OF SINGLE AMINO ACID RESIDUES TO THE STRUCTURAL STABILITY OF SPERM WHALE MYOGLOBIN. M. A. Flanagan, B. Garcia-Moreno E., F. R. N. Gurd, Chemistry Dept., Indiana University, Bloomington, IN 47405, S. H. Friend, Children's Hosp. of Philadelphia, R. Feldmann, Div. Computer Research & Technology, National Institutes of Health, Bethesda, MD 20014 & H. Scouloudi, Laboratory of Molecular Biophysics, Oxford University, Oxford, England.

The acid denaturation behavior of myoglobin from eleven closely related species of sea mammals representing the sperm whales, baleen whales, dolphins and beaked whales was studied at low ionic strengths. The observed acid stability falls into three groups, following roughly the phylogenetic groupings. The overall range of stability is small, suggesting evolutionary compensation. The observed stability differences were partitioned into contributions from different types of noncovalent interactions. These include electrostatic and hydrophobic interactions, hydrogen bonding and the free energy contribution of protein titration. The theoretical analysis roughly follows the over-all trends of the observed stability differences and in several cases predicts the observed differences due to single site substitutions. The interconvertibility of free energy makes an accurate prediction of the ultimate partitioning difficult, but the theoretical estimates are a reasonable measure of possible sources of the observed stability differences. Assignment of the contribution made to the overall structural stability by single amino acid substitutions and substitution of pairs of amino acids indicates that: (1) Substitutions involving methyl group deletion can have measurable effects on the stability of the myoglobin molecule. (2) The substitution of a lysine for an arginine can result in a substantial loss of stability, presumably due to loss of hydrogen bonding capability. (3) The net result of a particular type of substitution is strictly dependent on its specific location within the protein tertiary structure. (Supported by PHS HL-05556.)

M-AM-B5 FLUCTUATIONS IN THE HEME POCKET OF MYOGLOBIN MONITORED BY GENERAL BASE CATALYSIS OF HYDROGEN EXCHANGE FROM HISTIDINE F8. Neville R. Kallenbach, Leidy Laboratories, Department of Biology, University of Pennsylvania, Philadelphia, PA 19104, and Peter S. Kim, Department of Biochemistry, Stanford University, School of Medicine, Stanford, CA 94305.

The ring N_3H and peptide NH of the proximal histidine in cyanmet-myoglobin (MbCN) exchange with solvent at alkaline pH via a hydroxide catalysed reaction (Cutnell et al, J. Am. Chem. Soc. 103, 3567-72, 1981). Measurement of the exchange rate at low temperature of the imidazole N_3H in a soluble imidazole-cobalamine complex indicates that the rate of the His F8 N_3H in the heme pocket of MbCN is about 10^{-6} that of the rate this proton would have if it were fully exposed. We have investigated the nature of the fluctuations responsible for exposing these protons, using general base catalysts as a probe of the side-chain exchange reaction. The bases piperidine, pyrrolidine, as well as several substituted derivatives catalyse exchange of the His F8 side-chain, but not the peptide. Contrary to the predictions of a simple local unfolding model, in which exchange occurs in a milieu resembling bulk solvent, increasing pH and temperature strongly favor general base catalysis over that by OH^-. At pH 9.5 and 30°C, for example, only OH^- is effective, while at 40°C, the organic bases are more effective than OH^-. Thus the fluctuations mediating exposure to piperidine or pyrrolidine are different from those responsible for OH^- catalysis. One possibility is that larger amplitude fluctuational opening is required for access of the organic bases relative to OH^-. This work was supported by an NIH fellowship (GM 08466) as well as grants PCM 77-16834 (NSF), 2 R01 GM 19988-21 (NIH) to R.L. Baldwin, and grants NSF GP 23633, and NIH RR 00711 supporting the Stanford Magnetic Resonance Laboratories.

M-AM-B6 GEMINATE RECOMBINATION OF CARBON MONOXIDE, DIOXYGEN AND n-BUTYL ISOCYANIDE TO MYOGLOBIN AT AMBIENT TEMPERATURES. J.H. Sommer, E.R. Henry, J. Hofrichter and W.A. Eaton. Laboratory of Chemical Physics, NIADDK, National Institutes of Health, Bethesda. MD 20205

Transient absorption spectra have been measured on myoglobin complexed with carbon monoxide (MbCO), dioxygen (MbO_2) and n-butyl isocyanide (MbBuNC) following photolysis by a Nd:YAG laser (532 nm, 10 ns FWHM). The source for spectral measurements was the fluorescence of a dye excited by a second Nd:YAG laser (355 nm, 10 ns FWHM), and the transmitted intensity was detected with a vidicon and optical multichannel analyzer. In all cases, geminate recombination of the ligand to the parent myoglobin molecule was observed. MbCO and MbO_2 both exhibit one geminate recombination process with no spectral changes observed during or after the process. This suggests that the protein relaxes very quickly, with the iron having moved out of the heme plane in less than 3 ns, the time resolution of our instrument. The geminate recombination parameters for MbCO are ϕ=0.04 and τ=200 ns. For MbO_2, $\phi \sim 0.45$, $\tau \sim 60$ ns. In the simplest kinetic model, the photodissociated ligand either returns to the heme from a non-covalently bound site in the protein or escapes to the solvent. This model gives for MbCO: τ_{out}=200 ns and τ_{in}=5 μs and MbO_2: $\tau_{out} \sim \tau_{in} \sim 120$ ns. The out rates thus seem fairly insensitive to the ligand. The in rates is the same as the ratio of the bimolecular recombination rates, which suggests that the photoproduct prepared by our 10 ns pulses is also an intermediate in the thermal dissociation and association pathway. MbBuNC has at least two geminate recombination processes: $\phi_1 \sim 0.33$, $\phi_2 \sim 0.25$, $\tau_1 \sim 30$ ns, $\tau_2 \sim 1.3$ μs. Each geminate process in MbBuNC is accompanied by a spectral change in the Soret band, indicating changes in structure that are not observed for the less bulky CO and O_2 ligands.

M-AM-B7 STUDIES OF HEME-HEME INTERACTION IN HEMOGLOBIN BY MÖSSBAUER SPECTROSCOPY. A. Levy* and J.M. Rifkind. *The Johns Hopkins University, Baltimore, Maryland 21218 and The Gerontology Research Center, NIA/NIH, Baltimore, Maryland 21224.

ESR and Mössbauer studies of methemoglobin (A. Levy, J.C. Walker and J.M. Rifkind, J. Appl. Phys. 53, 2066-2068, 1982) indicate that there is appreciable mobility in the ligand pocket even at low temperature. Mössbauer studies have now been performed on carbonmonoxy hemoglobin, oxyhemoglobin and deoxyhemoglobin, as well as partially liganded hemoglobins in order to determine whether similar freedom of mobility exists in the ferrous hemoglobins and to delineate the perturbations that take place at the iron during binding of ligands. These results will be discussed in terms of their implications for helping to explain the interaction between hemes, which is responsible for cooperative binding of ligands.

M-AM-B8 HEAT CAPACITY CHANGES ACCOMPANYING OXYGENATION OF HUMAN HEMOGLOBIN, E. Battistel and R. Lumry, Chemistry Dept., University of Minnesota, Minneapolis, MN 55455 and C. Jolicoeur, Chem. Dept., University of Sherbrooke, Sherbrooke, Quebec, Canada J1K 2R1.

The heat capacity measures the mean square fluctuation in enthalpy and in entropy and is thus an important source of information for proteins which derive physical and functional properties from fluctuations. Using a Sodev calorimeter and densimeter the heat capacity of hemoglobin A solutions ($4x10^{-4}$M,unbuffered,salt and DPG free)was determined as a function of oxygen binding. There was no significant change in molar volume but $\bar{C}p$ increased by $5x10^{2}jK^{-1}mol^{-1}$ at 25% saturation then moved smoothly to the $Hb(O_2)_4$ value ($2.8x10^{2}$ $jK^{-1}mol^{-1}$ higher than Hb). Using the values of the single-step binding constants for a four-step mechanism published by Ackers et al, and Yonetoni and Imai to calculate concentrations of intermediates the data were found to be consistent with a model in which $Hb(O_2)_2$,$Hb(O_2)_3$ and $Hb(O_2)_4$ have the same $\bar{C}p$ value and $\bar{C}p$ for HbO_2 is larger by at least $1.2x10^{3}jK^{-1}mol^{-1}$ which is 1.6% of the total (91.5 $kjK^{-1}mol^{-1}$). The relaxation contributions to the heat capacity from oxygen and proton-binding fluctuations calculated using parameter values from the literature were too small to alter the pattern. Relaxation contributions from the several T to R processes calculated using T and R-state probabilities for the intermediates and the corresponding enthlpy changes (Ackers et al) were inconsistent in size and shape with the measured pattern. On the other hand the $\bar{C}p$ data follow closely the hydrogen-exchange behavior to be reported by Hallaway, Hallaway and Rosenberg. This measure of the dynamical aspects of fluctuations changes abruptly between 0 and 25% oxygenation and then remained constant to saturation. These observations reflect a major difference between Hb and HbO_2 consistent with other observations; e.g. the abrupt decrease in dimer affinity on first oxygen addition.Supported by the Nat'l.Heart,Lung&Blood,Inst.2P01 HL16833

M-AM-B9 SEMISYNTHETIC STUDIES ON HEMOGLOBIN: PREPARATION AND CHARACTERIZATION OF TRUNCATED DERIVATIVES OF HEMOGLOBIN: David E. Harris, Mary L. Crowl-Powers, William F. Heath and Frank R. N. Gurd, Department of Chemistry, Indiana University, Bloomington, IN 47405.

The four NH_2-terminal valine residues of the major component human hemoglobin are involved in interactions important for the function of the protein. Using methods similar to those developed for the semisynthesis of myoglobin (DiMarchi et al. (1980) Biochemistry 19, 2454) the NH_2-terminal valine residues of each of the chains have been removed by a single round of the Edman degradation The degradation was performed by coupling 3-sulfophenylisothiocyanate to hemoglobin under conditions favoring reaction at the NH_2-terminal amino groups. The chains that were modified by a single coupling were isolated and after treatment with trifluoroacetic acid des-Val^1-α chains and des-Val^1-β chains were prepared. The truncated apo chains have been combined with their complementary heme-containing chains and after heme reintroduction, the reconstituted proteins have been purified by cation exchange chromatography. By these methods des-$Val^{\alpha 1}$-hemoglobin and des-$Val^{\beta 1}$-hemoglobin have been prepared. The truncated hemoglobin derivatives exhibit physical and spectroscopic properties that are similar to those of the native protein. Work is in progress to further characterize the modified proteins to study the roles of the NH_2-terminal residues in the action of the protein. (This work was supported by PHS Grants HL-05556, HL-14680, & HL-21483.)

M-AM-B10 ISOLATION OF A HEMOGLOBIN-PROTEIN COMPLEX FROM HEMOLYZED PLASMA OF THE AMPHIBIAN TARICHA GRANULOSA. R. T. Francis, Jr., R. R. Becker and T. D. Yager, Department of Biochemistry and Biophysics, Oregon State University, Corvallis, OR 97331

Haptoglobin, a hemoglobin-binding protein (HBP), has been observed in mammals, birds and some snakes. In this study, the newt Taricha granulosa has been examined for the presence of haptoglobin or another HBP. The existence of a hemoglobin-HBP complex has been demonstrated by the following: Upon hemolysis of newt blood, a large peroxidase-active protein was seen on nondenaturing polyacrylamide gel electrophoresis (PAGE). Densitometric measurements of the plasma profile revealed the complex to be 10% more abundant than serum albumin. In clear plasma, old hemolyzed plasma, or hemolyzed plasma at pH 3.5 or lower, the complex was absent from the PAGE profile. Below pH 3.5, newt hemoglobin is denatured and incapable of complex formation. Hemoglobin was revealed to be part of the complex band in PAGE by the excision of the band from the gel and running it in a second dimension on SDS PAGE. Hemoglobin subunits and larger components were seen after Coomassie R-250 staining. When the large material was reduced with β-mercaptoethanol, a 72K dalton-sized doublet was produced. When clear plasma was eluted over a Sepharose 4B-CL-hemoglobin affinity column, the same doublet was seen after reduction. Whether the newt HBP is composed of subunits of that size remains to be demonstrated. Analytical ultracentrifugation of material previously separated from free hemoglobin showed 409 nm absorbing components with S values of 6.7 and 9.5 (approximately 120 and 200K daltons). This newt is one of the most primitive vertebrates to be shown to possess this mechanism. Dr. K. van Holde collaborated in the sedimentation analysis. NSF grant PCM 78 21784 supported this research.

M-AM-B11 FREE ENERGY COUPLING WITHIN MACROMOLECULES: THE CHEMICAL WORK OF LIGAND BINDING AT THE INDIVIDUAL SITES IN COOPERATIVE SYSTEMS G. K. Ackers, M. A. Shea, and F. R. Smith, Department of Biology, The Johns Hopkins University, Baltimore, MD 21218

A new treatment of thermodynamic coupling in multisite ligand binding systems has been developed. This treatment provides a theoretical framework for (a) evaluating from experimental data the chemical work (Gibbs free energy) of loading each individual site of a macromolecule with ligand, taking into account the effects of energetic coupling to binding processes at the other sites, and (b) predicting the contributions from binding events at each site to the total energy of binding. The availability of experimental techniques which directly measure binding at individual sites or at combinations of a few sites is becoming increasingly widespread. For a system of two interacting sites, a general analytical theory for partitioning of the binding free energy into contributions from reactions at the separate sites has been derived. Whenever the sites differ in their intrinsic affinities, an unequal partitioning of the cooperative energy occurs, with the larger portion contributed to the energy of loading the "weaker" site. This partitioning is independent of the molecular mechanism of coupling between the sites. Some applications to experimental data in the form of individual-site binding isotherms will be presented. Mechanisms whereby conformational transitions within the macromolecule may contribute to the individual-site binding energies will be discussed. Supported by grant PCM 80-14533 from the NSF.

M-AM-B12 ELECTRONIC STRUCTURE AND HYPERFINE INTERACTIONS IN FERRICYTOCHROME c_2. K.C. Mishra, Santosh K. Mishra and T.P. Das, Department of Physics, State University of New York, Albany, NY, 12222.

Using the self-consistent charge extended Hückel procedure, we have studied the electronic structure of ferricytochrome c_2. The sulfur atom of the methionine group is found to carry a small positive charge, in keeping with suggestions[1] that it interacts with the oxygen of tyrosine 70. The spin population is significantly delocalized with the iron atom carrying only 65 percent of the unpaired spin population. The porphyrin nitrogens all have significant hyperfine interactions different from each other and the proximal histidine nitrogen. Using our calculated ^{14}N hyperfine constants the ENDOR frequencies expected in the presence of a magnetic field have been obtained and four of them have been identified with the experimentally observed frequencies[2]. Proton hyperfine constants have also been studied for the mesoprotons and the protons of the imidazole of the proximal histidine, the major contributions to which arise from exchange polarization and dipolar effects, leading to negative hyperfine constants which explain four of the observed proton ENDOR frequencies[3]. The possible assignment of the remaining two observed ENDOR frequencies to methionine protons will be discussed. Theoretical results for the components of the g-tensor using the calculated electronic wave-functions and energy-levels will also be presented and compared with experiment. (Supported by NIH grant HL 15196).

1. F.R. Salemme et.al. J. Biol. Chem 248, 3910 (1973).
2. C.F. Mulks et.al. Jour. Am. Chem. Soc. 101, 645 (1979).
3. R. de Beer et.al. (private communication).

M-AM-B13 RAMAN DIFFERENCE SPECTROSCOPY OF HEME-LINKED IONIZATIONS IN CYTOCHROME C PEROXIDASE*, John A. Shelnutt, Division 1152, Sandia National Laboratories, Albuquerque, New Mexico, 87185; J. D. Satterlee, University of New Mexico, Albuquerque, New Mexico; J. E. Erman, Department of Chemistry, Northern Illinois University, Dekalb, Illinois.

The pH-dependence of the oxidation-state marker line of hemoproteins is investigated in cytochrome c peroxidase and its cyanide derivative with Raman difference spectroscopy. The frequency is sensitive to ionization of a group on the protein that regulates catalytic activity of the resting ferriheme enzyme. The oxidation-state marker line shows a transition with pK of 5.5 in good agreement with other spectroscopic measurements and with kinetic measurements of binding of peroxide and other ligands to the native enzyme. The shift of 0.8 cm^{-1} to higher frequency at pH 4.5 relative to the pH 6.4 value is interpreted in terms of a substantial decrease in π-electron density in the porphyrin ring. Charge density in the π-system is highest at maximal activity as would be expected if donor-acceptor interactions with residues of the protein stabilize the oxidized Fe(IV) reaction intermediate. Additional heme-linked ionizations with pK's near 7.5 involve deprotonation of several groups of the protein, conversion of iron from high to low spin, and denaturation of the protein.

*Work performed at Sandia National Laboratories supported by the U. S. Department of Energy under contract number DE-AC04-76-DP00789.

M-AM-C1 SPECTROSCOPIC PROPERTIES OF HALORHODOPSIN. H. J. Weber, M. Taylor and R. A. Bogomolni, Cardiovascular Research Institute, University of California, San Francisco, CA 94143

Although various bacteriorhodopsin-less halobacterium strains were recently made available, none exist which contain only halorhodopsin (hR), due to the presence of a third, newly discovered retinal pigment, sR (1). Previous data on hR have been confused by the spectral contribution of this unrecognized pigment (2). We therefore developed methods for the bleaching of sR alone in pigment-enriched membranes. Bleaching is accomplished by incubating membranes in the dark at 40°C with 0.4M NH_2OH and 4M NaCl at pH 9.0 for 90min. The treated membranes contain a photoactive pigment that absorbs maximally at 580nm and which we identify as hR based on its photocycle (3). hR reversibly converts at pH 11.0 (4M NaCl, 20°C) to a new form, P^a_{410} (λ_{max} = 410nm, a = alkaline). At pH 9.0, however, no shift in λ_{max} occurs in the dark, but upon illumination with red light (λ >630nm) a loss of the 580nm absorption band is accompanied by an absorption increase at 410nm. This new form, P^l_{410} (λ_{max} = 410nm, l = light) is stable in the dark but can be fully converted to hR_{580} by a pulse of blue light (λ_{act} <450nm), a reaction which cannot be observed for P^a_{410}.

(1) Bogomolni, R.A. and J.L. Spudich, Proc. Natl. Acad. Sci. USA (1982) 79, 6250-6254.
(2) Lanyi, J.K. and H.J. Weber (1980) J. Biol. Chem. 255, 243-250.
(3) Weber, H.J. and R.A. Bogomolni (1981) Photochem. Photobiol. 33, 601-608.

M-AM-C2 STATE OF PROTONATION OF THE RETINAL SCHIFF-BASE OF BACTERIORHODOPSIN: MAGIC ANGLE SPINING NMR OF PURPLE MEMBRANE USING CARBON-13 ENRICHED RETINAL, Dratz,E.A.[†], Gärtner,W.[‡], Oesterhelt,D.[‡] and Veeman,W.S.[&], [†]Div. of Natural Sciences, Univ.of Calif.,Santa Cruz 95064, [‡]M.-P.-I. für Biochemie D-8033 Martinsried, FRG and [&]Dept. of Molecular Spectroscopy, Univ.of Nijmegen, 6525ED Netherlands

It has been very difficult to obtain structural information on membrane proteins, especially when they are located in their unperturbed native membrane. We have used solid-state NMR methods to obtain information of the state of protonation of the retinal-Schiff Base chromophore in bacteriorhodopsin (BR) located in its native purple membrane.

The synthesis and incorporation of single site 95% enriched ^{13}C retinal (Gärtner, Oesterhelt and Hops, unpublished) has allowed us to obtain useful spectra (S/N about 4 for single carbon lines on ca. 16 mg. of BR in purple membranes in about 20 hours on a Brucker CXP-300 at 75MHz with a home-built MAS NMR probe (vanDijk etal., J. Physics E: Sci. Instr., 13, 1309110(1980)). More material provides a higher S/N and/or a shorter measuring time.

We have carried out a number of experiments with retinal ^{13}C enriched at carbon number 13, which is the retinal carbon that is most sensitive to the protonation state of model Schiff bases. The 13 carbon site in BR in native purple membrane has a chemical shift of ca. 159 ppm. This chemical shift is rather close to that of model Schiff bases in solution that have been protonated (eg. 162 ppm with HCl) but is quite different from unprotonated Schiff base model compounds (144-5 ppm). The difference between the model protonated Schiff bases(PSB) and BR indicates that there is more electron density on C-13 in BR than the model PSB. If the Schiff base in BR is in fact protonated any counter ion would seem to have less electron withdrawing power than Cl^-.

M-AM-C3 SPECTRAL AND CHEMICAL DISCRIMINATION OF hR AND sR. John L. Spudich, Department of Anatomy, Albert Einstein College of Medicine, Bronx, NY 10461 and Roberto A. Bogomolni, Cardiovascular Research Institute and Department of Biochemistry and Biophysics, University of California, San Francisco, CA 94143.

Membranes of halobacteria contain two photoactive rhodopsin-like pigments in addition to bR: the light-driven ion pump hR and the slower photocycling molecule sR, which absorbs in the same spectral region and appears to serve as a photosensory receptor (Bogomolni and Spudich, Proc. Natl. Acad. Sci. USA, 79: 6250-6254, 1982). The availability of mutants (Spudich and Spudich, Proc. Natl. Acad. Sci. USA, 79: 4308-4312, 1982) lacking one or both of these pigments has enabled us to separate spectral and chemical properties of hR and sR. The sR absorbs with λ_{max} = 589 ± 3 nm, whereas that of hR is 7 -10 nm to the blue of this value. sR shows a shift in λ_{max} to 550 nm with a slight decrease in extinction when taken from neutral pH to pH10.8, whereas similar treatment of hR causes an essentially total loss of extinction with the production of absorbance in the near UV/blue region. Both effects are completely reversible. This difference, as well as differing sensitivity of sR and hR to detergents and low ionic strength, provide criteria for distinquishing the two pigments. These criteria allow us to determine that several properties attributed to hR in other laboratories are actually properties of sR. (Supported by NIH GM 27750 and NIH GM 28767)

bR = bacteriorhodopsin; hR = halorhodopsin; sR = slow-cycling rhodopsin-like pigment.

M-AM-C4 THE STRUCTURE OF THE CHROMOPHORE IN THE O_{640} INTERMEDIATE OF BACTERIORHODOPSIN.
S.O. Smith and R. Mathies. Department of Chemistry, University of California, Berkeley, CA 94720.

Resonance Raman spectra of the O_{640} photointermediate of bacteriorhodopsin have been obtained using a dual-beam, time-resolved technique. A flowing purple membrane suspension at 40°C is first illuminated with a 514-nm pump beam to initiate photocycling. Raman scattering from O_{640} is excited 3-6 msec "downstream" using a probe beam at 752-nm. This far red excitation minimizes interference from the O_{640} fluorescence. Raman spectra of the O_{640} intermediate of native bacteriorhodopsin have been obtained in H_2O and D_2O, as well as from bacteriorhodopsin regenerated with 15-deuterio-, 14-deuterio-, and 12,14-dideuterio-retinals (obtained from Johan Lugtenburg and Hans Pardoen, Leiden University, Holland). Comparision of these O_{640} Raman spectra with spectra of both light-adapted bacteriorhodopsin (BR_{568}) and the 13-*cis* component of dark-adapted bacteriorhodopsin (BR_{548}) have been used to establish the configuration of the retinal chromophore in O_{640}. The deuteration induced frequency and intensity changes in the Raman spectra of O_{640} correspond closely with those displayed by BR_{568} which contains an all-*trans* retinal chromophore. However, the changes observed upon deuteration of the chromophore in BR_{548}, our 13-*cis* "model compound", are very different from those observed in O_{640}. This demonstrates that the O_{640} intermediate has an all-*trans* retinal chromophore that is formed from a thermal isomerization about the 13,14 double bond. In addition, resonance Raman spectra of O_{640} in H_2O and D_2O show a shift of the C=N stretch from 1630 cm^{-1} to 1589 cm^{-1}, demonstrating that the Schiff base nitrogen in O_{640} is protonated.

M-AM-C5 BACTERIORHODOPSINS CONTAINING CYANINE DYE CHROMOPHORES. SUPPORT FOR THE EXTERNAL-POINT CHARGE MODEL.
F. Derguini, C.G. Caldwell, M.G. Motto, V. Balogh-Nair, K. Nakanishi, Department of Chemistry, Columbia University, New York, N.Y. 10027.

Bacteriorhodopsins (bR) derived from merocyanines 1 and 2 have been prepared in order to check the validity of the external point-charge model which was forwarded to account for the dramatic red shift in the absorption maximum of bR (570 nm). The iminium salts of merocyanines 1 and 2 have symmetric charge distributions which should be retained in bR if the proposed model were valid. The two pigments formed from the merocyanines absorbed at 662 nm and had half-band widths (W1/2) of ca. 1300 cm^{-1}; the red-shifted maxima and the narrow bandwidth both provide excellent support for the point-charge model 3 and also furnish independent support for the protonated Schiff base structure of the chromophore. When these bR analogues were incorporated into asolectin vesicles no proton pumping activity was observed under constant illumination. Since the double bonds in iminium salts of 1 and 2 do not seem to be capable of existing in the cis form, the inability of 2 to pump protons indicates the necessity of cis/trans isomerization in the proton pumping process.

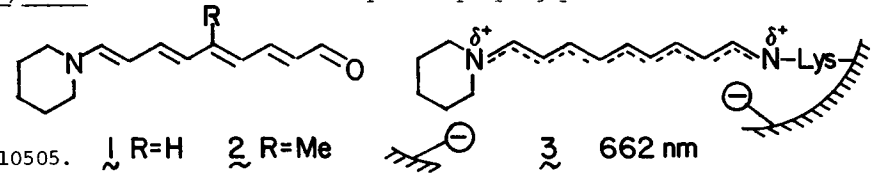

1 R=H 2 R=Me 3 662 nm

Supported by NSF Grant CHE81-10505.

M-AM-C6 AN ELECTRIC BIREFRINGENCE STUDY OF THE PURPLE MEMBRANE OF HALOBACTERIUM HALOBIUM.
Leo D. Kahn and Shu-I Tu. Eastern Regional Research Center, USDA, ARS, Philadelphia, PA 19118.

An electric birefringence study was carried out on aqueous suspensions of the purple membrane of Halobacterium halobium under various conditions of pH and ionic strength. The results indicate that purple membrane shows electric birefringence at a field strength as low as 1400 volts per cm. The permanent dipole moment and polarizability ranged from 20,500 debyes and 1.01 x 10^{-14} cm^3 for for a purple membrane concentration of 0.40 mg per ml to 40,000 debyes and 2.05 x 10^{-14} cm^3 for a concentration of 0.80 mg per ml. It was also found that removal of the retinyl group of bacteriorhodopsin substantially reduces the electric birefringence of the membrane. Solubilization of the membrane by Triton X-100, however, completely abolishes the electric birefringence. At low values of concentration and/or field strength the buildup curve shows a distinct anomaly. These experiments suggest that there are two types of interaction in purple membrane suspensions when placed in an electric field. One interaction is between bacteriorhodopsin molecules via their chromophore moieties. This builds up the permanent dipole moment and the polarizability of the membrane. The other interaction is a stacking of the particles following their alignment by the electric field, which is promoted by the induced dipole moment.

M-AM-C7 STRUCTURAL RELAXATION OF THE SCHIFF BASE BOND IN BACTERIORHODOPSIN'S PRIMARY PHOTOPRODUCT. Mark Braiman and Richard Mathies, Chemistry Dept., University of California, Berkeley, CA 94720.

We have obtained 60-nsec time-resolved resonance Raman spectra of bacteriorhodopsin's primary photoproduct K at room temperature. Two 25-nsec pulses are generated by cavity-dumping both an Ar^+ and a Kr^+ laser. The 514-nm photolysis pulse creates a quasi-steady-state mixture of BR_{570} and K. The delayed 647-nm probe pulse then selectively enhances the Raman scattering from K. Fluorescence excited by the photolysis pulse is eliminated by turning on the photon counting electronics only during the probe pulse. The red-probe resonance Raman spectrum of the 60-nsec room temperature species (K_{610}) is very similar to that of the primary photoproduct of BR_{570} trapped at 77°K (K_{625}). In particular, the configurationally sensitive fingerprint regions (1100-1300 cm^{-1}) of the two K species are identical, for both native and 15-deuterio (15-D) isotopic variants of the chromophore. Our 15-D "isotopic fingerprint" method thus demonstrates that the chromophore in K_{610} has a 13-*cis* configuration, as shown previously for K_{625} [Braiman and Mathies (1982) *P.N.A.S. 79,* 403]. The only major difference observed between the two K species is the shift of the C_{15}-H out-of-plane wag from 974 cm^{-1} in K_{625} to 987 cm^{-1} in K_{610}. The C_{15}-deuterium wag is also 10 cm^{-1} higher in K_{610} than in K_{625}, demonstrating that the force constant for this vibration is increased in K_{610} relative to K_{625}. These results suggest that there is a protein perturbation near the Schiff base bond in the 77°K frozen K_{625} species, which undergoes a relaxation within 60 nsec at room temperature. We are using a series of isotopic analogues to refine a vibrational force field for K_{625}, in order to determine the nature of this protein relaxation.

M-AM-C8 TOPOGRAPHY AND MOBILITY OF SPIN-LABELED CARBOXYL RESIDUES IN BACTERIORHODOPSIN. J. Herz R.J. Mehlhorn and L. Packer, Membrane Bioenergetics Group, Lawrence Berkeley Laboratory and the Department of Physiology-Anatomy, University of California, Berkeley, CA 94720.

Carboxyl groups on bacteriorhodopsin in purple membranes were covalently spin-labeled with Tempamine using N-(ethoxycarbonyl)-2-ethoxy-1,2-dihydroquinoline as a highly specific coupling agent. Spin-labeled bacteriorhodopsin (2 spins/mole) retained photocycling and proton pumping functions. Accessibility to paramagnetic broadening agents, $Fe(CN)_6^{-3}$ and Ni^{+2}, demonstrated the existence of two distinct spin populations in purple membranes: a high mobility surface group quenched at low concentrations of these agents, and buried immobilized groups whose ESR signal remained at high quencher concentration. Treatment with denaturing agents greatly increased the mobility and quenching of these buried residues. A series of stearic acid spin labels bound to purple membranes was used to define the depth of paramagnetic interactions. $Fe(CN)_6^{-3}$ interactions were limited to surfaces whereas Ni^{+2} and Cu^{+2} effects extended into hydrophobic domains. A double modification procedure in which surface groups were first blocked selectively spin-labeled only a buried carboxyl group having a strongly immobilized signal. Comparison of the quenching behavior of stearic acids with this double modified sample indicated that one carboxyl residue is buried about 20Å from the membrane surface. Cleavage of the carboxyl-terminal tail with trypsin increased the mobility of the spectrum, showing that this tail is moderately immobilized in the native structure. These data are consistent with bacteriorhodopsin models of tertiary structure which place carboxyls within hydrophobic domains of the protein-membrane matrix.

M-AM-C9 BROWNIAN DYNAMIC ANALYSIS OF ION MOVEMENT IN MEMBRANES. Kim Cooper, Eric Jakobsson, and Peter Wolynes, Department of Physiology and Biophysics, Program in Bioengineering, and Department of Chemistry, University of Illinois, Urbana, Illinois 61801.

It has been known since the work of Einstein in 1905-8 that the microscopic basis of all processes involving thermal motion of dissolved or suspended particles is Brownian motion. The widespread availability of digital computers has made it practical to apply Brownian dynamics to many-particle problems, such as ion permeation in membranes. This method treats the system in more detail and with fewer approximations than either bulk diffusion theory or absolute rate theory. We have used Brownian dynamics to consider the problem of single-file ion movement through membrane channels. We find that constant-field electrodiffusion results are reproduced to good accuracy when the electrostatic repulsion term between ions is turned off (obviously impossible experimentally). When the electrostatic repulsion term is turned on, we find the results to be different from the corresponding electrodiffusion calculation (simultaneous solution of the Nernst-Planck and Poisson equations). The apparent reason for this discrepancy is that electrodiffusion theory treats the charges as "smeared-out" spatial distributions with each element of the distribution repelling each other element. In the Brownian dynamic theory with reasonable parameters, there is only one ion in the channel a large fraction of the time. Since this ion does not repel itself, its behavior as it moves about in the channel does not correspond to that of the distributed charge described in electrodiffusion theory.

Support was received from the Bioengineering Program and the Research Board of the University of Illinois at Urbana-Champaign.

M-AM-C10 TEMPERATURE DEPENDENCE OF LIGHT-INDUCED PROTON MOVEMENT IN RECONSTITUTED PURPLE MEMBRANE Shu-I Tu and Howard Hutchinson. Eastern Regional Research Center, USDA, ARS, Philadelphia, PA 19118.

Bacteriorhodopsin was incorporated into egg yolk phosphatidyl choline (PC) vesicles which also contained different amounts of other lipids. Under the condition of nullified membrane potential, light-induced proton movement seemed to follow a kinetic scheme which assumed the existence of a proton pumping inhibition process characterized by a rate constant, k_L. In the temperature range of 5-30°C, both k_L and the proton leak rate constant (k_D) obeyed a simple Arrhenius equation. The presence of cholesterol in the membrane phase caused a significant increase of activation energy (E_a) for both rate constants. When phosphatidic acid was also present in the membrane, only the E_a associated with k_D increased. The initial proton pumping rate (R_o) of purple membrane vesicles reconstituted with PC showed a bell-shaped temperature dependence with a maximum at ∿20°C. The addition of cholesterol to the above system abolished this dependence; i.e., R_o increased as the temperature was raised, but did not reach a maximum within the experimental conditions used. These results suggest that the molecular origin of the process that inhibits proton pumping is different from that of R_o or k_D. The data also indicate that a membrane with low fluidity and negatively-charged surfaces enhances the pumping efficiency of bacteriorhodopsin in reconstituted vesicles.

M-AM-C11 BIOENERGETIC CHARACTERIZATION OF A BACTERIORHODOPSIN-OVERPRODUCING HALOBACTERIUM HALOBIUM STRAIN. S.L. Helgerson, H. Jurgen Weber and W. Stoeckenius, CVRI and Dept. of Biochemistry and Biophysics, UCSF, San Francisco, CA 94143.

Bacteriorhodopsin (bR) is an electrogenic proton pump which generates a protonmotive force (pmf) and drives photophosphorylation in H. halobium cells. Thus, bR-driven energetic systems can serve as models for studying proton-dependent energy coupling mechanisms. However, the contribution of other electrogenic ion pumps (i.e., the respiratory chain and halorhodopsin) must be systematically excluded. bR and halorhodopsin have similar absorption spectra with maxima near 570nm and 580nm, respectively. H. halobium strain JW-3 is an overproducer with approximately 500,000 bR molecules per cell. A daughter strain, JW-1, has been isolated which lacks bR but has halorhodopsin. Both strains exhibit oxidative phosphorylation driven with O_2 + glycerol and substrate level phosphorylation driven with L-arginine. In the dark under nitrogen both strains maintain a pmf of -125 to -175mV with similar values of $\Delta\Psi$ and ΔpH for external pH 5.5-7.5. Under nitrogen JW-3 shows illumination-dependent ATP synthesis and an increase in pmf (both $\Delta\Psi$ and ΔpH) while JW-1 lacks all of these functions. The presence of an electrogenic halorhodopsin in JW-1 can be demonstrated. The internal pH decreases and ΔpH collapses when JW-1 is illuminated in the presence of 10μM carbonyl cyanide-m-chlorophenyl hydrazone (CCCP). This light-mediated collapse of ΔpH does not occur in JW-3 with CCCP present or in JW-1 without CCCP. These results indicate that using JW-3 experimental conditions can be devised to study energy coupling mechanisms with protons pumped and pmf generated exclusively by bR. (Supported by NIH Program Project Grant GM-27057 and NIH Grant 28767.)

M-AM-C12 TIME RESOLVED X-RAY DIFFRACTION STUDIES OF PURPLE MEMBRANE FROM HALOBACTERIUM HALOBIUM* R. D. Frankel and J. M. Forsyth, Intr. by Bernard K. Fung, Laboratory for Laser Energetics, University of Rochester, Rochester, NY 14623

Single shot, nanosecond exposure x-ray diffraction patterns to 7Å resolution have been obtained on unstimulated and light stimulated stacked isolated Halobacterium halobium purple membrane fragments using a laser plasma x-ray source. The x-ray wavelength was 4.45Å and the samples were approximately 40μm thick. Patterns were recorded on an intensifier aided two dimensional TV system. The samples were placed directly in the evacuated chamber which houses the x-ray diffraction camera. Diffraction patterns from light stimulated specimens were acquired at times after stimulation which varied from 200 microseconds to 40 minutes. At one millisecond delay and longer, major changes are observed in the 9-14Å region of the patterns. Under some conditions, major, reversible lattice alterations are observed. Similar alterations have been observed in earlier, low resolution studies on hydrated samples.

*Work supported, in part, by the National Institutes of Health, the National Science Foundation, and the Laboratory for Laser Energetics.

M-AM-D1 MULTIPLE PHASES OF EP DECOMPOSITION ARE ASCRIBABLE TO KINETICALLY NON-EQUIVALENT SUBUNITS OF SARCOPLASMIC RETICULUM CA ATPASE. Noriaki Ikemoto and Ralph W. Nelson. Department of Muscle Research, Boston Biomedical Research Institute, and Department of Neurology, Harvard Medical School, Boston, MA. 02114

Our recent studies suggest that one of the subunits (E_I) of the sarcoplasmic reticulum Ca^{2+} ATPase is one step ahead of the other (E_{II}) in carrying out several sequential reaction steps, such as EP formation, translocation of enzyme bound Ca across the membrane and release of the translocated Ca^{2+} to the intravesicular lumen. The time courses of EP decomposition were investigated by chasing $E^{32}P$ formation with EGTA and cold ATP at various times of $E^{32}P$ formation. If chasing occurs at 10 ms, at which time only E_I has formed $E^{32}P$, EP decomposes rapidly in a monophasic fashion (scheme 1). Furthermore, simultaneous addition of EGTA and [γ-^{32}P] ATP to the SR that has bound Ca (the conditions in which only E_I can form $E^{32}P$) produces rapid and monophasic EP decomposition (scheme 1). Upon chasing after both E_I and E_{II} have formed $E^{32}P$, EP decomposition takes place in two phases, rapid and slow (scheme 2). These results suggest that rapid and slow phases of EP decomposition are ascribable to the sequential Pi liberation from different subunits, E_I and E_{II}, respectively.

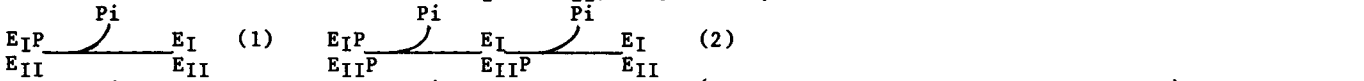

(Supported by grants from NIH and MDA).

M-AM-D2 IDENTIFICATION AND LOCALIZATION OF THE NUCLEOTIDE BINDING REGION OF THE CA - ATPASE OF SARCOPLASMIC RETICULUM T. Scott and N. Ikemoto, Dept. of Muscle Research, Boston Biomedical Research Institute and Dept. of Neurology, Harvard Med. School, Boston, MA 02114.

Initial attempts have been made to map the structure of the nucleotide binding site(s) of the SR Ca-ATPase and to determine its relation to the site of phosphorylation. To label the purine binding region of the enzyme, 8- azido ATP (AzATP), which has been shown to be a substrate of the ATPase (Cell Calcium,1:205,1980), has been used. Low (< 5 μM) concentrations of AzATP have been used in order to label only high affinity nucleotide sites. Upon photoactivated covalent labeling of the ATPase with ^{32}P-AzATP in the presence of Ca^{2+} and subsequent digestion of the protein with trypsin, the label appears in the A (~55K) fragment and its A1 (~30K) subfragment. This is consistent with the localization of the site of phosphorylation in the A and A1 fragments. Labeling with AzATP in the absence of Ca suggests that AzATP is incorporated into regions of the polypeptide other than the A-A1 fragments under these conditions. Using digestion of the tryptic fragments with S. Aureus V8 protease and a two-dimensional gel mapping technique, our preliminary findings indicate that the AzATP-labeled purine site can be further localized within a peptide of < 15K daltons which is derived from the A1 fragment. We are presently attempting to align the labeled peptides within the primary sequence of the ATPase and to determine their relation to the ATP-regulatory and the phosphorylation sites. (supported by grants from NIH and MDA).

M-AM-D3 ADP-REACTIVE PHOSPHOENZYMES (EP) IN SKELETAL AND CARDIAC SARCOPLASMIC RETICULUM (SR) CALCIUM ATPase REACTION. Taitzer Wang, Jun Nakamura, and Arnold Schwartz. Department of Pharmacology and Cell Biophysics, University of Cincinnati College of Medicine, Cincinnati, Ohio 45267

It is known that skeletal muscle utilizes the Ca^{2+} released from the sarcoplasmic reticulum (SR) for contraction; whereas, cardiac muscle depends upon extracellular Ca^{2+}. In muscle cells, the principal physiological function of the SR Ca^{2+}-ATPase is its active transport of cytoplasmic Ca^{2+} across SR membranes that brings about muscle relaxation. The Ca^{2+} released from SR through the reverse pathway of the Ca^{2+}-ATPase reaction may contribute only a small fraction to the total Ca^{2+} required for muscle contraction. Nonetheless, we have observed that, in the reverse reaction, the EP derived from skeletal SR interact with ADP in the presence of K^+ at a greater rate than cardiac EP. In the early phase of ATP hydrolysis the EP in the skeletal SR may be composed of three dominant conformers existing in equilibrium: $E_1'P$ $E_1''P$ E_2P. The $E_1'P$ and $E_1''P$ are ADP-sensitive. The overall ADP-enhanced EP decomposition is possible due to (1) rapid dephosphorylation of ADP·$E_1''P$ complex, (2) the transformation of ADP·$E_1''P$ to the highly-labile ADP·$E_1'P$, and (3) the influence of ADP favoring the transformation of E_2P to ADP·$E_1''P$ via E_1P in the reverse reaction. Dephosphorylation of ADP·$E_1'P$ is extremely fast, and the transformation of ADP·E_1P to ADP·$E_1'P$ is rapid but measurable. The E_2P is also kinetically identifiable, which, in line with widely published results, is likely to be ADP-insensitive. When ADP is present in less than saturating amount, the kinetics of EP decomposition is greatly complicated by the existence of unaltered $E_1'P$ and $E_1''P$. In cardiac SR, the unmeasurable dephosphorylation of ADP·$E_1'P$ is similarly observed, but the decomposition of the remaining EP is not enhanced by ADP and K^+. (Supported by NIH PO1 HL22619 IVA-05)

M-AM-D4 THE EFFECT OF CAMP-DEPENDENT PHOSPHORYLATION ON CA^{2+} AFFINITY OF CARDIAC SARCOPLASMIC RETICULUM. Mandel, F., Kranias, E.G., and Schwartz, A. Department of Pharmacology and Cell Biophysics, University of Cincinnati College of Medicine, Cincinnati, Ohio 45267.

Canine cardiac sarcoplasmic reticulum (SR) is known to be phosphorylated by adenosine 3',5', monophosphate (cAMP) dependent protein kinase on a 22,000-dalton protein. Phosphorylation is associated with an increase in both the initial rate of Ca^{2+} uptake and the Ca^{2+}-ATPase activity which is partially due to an increase in the affinity of the Ca^{2+}-Mg^{2+}-ATPase (E) of sarcoplasmic reticulum for calcium. We have examined the effect of cAMP-dependent protein kinase phosphorylation on the binding of calcium to the SR and on the dissociation of calcium from the SR. The rate of dissociation of the $E \cdot Ca_2$ was measured directly and was not found to be significantly altered by cAMP-dependent protein kinase phosphorylation. Since the affinity of the enzyme for Ca^{2+} is equal to the ratio of the on and off rates of calcium, these results demonstrate that the observed change in affinity must be due to an increase in the rate of calcium binding to the Ca^{2+}-Mg^{2+}-ATPase of SR. In addition, an increase in the degree of positive cooperativity between the two calcium binding sites was associated with protein kinase phosphorylation. (Supported by NIH grants HL26049 (FM), HL26057 (EGK), HL22619 (AS), and by Research Career Development Awards HL00789 (FM) and HL00775 (EGK).)

M-AM-D5 CONFORMATIONAL STATES OF SKELETAL SARCOPLASMIC RETICULUM AS DETECTED BY MalANS. THE EFFECT OF CATIONS AND NUCLEOTIDES ON THE SULFHYDRYL GROUP REACTIVITY. Frederic Mandel*, Sharmila Gupte#, and Arnold Schwartz*. *Department of Pharmacology and Cell Biophysics, University of Cincinnati College of Medicine, Cincinnati, Ohio 45267 and #Department of Anatomy, University of North Carolina, Chapel Hill, North Carolina 27514.

The fluorescent sulfhydryl probe 2-(4'-maleimidylanilino) naphthalene 6-sulfonic acid, MalANS, reacts covalently with the sulfhydryl groups of the Ca^{2+}-Mg^{2+}-ATPase of the SR. Control gel electrophoresis studies have shown that the probe reacts almost exclusively (>95%) with the Ca^{2+}, Mg^{2+}-ATPase and not with the other SR proteins. Both the rate and the magnitude of the reaction were monitored by the increase in the fluorescence intensity of the covalently bound probe. The rates of probe binding to the Ca^{2+}-Mg^{2+}-ATPase of SR were examined as a function of Ca^{2+},Mg^{2+},Na^{+}, K^{+},ATP and ADP concentrations. The control that was used consisted of 250 µg of SR in a solution containing 20 mM Tris-Maleate (pH 6.8), 150 µM EGTA and 50 µM EDTA. With the sole exception of large concentrations of lipophilic agents such as the N-acylethanolamines, the addition of ligands resulted in a protective effect (decrease in the rate of probe binding) which could be titrated versus the free concentration of ligand. This result is in contrast with the Na^{+}-K^{+}-ATPase where the presence of Mg and Ca^{2+} caused a 3-fold increase in the rates of probe binding and with the cardiac SR where Mg (but not Ca^{2+}) also increased the probe binding rate. This research was supported by NIH grant HL26049 (FM) and by a Research Career Development Award, HL00789, to F.M.

M-AM-D6 LIPID METABOLITE INDUCED CONFORMATIONAL CHANGES IN SKELETAL SARCOPLASMIC RETICULUM CA^{2+}-ATPase. DETECTION USING A COVALENT-BOUND SULFHYDRYL SPECIFIC FLUORESCENT PROBE. D.E. Epps, F. Mandel, and A. Schwartz. University of Cincinnati College of Medicine, Department of Pharmacology and Cell Biophysics, Cincinnati, Ohio 45267.

The sulfhydryl specific fluorescent probe 2-(4'-maleimidylanilino) naphthalene -6-sulfonic acid (MalANS) was used to study conformational changes in sarcoplasmic reticulum (SR) Ca^{2+}-ATPase induced by lipid metabolites. N-oleylethanolamine (NOE) and palmitylcarnitine (PCarn), two lipid metabolites which accumulate during myocardial ischemia and infarction, were found earlier to have biphasic effects on both the Ca^{2+} transport and ATPase activity of the SR. In the present study, we detected 3 classes of ATPase SH groups (characterized by their availability to bind MalANS) by semilogarithmic plots of MalANS fluorescence after equilibrium binding. NOE and PCarn at low concentrations (10 and 6 nmoles/mg SR, respectively) protected all 3 classes of SH groups from binding to the probe. The apparent rate constants for MalANS binding were also decreased. High concentrations of NOE and PCarn (1000 and 600 nmoles/mg SR) greatly enhanced MalANS binding to free SH groups with a concomitant increase in the apparent rate constants. The results suggest that concentrations of NOE and PCarn which stimulate skeletal SR Ca^{2+} transport produce a conformational state in which free SH groups of the ATPase are more shielded, whereas, inhibitory metabolite concentrations expose more SH groups to the external environment. These effects may be due to a direct effect on the ATPase or an indirect effect transmitted through the microenvironment of the annular lipid. This research was supported by NIH grant HL26049 (FM), a grant from the American Heart Association (DE) with funds contributed in part by the Southwestern Ohio Chapter, a Research Development Award, HL 00789 (FM) and a New Investigator Research Award, HL28902 (DE).

M-AM-D7 MEMBRANE CRYSTALS OF THE Ca^{2+} TRANSPORT ATPase IN SARCOPLASMIC RETICULUM. Laszlo Dux and Anthony Martonosi. Dept. of Biochemistry, SUNY Upstate Medical Center, Syracuse, New York 13210.

Two-dimensional arrays of protein crystals were observed in sarcoplasmic reticulum membranes and purified Ca^{2+} transport ATPase vesicles after treatment with 5 mM Na_3VO_4 in 0.1 mM KCl, 10 mM imidazole pH 7.4, 5 mM $MgCl_2$ and 0.5 mM EGTA, at 2°C. The crystalline arrays were best visualized by negative staining with 1% uranylacetate (pH 4.3); 1% K-phosphotungstate (pH 4.3 or 7.0) gave a similar but slightly disorganized crystal pattern. The dimensions of the crystal lattice in sarcoplasmic reticulum membranes and purified ATPase vesicles are similar, supporting the involvement of the Ca^{2+}-ATPase. Vanadate probably promotes crystallization of the ATPase by stabilization of the E_2 conformation, as reflected by inhibition of ATPase activity. The formation of protein crystals was prevented by 0.05 - 1 mM Ca^{2+}; addition of Ca^{2+} to preformed crystals caused the "cracking" and disappearance of the lattice. These observations are consistent with the protection afforded by Ca^{2+} against inhibition of ATPase activity by vanadate. The crystalline arrays are usually located on the surface of elongated cylinder-shaped vesicles of 500-700 A° diameter, with lattice lines oriented at approximately 45° to the long axis. The crystalline cylinders usually emerge from spherical vesicles with random particle distribution on their surface, suggesting that crystallization of the Ca^{2+}-ATPase imparts the cylindrical shape upon the membrane. Frequently rows of negatively stained particles are arranged in pairs forming ladder-like structures, which are separated from neighboring pairs by wider bands of negative stain. The unit cell dimensions are consistent with Ca^{2+} ATPase tetramers. These observations open a new approach for the analysis of the structure of Ca^{2+} ATPase in its natural environment. (Supported by the NIH and Muscular Dystrophy Association)

M-AM-D8 STRUCTURAL STUDY OF SARCOPLASMIC RETICULUM MEMBRANES FROM MOLLUSCAN MUSCLE. Peter Hardwicke and Loriana Castellani, Department of Biology and Rosenstiel Center, Brandeis University, Waltham, MA 02254.

A membrane preparation from scallop adductor muscles has been identified as sarcoplasmic reticulum (SR) on the basis of an oligomycin-insensitive Ca^{2+}-ATPase activity and an ATP-dependent Ca^{2+} uptake. The major polypeptide component has a mobility on SDS-polyacrylamide gels similar to that of Ca^{2+}-ATPase of rabbit SR. Negatively stained preparations of these membranes show a variety of highly ordered forms in the electron microscope, the most common being tubular structures. These sometimes branch and often originate in sacs or cisternae. A regular striation pattern, with a repeat of 10.5 nm, runs diagonally across these structures. Within each period rows of subunits may be distinguished whose size is comparable to that of the projections observed on the surface of negatively stained rabbit SR. Superimposition of top and bottom layers in collapsed tubes yields a characteristic diamond-type net, whose optical diffraction pattern shows two sets of reflections that can be assigned to the two surfaces. When the membranes are unidirectionally shadowed with platinum, only the top surface is seen, confirming this interpretation. A determination of the detailed structure of these membranes may provide an insight into the possible role of Ca^{2+}-ATPase oligomers in the pumping mechanism.

Supported by grants from NSF, NIH, MDA and by a Fellowship from MDA to L.C.

M-AM-D9 CA-DEPENDENT ALTERATION OF THE SECOND CLEAVAGE SITE OF THE CA ATPASE OF SARCOPLASMIC RETICULUM. Zoltan Marcsek, Ralph W. Nelson, Mario S. Rosemblatt and Noriaki Ikemoto. Department of Muscle Research, Boston Biomedical Research Institute, and Department of Neurology, Harvard Medical School, Boston, MA. 02114

It is generally accepted that limited tryptic digestion of the sarcoplasmic reticulum Ca^{2+} ATPase produces fragments A and B by the first cleavage, and subfragments A_1 and A_2 by the second cleavage.

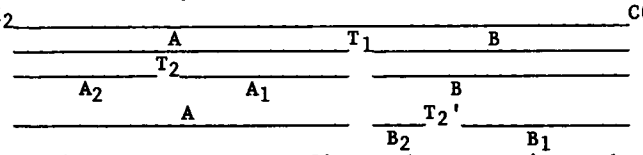

We have found that the second cleavage site, but not the first cleavage site, changes as a function of $[Ca^{2+}]$ and $[Mg^{2+}]$. In the presence of several μM Ca^{2+} with or without added Mg^{2+}, the second tryptic cleavage occurs at site T_2 as reported in the literature. In the absence of both Ca^{2+} and Mg^{2+}, however, second cleavage occurs in fragment B, producing two new types of subfragments which are designated as subfragment B_1 and B_2. Upon increase of $[Mg^{2+}]$ to 3 mM in the absence of Ca^{2+}, the site of second cleavage is switched from site T_2' to site T_2. These results suggest that conformational changes of the Ca^{2+} ATPase molecule induced by $\sim$ μM Ca^{2+} or by $\sim$ mM Mg^{2+} involve drastic changes in the susceptibility to trypsin of at least two domains represented by T_2 and T_2'. (Supported by grants from NIH and MDA).

M-AM-D10 AFFINITY LABELING OF CANINE CARDIAC SARCOPLASMIC RETICULUM CALMODULIN-BINDING COMPONENTS. Charles F. Louis and Bruce Jarvis. Department of Veterinary Biology, University of Minnesota, St. Paul, MN 55108

To determine the mechanism by which calmodulin promotes the phosphorylation of the M_r=23,000 cardiac sarcoplasmic reticulum (SR) protein phospholamban, SR (1 mg/ml) has been affinity labeled with ^{125}I-calmodulin using dithiobis(succinimidyl propionate) (DSP) in 20 mM HEPES (pH 7.0) at 20°C. Electrophoretic analysis in SDS demonstrated a ^{125}I-containing major product of M_r=40,000, and a minor component of M_r=120,000; formation of these components was maximal at Mg^{2+} and Ca^{2+} concentrations that maximally activated the calmodulin-dependent phosphorylation of SR. The M_r= 120,000 component probably represents a 1:1 complex between the M_r=100,000 Ca-ATPase and ^{125}I-calmodulin. The M_r=40,000 component dissociated to form M_r=26,000 and 28,000 components when SDS-solubilized samples were boiled; storage of these boiled samples for 1 week at -70°C resulted in the reassociation of the M_r=40,000 component. That phospholamban, phosphorylated in the presence of calmodulin + ^{32}P-ATP, could be dissociated and reassociated in a similar fashion indicated that the ^{125}I-labeled M_r=40,000 component represented a 1:1 complex between phospholamban and ^{125}I-calmodulin. This was confirmed in an experiment where a M_r=40,000 ^{32}P-containing component was formed when DSP was added to SR that had been phosphorylated in the presence of [γ-^{32}]ATP and calmodulin. We propose that phospholamban is the endogenous receptor for calmodulin in cardiac SR membranes. However, because of its small size, and unusual dissociation properties, it seems unlikely that phospholamban is the endogenous calmodulin-dependent protein kinase in this membrane. (Supported by N.I.H. HL-25880 and American Heart Association Minnesota Affiliate.)

M-AM-D11 ASSOCIATION OF PHOSPHOLAMBAN WITH A HIGHLY PURIFIED CA^{2+}-ATPase PREPARATION FROM CARDIAC SARCOPLASMIC RETICULUM. E.G. Kranias, J. Nakamura and A. Schwartz. Department of Pharmacology and Cell Biophysics, University of Cincinnati College of Medicine, Cincinnati, Ohio 45267.

Canine cardiac sarcoplasmic reticulum vesicles (SR) are phosphorylated by cAMP-dependent and by Ca^{2+}-calmodulin-dependent protein kinases on a 22,000 dalton protein, called phospholamban. Both types of phosphorylation are associated with an increase in the initial rate of Ca^{2+} transport. Therefore, phospholamban appears to be a regulator for the calcium pump in cardiac sarcoplasmic reticulum. However, there is conflicting evidence as to the degree of association of the Ca^{2+}-ATPase with its regulator, phospholamban. We have recently developed a simple procedure for purification of the Ca^{2+}-ATPase from cardiac SR using Triton X-100. The presence of $CaCl_2$ (20 mM) and ATP (5 mM) in the solubilization solution was necessary in order to maintain the high activity of the final purified Ca^{2+}-ATPase. The isolated Ca^{2+}-ATPase was phosphorylated on an 11,000 M_r protein but $^{32}P_i$-incorporation was much lower than in SR (32 pmol Pi/mg ATPase vs. 1,500 pmol Pi/mg SR). Solubilization of the Ca^{2+}-ATPase in the presence of [γ-^{32}P]ATP indicated that phospholamban was extracted from the membranes in the same fraction as the Ca^{2+}-ATPase but dissociated from the Ca^{2+} pump during subsequent purification steps. Our isolation procedure results in an increase of 5-8 fold in the specific activity of the Ca^{2+}-ATPase but a decrease of over 3 fold in the specific activity of $^{32}P_i$ incorporation (pmol Pi/mg) present as phosphoester bonds. These data suggest that phospholamban is not tightly associated with the Ca^{2+}-ATPase in cardiac SR. (Supported by NIH grants HL26057, HL00775 and HL22619).

M-AM-E1 RHEOLOGIC PROPERTIES OF F ACTIN. K.S. Zaner and T.P. Stossel (Intr. by Richard Niederman) Dept. of Hematology and Oncology , Mass. Gen. Hosp., Boston Ma.

We have measure the viscoelastic properties of F-actin and F-actin in the presence of Actin Binding protein (ABP) an actin crosslinking protein derived from rabbit pulmonary macrophages. The time dependent compliance of 1 mg/ml F-actin does not demonstrate an equilibrium value but rather continues to rise over the period of the measurement. The fact that the compliance remains the same when the stress is varied over a four-fold range and that the rising compliance was evident at strains of <5% is strongly suggestive that this finding is not due to the breaking of filaments or of any interfilament bonds. The filament lengths were varied by the addition of Ca-gelsolin complex and measured by the gel-pount method. It was found that the complex dynamic viscosity, $|\eta^*|$, showed a -.8 power dependence on frequency for all concnetrations and lengths measured. From this data it was determined that at any particular frequency, $|\eta^*| \propto cL_w^{7}$. These results are quite close to those predicted by a recent formulation of the rheologic properties of stiff rods in solution, based on the fact that long thin rods in concentrated solutions will severely impede each others' rotary diffusion. This suggests that the flow properties of F-actin are mainly due to the diffusional constraints on the rods , and does not require the postulation of interfilament "bonds". In contrast, the introduction of ABP at a ratio of 1:500 greatly decreases the compliance and causes the appearance of a plateau modulus. This suggests that ABP is causing stable crosslinkages between actin filaments drastically reducing the rotary diffusion constant, and probably causing a gelled state.

(This work supported by NHLBI grant No. K08 HL00912-1)

M-AM-E2 CILIARY MEMBRANE RECONSTITUTION: MEMBRANE TUBULIN-LIPID INTERACTION. R. E. Stephens, Marine Biological Laboratory, Woods Hole, Massachusetts 02543.

Scallop gill ciliary membranes contain a hydrophobic tubulin dimer (>60%) and numerous minor proteins. These may be solubilized by the nonionic detergents Nonidet P-40 or octyl β-D-glucoside. When the detergents are removed by adsorption or dialysis, respectively, the proteins remain soluble as mixed micelles of low sedimentation rate. When the solution is concentrated or frozen and thawed, unilamellar vesicles form. With Nonidet solubilization in low ionic strength Tris at pH 8, isopycnic centrifugation of the vesicles reveals a single, monodisperse band (d = 1.167 g/cc) with lipid and protein compositions nearly identical to those of the original membrane. Reconstitution is independent of divalent cation or nucleotide at millimolar levels. If solubilized with Nonidet in 0.1 M MES at pH 6.4 (or octyl glucoside, pH 8), a monodisperse major band of lower density (1.146 g/cc) and heterodisperse bands of much lower density are obtained upon freeze-thawing; an 8-fold excess of elasmobranch brain tubulin does not incorporate into the vesicles. Using a 0.1 M MES microtubule polymerization buffer, vesicles rather than microtubules form when the detergent-free solution is warmed. When brain tubulin is included, it forms microtubules but does not incorporate into the membrane tubulin-containing vesicles. Conversely, membrane tubulin does not incorporate into brain microtubules when the polymerization is carried out in either the presence or absence of detergent. Addition of the tubulin-binding drug Taxol to the extract induces protein-depleted vesicles, not microtubules. These data suggest that membrane tubulin forms a stable mixed micelle with lipids, enabling it to "sort out" from soluble brain tubulin and incorporate directly into membranes. Support: NIH Grants GM 20644 and 29503.

M-AM-E3 COMPARISON OF THE MECHANISM OF ACTION ON ACTIN FILAMENT ASSEMBLY OF THE SERUM PROTEINS BREVIN AND VITAMIN D BINDING PROTEIN. A. Lees, J.G. Haddad* and S. Lin, Dept. of Biophysics, Johns Hopkins U., Balto., MD 21218, and the U. of Penn., School of Medicine, Phila., PA 19104.

We have found that two serum actin-binding proteins, 90Kd brevin and 58Kd vitamin D binding protein (DBP), interact with actin by distinctly different mechanisms. Polymerization curves determined viscometrically with a brevin:actin ratio of 1:250 were hyperbolic, whereas control curves were sigmoidal, indicating that brevin nucleates filament assembly. Under the same conditions, DBP accentuated the lag phase of the sigmoidal curve, suggesting an inhibition of nucleation. Brevin, at a ratio of 1:120 actins, blocked barbed end filament elongation nucleated by red cell spectrin-4.1-actin complex in 0.4 mM $MgCl_2$. Pyrene-labeled actin was used to quantitate polymerization in the presence of DBP. Unlike brevin, it took nearly an equimolar quantity of DBP to completely inhibit nucleated polymerization. Even high brevin:actin ratios only slightly increased the critical concentration of actin, whereas DBP caused a nearly stoichiometric release of G-actin from filaments as measured with the pyrene-actin probe in 2 mM $MgCl_2$. Actin polymerized in the presence of brevin had an increased number of filament ends as measured by [^{3}H]cytochalasin B binding. At a brevin:actin ratio of 1:20, cytochalasin binding increased 8x. This study supports the notion that brevin binds to the barbed end of the actin filament and that DBP acts by sequestering monomers. Assuming that DBP binds G-actin 1:1 and does not bind F-actin, the increase in the critical concentration as a function of DBP added indicated a K_D of = 5 x 10^{-8} M in 2 mM $MgCl_2$. Since both brevin and DBP are found in high concentrations in human serum, their combined actions should rapidly remove actin filaments from the blood. Supported by Grants GM22289, AM28292, and ACS-CD73.

M-AM-E4 TWO DIFFERENT ACTIN BINDING PROTEINS FROM DICTYOSTELIUM AMOEBAE HAVE OPPOSITE EFFECTS ON THE INTERACTION BETWEEN ACTIN AND MYOSIN FILAMENTS. J. Condeelis and M. Vahey, Albert Einstein College of Medicine, Department of Anatomy, Bronx, New York.

We have characterized the properties of two actin binding proteins called 120K and 95K. Both are homodimers with native molecular weights of 267,000 and 217,000, respectively. The 95K protein is very similar in subunit and amino acid composition, strokes radius, S20,w, native molecular weight, appearance in rotary shadowing, f/fo and D20,w to α-actinin from rabbit muscle. The 120K protein differs in these properties from both 95K and α-actinin. Like non-muscle α-actinins, the interaction between 95K and F actin is inhibited by Ca^{++} while that between 120K and F actin is not. The 120K protein cross-links actin to form meshworks composed of branched microfilaments. The 95K cross-links actin to form filament bundles. To determine the physiological consequences of these two different geometries on the ability of actin to interact with myosin, complexes of 95K or 120K were made with F actin in the absence of Ca^{++}. Myosin thick filaments and ATP were then added and the rate of superprecipitation of the actomyosin complex was measured as the rate of liberation of inorganic phosphate. The 120K-actomyosin complex exhibited less than half of the activity of actomyosin alone while the 95K-actomyosin complex showed 2-3 fold greater activity. However, the 95K induced stimulation was increased to over 10-fold if micromolar Ca^{++} was added with the ATP. This presumably results from Ca^{++} induced release of 95K cross-links between actin filaments which would inhibit sliding between actin and myosin filaments during superprecipitation.

Supported by GM 25813 and the Rita Allen Foundation.

M-AM-E5 ROLE OF ACTIN BINDING PROTEIN PHOSPHORYLATION AND THE STATE OF ACTIN IN PLATELET CYTOSKELETAL STRUCTURE. Alfred Stracher, Qing-Qi Zhuang*and John Lawrence* SUNY Downstate Medical Center, Brooklyn, N.Y. 11203.

We have recently isolated the platelet cytoskeleton (S. Rosenberg, R. Lucas and A. Stracher, J. Cell. Biol. 91, 201 (1981) and have shown it to be comprised of three proteins, actin binding protein (ABP), α-actinin and F-actin. We have purified these three proteins and have demonstrated that they are capable of recombining, in vitro, to form a structure resembling that in vivo. Preliminary investigations from our laboratory had suggested that reformation of the cytoskeleton necessitated that ABP be in the phosphorylated state and that actin be in the F-form. This requirement dictated that if, as we believe, the cytoskeleton is a pre-existing structure then ABP must exist as a phosphoprotein and F-actin must be the predominant form in the "resting platelet". Using a malachite green micro assay for P_i we have been able to determine that ABP isolated from the cytoskeleton of either gel filtered or centrifuged platelets contained 3.96 ± 0.4 moles Pi/mole ABP. All of the P_i could be accounted for as phosphoserine by amino acid analysis (4.61 ± 0.4 moles PS/mole ABP). Removal of 1.78 ± 0.2 moles Pi/mole ABP by E. Coli Alk. Phosphatase resulted in the inability of ABP to cross link F-actin into a low speed sedimentable complex as well as an apparent loss of its ability to bind to an F-actin affinity column. These results and the rapid, near quantitative isolation of the cytoskeleton upon the addition of 1% Triton-10mM EGTA, as originally described by us, reaffirm our earlier contention that ABP exists in situ as a phosphoprotein crosslinking the existing F-actin into a cytoskeletal network.

(Supported by HHS grant HL 14020).

M–AM-E6 ACTIN SPECIES IN EQUILIBRIUM WITH ASSEMBLED FILAMENTS: NANOSECOND EMISSION ANISOTROPY STUDIES. J.D. Pardee, J. Reidler, L. Stryer, and J.A. Spudich. Department of Structural Biology, Stanford University School of Medicine, Stanford, CA 94305.

After assembly of actin is complete, a small amount of non-filamentous actin called the critical actin concentration (C_A) remains in equilibrium with actin filaments. We have determined the size of the C_A actin by nanosecond fluorescence polarization spectroscopy. Highly purified skeletal muscle actin was covalently labeled with the fluorescent probe 5-(iodoacetamidoethyl) aminonaphthalene-1-sulfonic acid (IAENS) and assembled. Nanosecond anisotropy correlation times (ϕ_1, ϕ_2) were obtained on solutions of unassembled actin, filamentous actin, and the C_A actin separated from filaments by centrifugation. A correlation time of 20 nsec was obtained for unassembled actin compared to >500 nsec for filaments. However, correlation times for the C_A actin was highly dependent on the ionic species used for polymerization. Values of ϕ_2 were 21 nsec when actin was assembled with 0.1 M KCl + 1 mM $CaCl_2$, 42 nsec for assembly by KCl alone, and 90 nsec for assembly by 0.1 M KCl + 1 mM $MgCl_2$. A comparison of these correlation times to those for proteins of known molecular weight indicate that the actin in equilibrium with filaments after assembly is monomeric in 0.1 M KCl + 1 mM $CaCl_2$, dimeric in 0.1 M KCl alone, and tetrameric in 0.1 M KCl + 1 mM $MgCl_2$. The data suggest that in the presence of physiological concentrations of K^+ and Mg^{2+}, the species in equilibrium with F(ADP)-actin filaments are actin tetramers. Combined fluorescence and ATPase studies suggest that actin assembly is divided into two distinct stages of assembly and steady-state with unique actin species associated with each stage. NIH GM-25240 to J.A.S.; NIH Fellowship to J.D.P.; NIH GM-24032 to L.S.

M-AM-E7 DIRECT MEASUREMENT OF ACTIN FILAMENT CRITICAL CONCENTRATIONS. E.M. Bonder, D.J. Fishkind, and M.S. Mooseker, Biology Depts., Yale Univ., New Haven, Ct. 06511 and Univ. of Penn., Phila., Pa. 19104. (Intro. by Robert M. Macnab)

Previously, we had established use of the acrosomal process fragments from Limulus sperm for examining actin filament assembly and structure. The fragments are particularly advantageous for such studies because they nucleate large numbers of both barbed and pointed end filaments. In addition, the morphology of the fragments identifies the polarity of the newly grown filaments. Using the analysis of Bergen and Borisy, the assembly rate constants for barbed and pointed filament end elongation were calculated. We have extended our analysis of actin assembly and directly determined the critical concentration (C_o) for each end of an actin filament. By titrating the monomer concentration and assaying for the presence or absence of filament nucleation off the ends of the fragments we can identify the C_o. Because elongation rates are linearly dependent upon the monomer concentration, the incubation times were increased in proportion to the decrease in monomer concentration. In 75mM KCl and 1-5mM $MgSO_4$ at pH 7.2 the C_o's for filament assembly were 0.1μM and 0.5μM for the barbed and pointed ends. These values are in close agreement with the estimates obtained via the Bergen and Borisy analysis (0.2μM and 0.4μM). These same C_o's were obtained when the experiments were done in the absence of both Ca^{++} and Mg^{++}. In the absence of Mg^{++} but in the presence of Ca^{++} (20-200μM) the barbed and pointed filament ends were found to have the same C_o. These findings illustrate the dependence of the individual C_o's on the salt and divalent cations present, which in turn may have a major effect on the degree of monomer treadmilling.

Supported by NIH (AM25387) and a Basil O'Connor Starter Grant from the March of Dimes and NIH training grant T32-GM07229-06.

M-AM-E8 KINETIC EVIDENCE FOR MULTIPLE DYNEIN HEADS **Takashi Shimizu* and Kenneth A. Johnson Department of Biochemistry, Pennsylvania State University, University Park, PA 16802. *Current Address: Research Institute for Polymers and Textiles, Tsukuba, Ibaraki Pref. 305, JAPAN.**

Previous analysis of the effect of vanadate on the presteady state hydrolysis of ATP by the Tetrahymena 30S dynein ATPase has shown that vanadate does not inhibit the binding nor the hydrolysis of a single turnover of ATP (Shimizu and Johnson, Biophys. J. 37:346). However, steady state turnover of ATP was completely blocked after the hydrolysis of one ATP per dynein site. These results and others have established that vanadate (V) inhibits the enzyme by forming an E•ADP•V complex immediately after the release of phosphate from the E•ADP•P_i intermediate. More important to the present study, these results provide a method to examine the reaction of ATP with dynein under conditions where only one ATP per site is able to bind to dynein. We have analyzed the ATP-induced dissociation of dynein from the dynein-microtubule complex by stopped flow light scattering measurements in the presence and absence of vanadate at low ATP concentration to obtain the following results: (1) Titration of the light scattering signal versus ATP concentration provided a measurement of 800-900 daltons per ATP site, indicating at least two ATP sites per dynein. (2) At low ATP concentration (1 μM) there was no dissociation in the absence of vanadate, but dissociation was complete and the kinetics exhibited a lag in the presence of vanadate. (3) At low ATP concentration, a graph of the rate of dissociation versus ATP concentration was concave upward in the absence of vanadate, but was linear in the presence of vanadate. These results indicate that at least two dynein heads interact with the microtubule and ATP must bind to each head in order to induce dissociation of the dynein molecule. Supported by NIH 26726.

M-AM-E9 MOIRÉ DISPLAY OF MICROTUBULE/SOLITON Ca^{++} RELEASE. Hameroff SR, Watt RC, Lerman JC, Lipchitz YH, Depts of Anesthesiology & Geoscience, University of Arizona HSC, Tucson, AZ

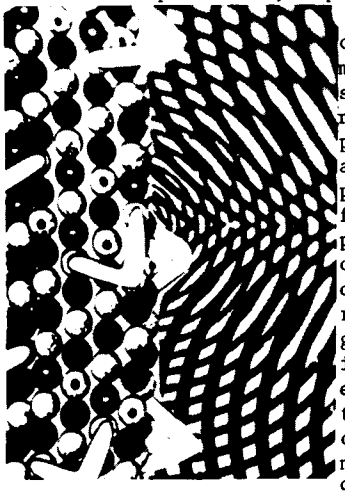

Trophic information processing, real time imaging, and other communicative cellular functions have been theoretically linked to Ca^{++}/conformationally coupled parallel computing in cytoskeletal polymer proteins such as microtubules (MT) (J Theor Biol 98:549-561, 1982). Nonlinear phonon/exciton oscillations, Davydov solitons propagating in MT could compute on genetic and learned MT programming and radiate coherent energy and ionic waves (Biology and Quantum Mechanics, Pergamon, Oxford, 1982, pp 185-212). Coordinated Ca^{++} release by MT subunits may induce Ca^{++} fluxes of about 8mM (16 low affinity Ca^{++}/MT subunit; 1 subunit/4nm; 13 protofilaments/MT; MT density ≈ $1/100nm^2$). The repetitive spatial array of MT subunits and temporal coordination (e.g., nerve action potential) could impart coherence to Ca^{++} fluxes and radiant energy. Coherently-released Ca^{++} and Cherenkov phonons from solitons in multiple MT could generate waves as depicted in Moiré-type interferences (Fig). Holographic imaging and standing waves could influence other structures, organelles and molecules via Ca^{++} gradient patterns or resonance effects and thus manifest mitotic, growth and differentiation patterns. Membrane coupled ongoing activity in massive parallel brain MT arrays could mediate conscious awareness and thought. Moiré patterns can illustrate 2-dimensional implications of parallel computing in MT.

M-AM-E10 MICROTUBULES IN MYOCYTES FROM RAT HEARTS SUBMITTED TO PRESSURE OVERLOAD.
L. Rappaport[x], L. Bugaisky[xx], B. Bertier[x], F. Marotte[x] and J.L. Samuel[xxx] and K SCHWARTZ[x]
[x]Inserm, U 127, Hop. Lariboisière 75010 Paris ; [xx]Institut Pasteur rue du Dr. Roux 75015 Paris ; [xxx]Faculté X. Bichat, Lab. Histo-cyto-génétique 75018 Paris.

It has been suggested that in skeletal muscle microtubules may be involved in the assembly of sarcomeres (1). In heart, in response to chronic pressure overload myocytes growth occurs with an increase in the number of sarcomeres and changes in the isomyosins content. The aim of this work was to determine whether these changes were related to the microtubules organization. Pressure overload, secondary to aortic stenosis, was induced in 3 week old and adult rats. Cardiac myocytes were isolated and microtubule network labeled by an immunofluorescence technique.
- A few days after constriction of aorta, the orientation of microtubules pattern was clearly altered in both cases. As compared to controls, microtubules were, still, mainly localized around the nuclei but the tortuous network observed in the sarcoplasm of controls was frequently replaced by an alignment of microtubules into parallel arrays. They were similar to those observed in cell cultures of fetal rat heart treated with DBcAMP (3). These variations were not linked with cell division, or isomyosin pattern. In conclusions, a reorganization of the microtubule network was observed at the beginning of the adaptation of myocytes to pressure overload. It may be related to the increase in protein synthesis occuring at that time (2).
(1) P.B. Antin et al. J. Cell. Biol. (1981) 90 300-308 ; (2) B. Swynghedauw et al. Europ. Heart J. (1982) 3 75-82 ; (3) A.P. Bollon et al. Cell and Muscle Motility (1982) 2 93.

M-AM-E11 NEAREST NEIGHBOR ANALYSIS OF NEUROFILAMENTS AND NEUROTUBULES IN LOBSTER CORD AND TOAD PERIPHERAL AXONS IS CONSISTENT WITH AN HEXAGONALLY ORDERED NEUROPLASMIC LATTICE. A. J. Hodge, W. J. Adelman, Jr., and R. B. Waltz, Laboratory of Biophysics, NINCDS, NIH at the MBL, Woods Hole, MA 02543.

We have carried out computer analyses on the coordinate position arrays of neurotubules as recorded from electron micrographs of transverse sections through lobster ventral cord axons and both neurofilaments and neurotubules in toad peripheral myelinated axons especially in the axonal constrictions associated with Schmidt/Lanterman "clefts". In all cases, when the point arrays were analyzed with respect to both vectorial and angular separation, there was a clear tendency toward an hexagonal packing arrangement of the longitudinal filamentous elements. This tendency was most clearly illustrated by "dynamic" three-dimensional presentation of the vectorial and angular data using the length of the scanning vector as the third coordinate. Interpretation of the toad axon neuroplasmic lattice data was complicated by the presence of both neurofilaments and neurotubules, the latter occurring both singly and in clusters with no apparent preferred cluster size. In toad axons so far analyzed, the neurotubule clump sizes have ranged between 2 and 12. In lobster axons, the lattice was composed entirely of cross-bridged neurotubules. The observed constraints on close-packing as reflected in the closest approach values are consistent with a lattice model involving specific interaction between cross-bridges and longitudinal filamentous elements. The nearest neighbor data support an hexagonal lattice structure for the model.

M-AM-F1 **TWO DIMENSIONAL GEL ELECTROPHORESIS OF PHYCOMYCES PHOTORECEPTOR MUTANTS.** J. A. Pollock, D. T. Sullivan, and E. D. Lipson. Departments of Physics and Biology, Syracuse University, Syracuse, NY 13210

The fungus Phycomyces shows several responses to blue light. In particular the sporangiophore, or fruiting body, exhibits positive phototropism. The photoreceptors in Phycomyces and other organisms with blue light responses have yet to be isolated and identified. Several lines of evidence indicate that the photoreceptor for phototropism in Phycomyces is a flavoprotein in the plasma membrane of the sporangiophore. Action spectra for phototropic threshold show that night-blind mutants affected in genes madB and madC are photoreceptor mutants, and that several chromophores are involved in phototropism (Galland, Photochem. Photobiol., in press). In order to identify the photoreceptor molecules, we are employing two-dimensional gel electrophoresis of proteins from a plasma-membrane-enriched fraction. During growth, proteins in general are labeled with ^{35}S-sulfate. Alternatively, those proteins with a covalently-bound flavin are specifically labeled by growth on medium with ^{14}C-riboflavin. With the ^{14}C label, two major spots appear in autoradiographs of the gels. These have pI 6.5 and 6.6, and molecular weights 60 kdal and 70 kdal respectively. We have analyzed several strains with independently-induced madC mutations. Three strains do not show the 60 kdal flavoprotein. However, this protein is present in six other madC strains. Genetic analysis of one of the former strains indicates that the absence of the spot segregates from the madC phenotype. Evidently mutations at both loci are coinduced at a high frequency. We are studying the behavior of segregants to determine whether this 60 kdal plasma-membrane flavoprotein plays a role in phototropism. (Supported by NSF grant PCM 8003915)

M-AM-F2 NUCLEOTIDE INJECTION IN LIMULUS VENTRAL PHOTORECEPTORS: EFFECTS ON DISCRETE WAVE PRODUCTION. Alan Fein and D. Wesley Corson, Marine Biological Laboratory, Woods Hole, MA 02543.

Nucleotides were injected into ventral photoreceptor cells by applying short duration pressure pulses to the back of intracellular micropipettes. In four cells we found that injection of 20 mM Na_2ATP, 100 mM KAsp, pH 7.0 reduced the rate of spontaneously occurring discrete waves. For the two most active cells having spontaneous rates greater than 1/sec the reduction was greater than 2-fold. Injection of KAsp alone was without effect. The ATP induced reduction in spontaneous rate occurred without any apparent change in the ability of light to induce discrete waves. We have previously shown that extracellular application of 5 mM vanadate in low calcium (1 mM) artificial seawater induces the production of discrete waves in the dark and prolongs the response to a dim flash. We now report that injection of GTP (3 cells) or ATP (5 cells) abolishes for a few minutes both the discrete waves evoked by vanadate in the dark and the prolongation of the response to a dim flash. We suggest that either the nucleotides or their reaction products are responsible for these effects.

M-AM-F3 SINGLE-CHANNEL CURRENTS ACTIVATED BY LIGHT IN LIMULUS VENTRAL PHOTORECEPTORS. J. Bacigalupo and J.E. Lisman. Dept. of Biology, Brandeis University. Waltham, MA 02254

We have studied the light-dependent conductance by means of the patch-clamp technique in Limulus ventral photoreceptors. In order to have access to the photoreceptor membrane with the patch-pipette we removed the glial cells and connective tissue by teasing them away using a suction pipette. We have resolved inward single-channel currents whose probability of opening is greatly increased by light and is proportional to light intensity. At high light intensities, there is high initial level of channel activity followed by a markedly decreased level that is maintained until the light is turned off. This is similar to the transient and plateau phases of the macroscopic light-induced current. Depolarizing the patch membrane in the dark does not activate the channel. This indicates that light, and not the depolarization induced by light, activates the channel. Light given while the patch is highly depolarized(+55mV) induces outward single-channel activity. The zero-current potential for the channel is similar to that of the macroscopic light-induced current. The single-channel conductance is 50 pS in the absolute membrane potential range of -40 to -20 mV. The mean open time of the channel, at 21°C, is in the msec range. The evidence presented strongly suggests that the channel we have found is light-activated and might represent the basis for the light-activated conductance change in Limulus ventral photoreceptors.

M-AM-F4 LIGHT MODULATION OF VOLTAGE-DEPENDENT INWARD AND OUTWARD CURRENTS IN LIMULUS VENTRAL PHOTORECEPTORS. K. Chinn and J. Lisman. Dept. of Biology, Brandeis University, Waltham, MA 02254

In addition to its effect on the light-activated Na conductance light reduces the voltage-dependent K current (i_k) in Limulus ventral photoreceptors (Science 212:1273, 1981). To test whether a light-induced decrease in pH causes the reduction of i_k, we pressure injected pH buffer (MOPS, pH 7.2) into photoreceptors while monitoring the injection volume using dye absorbance. MOPS (100 to 200 mM) did not affect the light-induced reduction of i_k, indicating that changes in pH are not involved. To test whether pCa, which rises in light, might be responsible we injected the Ca buffer, EGTA (pCa 7.1). At concentrations of about 60mM EGTA the effect of light on the maintained outward current was blocked or reversed (in these cases light increased the maintained outward current). These increases could be explained if there is a voltage-dependent maintained inward current that is decreased by light. We have therefore begun to study in more detail the voltage-dependent inward currents in these photoreceptors. In uninjected cells, early inward current is reduced about 10% by light. Tail currents measured 2 seconds after a depolarizing pulse indicate that there is a component of maintained inward current. Thus i_{in} is maintained and can be reduced by light. We are presently investigating how EGTA affects i_{in} and whether the effect of light on i_{in} in EGTA injected cells can account for the light-induced increase in net outward current seen in such cells. It remains uncertain whether Ca is involved in modulation of i_k.

M-AM-F5 LIGHT ACTIVATES CHOLERA TOXIN-CATALYZED LABELING OF A 44,000-DALTON PROTEIN IN SQUID PHOTORECEPTORS. Carol A. Vandenberg and Mauricio Montal, Depts. of Neurosciences, Physics & Biology, UCSD, La Jolla, CA 92093.

Guanine nucleotide-binding proteins can be identified biochemically through their specific labeling by bacterial toxins. Cholera toxin catalyzed the transfer of label from [^{32}P]NAD to a protein in squid (Loligo opalescens) photoreceptor membranes with an apparent molecular weight of 44,000. Labeling required illumination of the membranes: light increased the extent of ^{32}P incorporation 7 fold. The addition of ATP to the membrane suspension enhanced labeling of the 44,000-dalton protein, while guanine nucleotides inhibited labeling with the relative potency GTPγS>>GDP>GTP>Gpp(NH)p. The 44,000-dalton protein was membrane bound irrespective of variations in ionic strength and divalent ion concentration over a wide range. An additional protein of molecular weight 94,000 also was labeled using cholera toxin, but labeling was more extensive in dark than in illuminated membranes. We suggest that the 44,000-dalton protein is a component of the light-activated guanine nucleotide-binding protein/GTPase of squid photoreceptors. (Supported by NIH EY 02084)

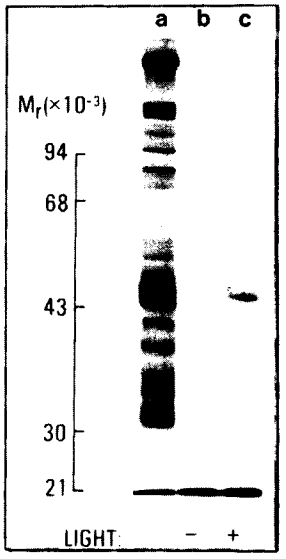

Figure legend: SDS polyacrylamide gel of labeled squid retinal membranes. a) coomassie-stained gel; b & c) corresponding autoradiograph from membranes labeled in the dark (b) or light (c).

M-AM-F6 PHOTOELECTRIC SIGNALS FROM ROD OUTER SEGMENT DISK MEMBRANES BOUND TO PLANAR LIPID BILAYERS. Paul J. Bauer, A. Fahr, E. Bamberg, Institute of Neurobiology, KFA, D-5170 Jülich and Dept. of Biology, Univ. of D-7750 Konstanz

Purified bovine rod outer segment disk membranes were bound to a planar lipid bilayer. After excitation with a 500 nm laser flash, a transient voltage signal was observed which at medium ionic strengths was negative on the rhodopsin containing side measured vs. the rhodopsin-free side. No photoelectric signal was detected when fully bleached disk membranes were bound to the lipid bilayer, however, after regeneration of rhodopsin with 11-cis-retinal, the signal recovered. The signal was already detectable after a flash bleaching about 1 percent of the bound rhodopsin. For successive flashes bleaching only a few percent of the bound rhodopsin, the amplitude of the signal decreased reaching a final value of about 20 percent of the original amplitude. The time constant of the rising phase was temperature dependent. At 20 °C it was 1 - 3 msec, presumably depending somewhat on the size of the disk vesicles. The decay phase was in the range of several tens of milliseconds. In the pH-range of 6 to 8, there was qualitatively no change of the signal at 20 °C, however, at 2 °C the signal was much greater at pH 6 than at pH 8. When osmotically swollen disks were attached under hypotonic conditions, a positive voltage signal was observed. These experiments, especially the latter finding suggest that the observed voltage signal is generated by ionic fluxes which are due to permeability changes triggered at the meta I - meta II transitions of rhodopsin.

M-AM-F7 INTRACELLULAR ATP AND GTP LEVELS AFFECT VISUAL TRANSDUCTION IN LIMULUS VENTRAL PHOTORECEPTORS. Jeff Stern, Kevin Chinn, Phyllis Robinson, and John Lisman. Brandeis University, Waltham, MA 02254

Limulus photoreceptors respond to single photons with a transient increase in membrane conductance termed a quantum bump. Similar events spontaneously occur at a low rate in the dark. We report that the spontaneous quantum bump rate was dramatically increased after cytoplasmic ATP and GTP concentrations were reduced. The spontaneous quantum bump rate was elevated by internal dialysis with a solution lacking ATP and GTP (together termed NTP). Elevated rates were then returned to a normal, low value when NTP levels in the internal solution were raised. The initial increase in quantum bump rate occured slowly (10-20 min.), but after this initial slow increase, bump rates were affected by NTP with a time course similar to the limiting rate for introducing molecules into cells using the internal dialysis technique (2-5 min. for 90% effect of Mg^{++}, TEA^{+}, or $EGTA^{=}$). These results suggest that NTP suppresses spontaneous quantum bumps. This hypothesis has been confirmed using an independent method. Extracellular application of the metabolic inhibitor 2-deoxy-D-glucose also elevated the spontaneous quantum bump rate, and this effect was reversed by intracellular injection of ATP through a microelectrode. These results suggest that an NTP-dependent mechanism turns off or keeps off an early reaction in visual transduction.

M-AM-F8 INTRACELLULAR PH OF LIMULUS PHOTORECEPTORS STUDIED WITH PHENOL RED. S.R. BOLSOVER, J.E. BROWN AND T.H. GOLDSMITH, SUNY, STONY BROOK, NY, 11794 AND YALE UNIVERSITY, NEW HAVEN, CT, 06520

The pH indicator dye phenol red was used to measure intracellular pH in Limulus ventral photoreceptor cells. In vitro, phenol red has absorbance peaks at 560 nm and 430 nm, an isosbestic wavelength at 480 nm and a pK of 7.78. Phenol red was pressure-injected into single cells out of an intracellular micropipette and the absorbance measured at single wavelengths or over the range 400 to 700 nm using a rapid scanning microspectrophotometer. The absorbance spectrum of intracellular dye in dark-adapted cells indicated a pH of 6.98 $\pm$ 0.04 (n = 15). When dark-adapted cells were illuminated for 10 sec with bright light (monochromatic 560 nm, 4 mW/cm^2) the absorbance at 560 nm fell, indicating a pH change of -0.03 $\pm$ 0.01 units. Most of the absorbance change occurred in the first 2 sec of illumination. We believe that the fall in absorbance at 560 nm results from an intracellular acidification because (1) the difference spectrum for intracellular phenol red has a minimum at 560 nm, a maximum at 430 nm and an isosbestic wavelength around 480 nm. (2) Injection of the pH buffer HEPES reduces the light-induced absorbance change. (3) No light-induced dye absorbance changes are seen in cells injected with the related dye bromphenol blue, pK = 4.0. The absorbance at the onset of a second bright flash indicated that after the first flash the intracellular pH in the dark had continued to fall for 1 min, to 0.06 $\pm$ 0.02 (n = 5) units more acid than the dark-adapted value, then recovered over 15 minutes. In contrast, the sensitivity of the cell to light began to increase immediately after a bright flash and recovered monotonically. The pH change elicited by the second flash increased exponentially with time in darkness, τ = 4.3 $\pm$ 0.9 min, (n = 7). Supported by NIH grants EY01914, EY01915 and EY00222.

M-AM-F9 VISUAL PIGMENTS OF TWO FRESHWATER TURTLES, Leo E. Lipetz, Dept. of Zoology, The Ohio State University, and Edward F. MacNichol, Jr., Marine Biological Laboratory.

A computer-controlled, photon-counting microspectrophotometer was used to measure visual pigments (VPs) in Chrysemys scripta elegans (Cse) and Chrysemys picta (Cp), the red-eared and painted turtles. Both species had 4 cone types (O, A, R, N) with red-sensitive VP (r), 1 (Y) with green-sensitive (g), and 1 (C) with blue-sensitive (b), and rods. The VP was identified in each type of cone in the following numbers: For Cse-- O, 39r; A, 34r; R, 62r; Y, 76g; C, 32b; N, 11r. For Cp -- O, 102r; A, 86r; R, 113r and 2g; Y, 95g; C, 88b; N, 10r.

Those VP direct absorbance spectra (DA) and bleaching difference spectra (BD) which showed negligible distortion were selected for analysis. The mean frequencies of peak absorbance (Fp) were compared by the Student t-test. For each species, there was no significant difference (SD) in the Fp's: (a) for DA vs BD spectra in each of the 6 cone types; (b) between O, A, R and N type cones, except that for Cse the N spectra were too poor to compare. For DA spectra, there was no SD in Fp between Cp and Cse for rods and for all cones. For BD spectra, there were SDs in Fp between Cp and Cse only for rods, and for C (6% level), Y (1%) and A (2%) cones; attributable to variations in amount of bleaching products under the different retinal conditions. For the pooled spectra of R, O and A cones, for DA and for BD, the Fp of Cse differed from Cp's at <1% level.

Means of the measured DA spectra are listed below as: number of cells averaged, Fp in TeraHertz, standard deviation of Fp, mean optical density, mean halfwidth in TeraHertz. For Cse: rod, 10, 577.64, 3.56, 0.048, 148; Y, 12, 576.05, 3.00, 0.029, 134; C, 12, 649.42, 4.81, 0.019, 140; pooled ROA, 38, 482.90, 4.27, 0.030, 136. For Cp: rod, 13, 575.47, 1.12, .048, 123; Y, 8, 576.31, 2.91, 0.025, 133; C, 9, 650.67, 5.22, 0.022, 133; pooled ROA, 40, 481.33, 3.39, 0.032, 125.

M-AM-F10 EXAMINATION OF ROTATIONAL CONFORMERS OF THE RETINYLIC CATION BY MOLECULAR ORBITAL CALCULATIONS. PAUL E. BLATZ, DEPARTMENT OF CHEMISTRY, UNIVERSITY OF MISSOURI KANSAS CITY, KANSAS CITY, MO 64110.

In this study, the retinylic cation is examined by application of molecular orbital methods. In particular conformers are investigated which are generated by rotation, separately, about the 6,7 and 13,14 bonds. Values for the required standard input integrals have been estimated previously by calibrating against electronic absorption and NMR spectroscopic data. The standard integrals for atoms 5 and 6 were adjusted to accept the alkyl substituents at these atoms and then calibrated against electronic absorption spectral data. Next the standard input integrals were adjusted to reflect rotation about the 6, 7 and 13, 14 bonds.

Rotation about the 13,14 bond causes the λmax to decrease continuously in length. At the same time the extinction coefficient decreases appropriately. Rotation about the 6,7 bond gives a different picture. For the first excited state, the λmax goes to very long wavelengths, and the extinction falls off to zero. Meanwhile the second excited state shows a wavelength increase to about the value for a 13,14 rotation, and the extinction goes from near zero to a value expected for a tetrainylic cation. Implications to visual pigments will be discussed.

M-AM-G1 EFFECTS OF PRESSURE, TEMPERATURE AND DIVALENT CATIONS ON PHOSPHATIDYLSERINE MEMBRANE FUSION. S. Ohki, Dept. of Biophysical Sciences, SUNY at Buffalo, New York 14214

Phosphatidylserine membrane fusion was studied with respect to the variation of environmental parameters; i) a pressure gradient across the membrane, ii) temperature and iii) divalent cation concentrations in the environmental solution of the membranes. Fusion was followed by the Tb/DPA assay monitoring the fluorescent intensity for mixing of internal aqueous contents of unilamellar lipid vesicles. Also, the surface tension of the lipid monolayers was measured with respect to the variation of the environmental parameters mentioned above. The degree of membrane fusion was correlated with the surface free energy of the membrane which was obtained in the monolayer membrane systems. Although the molecular pathways for the above mentioned membrane fusion appeared to be different with respect to the change in each environmental parameter, it was found that they all have a common feature of an increase in the surface free energy of the membrane under the environmental conditions necessary to induce fusion of the membrane. A theory for lipid membrane fusion is proposed. (Supported by NIH Grant GM-24840).

M-AM-G2 FUSION OF SMALL UNILAMELLAR VESICLES INDUCED BY PEPTIDES OBTAINED BY CONTROLLED PROTEOLYSIS OF SERUM ALBUMIN

Hernan Chaimovich,Lenise A.M.Garcia,Sergio Schenkman and Pedro S.Araujo
Dep.Bioquimica,Inst. Química,U.de São Paulo,CP20780,São Paulo,SP,Brasil

Controlled pepsin cleavage of serum albumin yields two peptides (A and B) that induce fusion of egg phosphatidylcholine small unilamellar vesicles.The fusion was demonstrated and analyzed on the basis of: i,time-dependent changes in absorbance;ii,dilution of the fluorescent label 2-(10-(1-pyrene)decanoyl) phosphatidyl choline,incorporated in a small proportion of the vesicles,as measured by the decrease of the excimer to monomer(E/M) ratio; iii,increase of the average hydrodynamic radius of the liposomes,estimated by Sepharose 4B filtration and iv,strict inverse relationship between the size of the liposomes and their E/M ratios.Peptide B,like albumin(Schenkman et.al.Biochim.Biophys.Acta 649,633;1981) induced the formation of large aggregates in which rapid cooperative fusion produced vesicles of large hydrodynamic radius.Peptide A did not produce large aggregates and the initial fusion products exhibited a hydrodynamic radius smaller than those observed with peptide B.Albumin and peptides A and B are fusogenic only at low pH.These data are discussed in terms of a general model for a signal-dependent protein-induced membrane fusion

M-AM-G3 Ca^{2+}-INDUCED FUSION OF NEGATIVELY CHARGED SMALL UNILAMELLAR VESICLES IS RAPID BUT LEAKY TO ENTRAPPED MATERIAL; FUSION OF LARGE UNALAMELLAR VESICLES IS RAPID BUT NON-LEAKY. Stephen J. Morris[1], Paul D. Smith[2], Carter C. Gibson[2], Duncan H. Haynes[3] and Robert Blumenthal[4], (1) Neurotoxicology Section, NINCDS, (2) Bioengineering and Instrumentation Branch, DRS, and (4) Laboratory of Theoretical Biology, NCI, NIH, Bethesda, MD 20205 and (3) Dept. of Pharmacology, Univ. of Miami Medical School, Miami, FL 33101.

Small unilamellar vesicles (SUV's) and large unilamellar vesicles (REV's) formed by the reverse evaporation technique from 1:1 (mol/mol) mixtures of bovine phosphatidyl serine (PS) and E. coli phosphatidyl ethanolamine (PE) were used to study the kinetics of membrane fusion. Stopped-flow measurements of the calcium-induced changes in turbidity were used to follow particle aggregation. Simultaneous measurements of the fluoresence resonance energy transfer from NBD-PE to rhodamine-PE incorporated into the vesicle bilayers (probe:lipid 1:100), established that the mixing of membrane contents followed the same kinetics and was as rapid as aggregation. Parallel experiments, which simultaneously measured aggregation and the relief of fluorescence self-quenching of encapsulated carboxy fluorescein (CF) in the presence and absence of anti-fluorescein IgG in the suspension medium, demonstrated that the small unilamellar vesicles rapidly lose their contents of CF as they fuse. On the other hand, the first few cycles of fusion of the large unilamellar vesicles are non-leaky, but leakage develops within 1 - 2 seconds as the particles grow in size.

Thus for this lipid mixture, aggregation is the rate limiting process in the fusion of Ca^{2+}-activated vesicles. The results also demonstrate that the SUV's are poor models for the study of fusion, while the REV's must be carefully tested before unambiguous interpretation of fusion assays, especially those involving the formation of tight complexes, can be made.

M-AM-G4 KINETICS OF DIVALENT CATION INDUCED FUSION. Joe Bentz, Nejat Duzgunes and Shlomo Nir. Schools of Pharmacy and Medicine, University of California, San Francisco, CA 94143.

Fusion and aggregation of sonicated phosphatidylserine vesicles (PS SUV) induced by the divalent cations Ba^{2+}, Ca^{2+}, Sr^{2+} and Mg^{2+} is studied and correlated with cation binding. Fusion is monitored with the terbium/dipicolinic acid (Tb/DPA) assay which is supplemented by measuring the dissociation of the Tb(DPA) complex due to leakage and entry of medium into the vesicles. The separate contributions of aggregation and fusion rates to the overall kinetics of membrane fusion are analyzed. In the presence of Na^+ or Li^+ concentrations of 300 mM or less both aggregation kinetics and bilayer destabilization are shown to affect the overall rate of fusion. In the presence of 500 mM of Na^+ or Li^+ and subfusogenic concentrations of each of the divalent cations, the PS SUV will reversibly aggregate; thus, the effect of the divalent cations (at larger, fusing concentrations) on the rate of bilayer destabilization can be examined directly. Here, Ba^{2+} and Ca^{2+} appear to be equally effective at inducing fusion. However, when the rate constant of fusion is compared with the amount of divalent cation bound per PS (calculated from binding constants which apply to the vesicles before aggregation and fusion), the fusogenic capacities of these divalent cations follows the sequence $Ca^{2+} > Ba^{2+} > Sr^{2+} > Mg^{2+}$. This is the same sequence found in other studies for the divalent cations' ability to increase the phase transition temperature of PS bilayers and to induce lateral phase separation of mixed PS/phosphatidylcholine (PC) bilayers. The concordance of these sequences is discussed relative to the initial events of fusion and the equilibrium structures of PS and the divalent cations. Supported by NIH Grant GM-31506.

M-AM-G5 ATTRACTIVE FORCES BETWEEN LECITHIN BILAYERS. By S.A. Simon, R.V. McDaniel, and T.J. McIntosh. Departments of Physiology and Anatomy. Duke University, Durham, N.C. 27710.

Between two large bodies in a fluid medium there exists a long range attractive van der Waals force, Fv. For uncharged multilamellar bilayers, the fluid spacing is determined by the balance of Fv and the repulsive hydration force. Fv is directly proportional to $(\varepsilon_m-\varepsilon_f)^2$, where ε_m and ε_f are the dielectric permitivities of the membrane and fluid space respectively. Thus it is expected that a plot of repeat period, d, versus ε_f should be symmetric and maximum about $\varepsilon_f=\varepsilon_m$ (see Le Neveu et al., Biophys. J. 18: 209, 1977). For egg PC (EPC) bilayers in a series of glycerol-water solutions we have found that d is maximum at an index of refraction of $n_f=1.37$, and symmetric about this point with d being the same in pure water and pure glycerol. Also, we have modified ε_m by using gel phase DPPC liposomes in glycerol-water solutions and observed maximum d at $n_f=1.40$, a value consistent with the measured optical changes in ε_m. However, when EPC is equilibrated with sucrose or glucose to change ε_f, the results obtained depend on the sample preparation. For slightly sonicated EPC vesicles, d is maximum at $n_f=1.37$, but for higher sugar concentrations decreases significantly below the value observed in pure water (Le Neveu et al.). When the sugars are equilibrated with unsonicated EPC dispersions, d monotonically decreases until ≈50 wt% sugar. The implications of these results in terms of attractive forces between bilayers will be discussed.

M-AM-G6 ASSOCIATION AND FUSION OF PHOSPHOLIPID VESICLES TO PLANAR BILAYER MEMBRANES. F.S. Cohen, M.H. Akabas, and A. Finkelstein. Departments of Physiology, Rush Medical College, Chicago, IL. 60612 and Albert Einstein College of Medicine, Bronx, New York, 10461. Intr. by B.R. Eisenberg.

In order to model exocytosis, we are studying the fusion of phospholipid vesicles to planar bilayer membranes. Divalent cations promote close and irreversible association of vesicles to planar membranes and subsequent osmotic swelling of vesicles in contact with the planar membrane results in fusion. Criteria used for scoring fusion have included transfer of internal contents of the vesicles to the other (trans) side of the planar membrane and, routinely, the simultaneous incorporation of several integral membrane channels from reconsitituted vesicles into the planar membrane. Recently we have monitored the discrete capacitance increases of the planar membrane which result from the fusion of large (several micron) vesicles to solvent-free planar membranes. These capacitance increases, approximately 1 pF, show that the vesicular membrane incorporates in toto (rather than only a portion transferring) into the planar membrane. Fusion occurs without conductance increases, and after fusion the capacitance of the planar membrane does not decay back to its original value. (Supported by Grants USPHS GM 27367, NS 14246 and 5T 32GM7288.)

M-AM-G7 COMPARISON OF TWO LIPOSOME FUSION ASSAYS MONITORING INTERMIXING OF AQUEOUS CONTENTS AND MEMBRANE COMPONENTS. C. Kayalar, J. Rosenberg, and N. Düzgüneş. Department of Chemistry, University of California, Berkeley, CA 94720 and Cancer Res. Inst. University of California, San Francisco, CA 94143.

Calcium-induced fusion of large unilamellar vesicles (d=0.1μm) made of phosphatidylserine (PS) or phosphatidylglycerol (PG) has been studied. Intermixing of aqueous contents during fusion was followed by the Tb/dipicolinic acid fluorescence assay (1), and intermixing of membrane components by resonance energy transfer between fluorescent lipid probes (2). Both assays gave identical threshold concentrations for calcium which were 2 mM for PS and 10 mM for PG. The dependencies of the initial rate of fusion on the vesicle concentration determined by either assay were very similar. The order of this dependence was about 1.2 for PG and 1.5 for PS in the concentration range of 5-200μM lipid. No leakage of contents were detected during fusion of PG vesicles. Magnesium inhibited the calcium-induced fusion of PS vesicles but did not cause any fusion by itself. There was no lipid transfer during magnesium-induced aggregation of PS vesicles.

1. Wilschut,J., Düzgüneş,M., Fraley,R. and Papahadjopoulos,D. (1980) Biochemistry 19, 6011.
2. Struck,D.K., Hoekstra,D. and Pagano,R.E. (1981) Biochemistry 20, 4093.
(Supported by grants from Dreyfus Foundation and NIH, AI-18578-01).

M-AM-G8 MODULATON OF DIVALENT CATION-INDUCED MEMBRANE FUSION BY IONOTROPIC AND THERMOTROPIC PHASE TRANSITIONS. N. Düzgüneş, J. Paiement, K. Freeman, N. Lopez, J. Wilschut and D. Papahadjopoulos. Cancer Res. Inst. and Depts. of Pharmacology and Anesthesia, UCSF, San Francisco, CA 94143 and Lab. of Physiological Chemistry, Univ. of Groningen, Groningen, The Netherlands.

We have studied the effect of isothermal phase transitions induced by Ba^{2+} and Sr^{2+} in large unilamellar vesicles (LUV, 0.1 μm diam.) made of phosphatidylserine (PS) on the initial rate of membrane fusion induced by these ions. Gel-liquid crystalline phase transitions were detected by differential scanning calorimetry and intermixing of internal aqueous contents of fusing vesicles by the Tb/dipicolinic acid fluorescence assay. Fusion was slow below the transition temperature Tc of the ion/PS complex and increased by more than an order of magnitude above it, indicating that fusion can occur in this system under conditions where the bilayers are still fluid. Ca^{2+}-induced fusion of membranes composed of an equilmolar mixture of PS with dipalmitoylphosphatidylcholine (DPPC) or dimyristoylphosphatidylethanolamine (DMPE) exhibited a complex dependence on temperature. PS/DPPC membranes were completely resistant to fusion above the endothermic transition, but fused within a narrow temperature range within the transition, suggesting the involvement of segregated PS domains. PS/DMPE vesicles fused at a slow initial rate below the Tc but the rate increased by more than 10-fold above it, going through a local minimum at the Tc. Ca^{2+}, but not Mg^{2+}, induced phase separation of the DMPE. Although both ions induced fusion, Mg^{2+} was less effective. This work was supported by NIH Grant GM28117 and NATO Research Grant 151.81.

M-AM-G9 RETENTION OF AQUEOUS CONTENTS DURING Ca^{2+}-INDUCED FUSION OF PHOSPHOLIPID VESICLES. N. Düzgüneş, J. Wilschut, K. Hong, D. Hoekstra and D. Papahadjopoulos. Cancer Res. Inst. and Depts. of Pharmacology and Anesthesia, UCSF, San Francisco CA 94143, and Lab. Physiological Chem., Univ. Groningen, The Netherlands.

We have investigated the relative kinetics of intermixing and release of contents during Ca^{2+}-induced fusion of phospholipid vesicles. Fusion was monitored by the Tb/dipicolinic acid (DPA) fluorescence assay. Release was followed by the relief of self-quenching of carboxyfluorescein (CF) or by Tb fluorescence with identical results. Fusion of large unilamellar vesicles (LUV) made of phosphatidylserine (PS), in 100 mM NaCl, pH 7.4, was initially non-leaky, whereas the fusion of small unilamellar vesicles (SUV) was accompanied by partial release of contents. After several rounds of fusion, the internal aqueous space of the vesicles collapsed. The rate of intermixing of lipids, measured by a resonance energy transfer assay, and the rate of coalescence of aqueous contents during fusion were similar over a range of Ca^{2+} concentrations. Release of contents from heavily aggregated LUV (PS) in Ca^{2+} and Mg^{2+} did not contribute to the Tb intermixing with DPA outside the vesicles. LUV made of a mixture of 1:1 cardiolipin (from *Bacillus subtilis*) and phosphatidylcholine went through 2 rounds of fusion in the presence of Ca^{2+} at 10°C with complete retention of contents. Similar results were obtained with vesicles made of a 1:2:3:2 mixture of phosphatitdate/PS/phosphatidylethanolamine/ cholesterol in the presence of Ca^{2+} and synexin at 25°. Our results emphasize the diversty of relative fusion/release kinetics in different phospholipid vesicle systems, and also point to the reliability of the two fusion assays. Supported by NIH grant GM28117 and NATO Research Grant 151.81.

M-AM-G10 KINETICS OF SYNEXIN-FACILITATED MEMBRANE FUSION K. Hong, R. Ekerdt, J. Bentz, S. Nir and D. Papahadjopoulos. Cancer Res. Inst. and Depts. of Pharmacology and Pharmacy, UCSF, San Francisco, CA 94143 and Hebrew University of Jerusalem, Rehovot, Israel.

Synexin, a Ca^{2+}-binding protein present in many secretory tissues, facilitates fusion of specific phospholipid membranes at divalent cation concentrations found intracellularly. The kinetics of synexin-facilitated membrane fusion was examined experimentally and theoretically. The fusion was studied by monitoring intermixing of the aqueous contents of phospholipid vesicles. Data was analyzed by a general mass action model which explicitly separates the rate of vesicle aggregation from that of the overall fusion process. The initial reaction of this model is

$V_1 + V_1 \underset{D_{11}}{\overset{C_{11}}{\rightleftharpoons}} V_2 \xrightarrow{f_{11}} F_2$, where V_1 denotes the vesicle monomer, V_2 denotes the dimer aggregate and F_2 denotes the fused doublet. For these vesicle systems, with a given Ca^{2+} concentration, synexin increased the dimerization rate constant C_{11}, while the fusion rate constant f_{11} is essentially unchanged. Thus, the enhancement to the overall fusion process induced by synexin is due to its ability to facilitate the close apposition of vesicles. The subsequent bilayer destablization may be prescribed by the bound divalent cations. This work was supported by NIH grants GM31506, GM26369, and a Central Research Grant from the Hebrew University of Jerusalem.

M-AM-G11 MEMBRANE ADHESION AND CONDUCTANCE INCREASES MEDIATED BY GANGLIOSIDES, Gregory J. Brewer* and P.D. Thomas, Department of Medical Microbiology and Immunology, Southern Illinois University School of Medicine, Springfield, Illinois 62708.

The formation of two spherical model membranes at the tips of two syringes has allowed us to study the role of gangliosides in membrane adhesion and look for changes in conductance between two such membranes during the process of adhesion. The membranes are formed in aqueous 100 mM NaCl, 10 mM KCl, 1 mM $CaCl_2$ from 1% (w/v) egg phosphatidylcholine, 0.1% (w/v) crude beef brain gangliosides in n-decane. After thinning to the "black" bilayer state, two membranes were moved into contact. After a lag of 10 to 20 min, the contact area increased linearly with time over a 5 to 20 min period dependent on ganglioside concentration. During this period, the conductance between the two membranes also increased significantly from 4 nS/cm^2 to 12 nS/cm^2. Membranes containing pure GM1, $GD1_a$ or GT1 behaved similarly. When membranes were formed in the absence of gangliosides, neither an increase in contact area nor an increase in conductance were observed. The role of electrostatic bridging by calcium was investigated. In the absence of calcium or in the presence of 2 mM EDTA, adhesion proceeded after a longer lag time at about one-half the normal rate. Membrane fusion during adhesion is unlikely because, 1) the adhesion process can be reversed by physically moving one membrane away from the other, 2) capacitance readings do not indicate a decrease in membrane thickness, 3) two different fluorescent probes do not mix across the junction. These data will be discussed in terms of calcium-mediated initial adhesion, followed by hydrogen bonding between carbohydrate chains and a possible electrical signal for contact sensation.

(Supported in part by NIH grant #CA34145).

M-AM-G12 CLATHRIN-INDUCED pH-DEPENDENT FUSION OF PHOSPHATIDYLCHOLINE VESICLES. Robert Blumenthal, Maryanna Henkart. NCI, NIH, and Clifford J. Steer, NIADDK, NIH, Bethesda, MD 20205

Interaction of clathrin coat protein with dioleoyl phosphatidylcholine (DOPC) vesicles at pH 6.5 and below results in the formation of stable vesicle - clathrin complexes (Steer et al, J. Biol. Chem. 257, 8533-8540, 1982). In this report we show by gel chromatography and sedimentation analysis that the interaction of clathrin coat protein with unilamellar DOPC vesicles at pH=6.0 results in the formation of larger structures. As shown by electron microscopy and an increase in trapped volume of both sucrose and inulin those larger structures represent fused bilayers. We examined the mixing of membrane lipid as a result of membrane fusion using resonance energy transfer between two fluorescent lipid probes incorporated into the same vesicle membrane. At a protein:lipid ratio of 1:500 there was 50% vesicle-vesicle fusion, at pH 6.0, as indicated by the change in efficiency of energy transfer between the fluorescent probes. Fusion was completed within 60 sec. A number of other proteins (ovalbumin, rabbit IgG, trypsin, pronase, calmodulin, tubulin, synexin, bovine serum albumin) at ten-fold or higher concentrations, did not induce fusion of dioleoyl phosphatidylcholine vesicles, either at pH 7.4 or at pH 6.0. This system provides a model for pH-dependent and protein-mediated fusion of uncharged lipid bilayers.

M-AM-H1 LIGHT DIFFRACTION STUDIES OF LIMULUS MUSCLE FIBERS. R. J. Baskin, K. Burton, Y. Yeh, and M. Corcoran, Depts. of Zoology and Applied Science, University of California, Davis, CA 95616.

Limulus striated muscle, unlike vertebrate striated muscle, exhibits a change in A-band width upon change in sarcomere length. Evidence has been presented to indicate a change in A-filament length at short sarcomere lengths (Dewey, et al. J. Cell Biol. 75, 366:1977). The increase in A-band width at long sarcomere lengths has been attributed to thick filament mis-alignment. In many of these studies sarcomere length has been determined using a light diffraction technique. Recent studies (Baskin, et al. Biophy. J. 36, 759:1981) have shown that interpretation of light diffraction measurements from striated muscle is more complicated than was initially realized. In this investigation we have studied the effect of the "anamolous" behavior of Limulus muscle during sarcomere length changes on the light diffraction pattern.

The angle of beam incidence to the fiber was varied (ω scan) and the order line intensity measured as a function of sarcomere length. Intensity of the first order line was a function of incident angle. Left and right first order peak separation was a function of sarcomere length. At some sarcomere lengths the tilt of a skew plane satisfied the Bragg condition resulting in an increase in the intensity of the second order diffraction line. Mis-alignment of A-band filaments which occurs at long sarcomere lengths may be the structural basis for the reversal in the first and second order line intensities.

M-AM-H2 INTERSARCOMERE DYNAMICS DURING ISOMETRIC TETANII OF SINGLE MUSCLE FIBERS. Richard L. Lieber and Ronald J. Baskin, Department of Zoology, University of California, Davis, CA 95616.

We have measured the contraction dynamics of "end" and "center" regions of single fibers during the "creep" phase of fixed-end tetanii. Experimental control is provided by a digital data acquisition system which acquires diffraction data as fast as every 260 μs for 300-700 ms. Tension records are simultaneously displayed on a storage oscilloscope.

Resting sarcomere length variation between the end and center regions was analagous to that of Gordon, Huxley and Julian (1966). During the rapid rise in force (<35 ms) the end regions contract almost twice as fast as the center regions (.782 SL/s vs. .396 SL/s). During the creep phase of force development, the velocity of contraction of the end regions was 3.8 times the velocity of stretch of the center regions. In addition, factors which effect the rate and extent of the slow phase of tension rise effected the rate and extent of shortening in the end sarcomeres.

These and other data support the explanation of creep first proposed by Hill (1953) and used by Gordon et al. to justify their use of the back extrapolation technique in measuring tetanic tension in single fibers. These data also indicate that laser diffraction may provide an effective method for studying the dynamics of creep and related phenomena.

R. L. Lieber's present address is Department of Orthopedic Research, Veterans Administration Medical Center, San Diego, CA 92161

M-AM-H3 THE STIFFNESS OF SKINNED RABBIT PSOAS FIBERS IN ATP OR PP_i: EFFECT OF SPEED OF STRETCH. M.Schoenberg*,B.Brenner*,J.Chalovich†,L.E.Greene†,and E.Eisenberg†.*NIADDK,†NHLBI, NIH.

We previously reported (Brenner et al., PNAS, 1982) that, at low ionic strength (μ=0.02 M), 5°C, in the presence of ATP and absence of Ca^{++}, the stiffness of single skinned rabbit psoas fibers measured with rapid stretches is approximately proportional to the amount of overlap between the thick and thin filaments. On this basis, we concluded that the stiffness was due to the binding of myosin heads to actin. In the present study we varied the speed of stretch over several orders of magnitude to determine if we could obtain a maximum value for the measured stiffness. When stiffness was plotted as a function of speed of stretch on a log scale, the measured stiffness never reached an upper limit. Rather, at μ=0.02 M, measured stiffness increased from 5% to 40% of the rigor value as the speed of stretch increased over two orders of magnitude from 10^3 to 10^5 nm/half-sarcomere/sec. As the ionic strength was increased, even lower stiffness levels were obtained over this range of speeds. To determine whether the measured stiffness also varies so widely with velocity of stretch in the presence of ATP analogues, we measured the speed dependence of the stiffness in the presence of 4 mM PP_i, 6 mM $MgCl_2$, 1 mM EGTA, 20 mM imidazole and 80 mM KCl. In this solution the in vitro binding constant of myosin subfragment-1 to actin is about the same as in ATP at μ=0.02 M. The data showed that, at a given stiffness, the speed of stretch was about 10^{-3} slower than in ATP solution. Nevertheless, the measured stiffness continually increased as the velocity was increased about four orders of magnitude, reaching the rigor value at the fastest speeds tested. We conclude that both in PP_i and ATP, myosin cross-bridges are attached to actin and in rapid equilibrium with their detached states. However, the rates of attachment and detachment seem to be much slower in PP_i than in ATP solution.

M-AM-H4 EFFECTS OF KCl CONCENTRATION ON EQUATORIAL X-RAY DIFFRACTION OF SINGLE SKINNED RABBIT PSOAS FIBERS. B. Brenner, L. C. Yu and R. J. Podolsky, NIADDK, NIH, Bethesda, MD.

Diffraction patterns were obtained from relaxed single skinned psoas fibers at ionic strengths between μ = 20 and 230 mM by varying KCl. The lattice spacing d_{10} was 384 Å between μ = 20 and 50 mM and increased gradually to 470 Å as ionic strength was increased to 230 mM. The intensity ratio I_{11}/I_{10} decreased continuously when ionic strength was raised above 20 mM, while the rigor pattern remained essentially the same. Between μ = 20 and 120 mM, intensities of the individual reflections changed in a reciprocal way. This change was more prominent after correction for the lattice volume change was made. Above 120 mM, both intensities decreased, although the relative decrease was greater for I_{11}; the peak widths of the reflections were broader compared to those in patterns below 120 mM. The intensity changes do not appear to be due to spacing changes since the intensities are not sensitive to a change in d_{10} from 440 to 380 Å produced by 3% gm-wt dextran. The reciprocal change in I_{11} and I_{10} between 20 mM and 120 mM indicates a mass shift from the thin filament region towards the thick filament region. The parallel decrease above 120 mM suggests the development of a strong disordering effect in the lattice in this range of ionic strength. These data support the idea that crossbridges are attached at μ = 20 mM, as deduced from stiffness measurements (Brenner *et al.*, PNAS, 1982), and they provide evidence that crossbridges detach gradually as a function of KCl concentration between μ = 20 and 120 mM. Above 120 mM, deductions from the diffraction pattern regarding crossbridge number are obscured by increasing disorder in the filament lattice. The lattice spacing data suggest that crossbridges formed in the presence of ATP may exert an inwardly directed radial force (without producing a net axial force) and that the magnitude of the radial force (or the radial compliance of the lattice) depends on lattice spacing.

M-AM-H5 COOPERATIVE CROSSBRIDGE FORMATION IN SKINNED RABBIT PSOAS FIBERS IN THE PRESENCE OF $MgPP_i$

B. Brenner*, L. C. Yu*, L. E. Greene†, E. Eisenberg†, M. Schoenberg* and R. J. Podolsky*. *NIADDK, †NHLBI, NIH, Bethesda, MD, 20205.

Myosin subfragment-1 (S-1) binds cooperatively to regulated actin in the presence of ADP and AMP-PNP (Greene, JBC 257) as well as PP_i. To study this behavior in muscle fibers, stiffness and equatorial X-ray diffraction patterns were measured in single skinned rabbit psoas fibers at 5°C in PP_i solution (20 mM imidazole, 1 mM EGTA or CaEGTA, 6 mM $MgCl_2$, 4 mM PP_i, 130-200 mM KCl). Both with and without Ca^{++}, stiffness measured with rapid stretches was close to the rigor value at μ = 170 mM. In contrast, at μ = 240 mM the stiffness was still close to the rigor value with Ca^{++}, but without Ca^{++} the stiffness was equal to the relaxed value suggesting that almost all bridges had detached. Equatorial X-ray diffraction studies show similar behaviour. At μ = 170 mM the diffraction pattern was similar to the rigor pattern both with and without Ca^{++} while at μ = 220 mM the diffraction pattern was shifted only slightly towards a relaxed pattern in the presence of Ca^{++} but was close to a relaxed pattern in the absence of Ca^{++}. Therefore, without Ca^{++} a marked decrease in the number of attached crossbridges occurs between μ = 170 and μ = 220 mM. Since *in vitro* data suggest that over this range of ionic strength the binding constant of S-1 to unregulated actin changes only 2-3 fold, it seems likely that detachment of bridges in the fiber is a cooperative phenomenon that can be analysed in terms of the model of Hill *et al.* Using cooperativity parameters obtained in *in vitro* binding studies between S-1 and regulated actin carried out under similar conditions to the fiber experiments, this analysis suggests that the average binding constant of the crossbridge to the strongly binding form of regulated actin in the fiber is about 1-10 (no units) under conditions where the binding of S-1 to actin is about 4×10^2 M^{-1} *in vitro*.

M-AM-H6 CROSSBRIDGE ATTACHMENT DURING ISOTONIC SHORTENING IN SINGLE SKINNED RABBIT PSOAS FIBERS.

B. Brenner. Institute of Physiology II, University of Tübingen, FRG and NIADDK, NIH, USA

The effect of isotonic motion on crossbridge attachment was studied by measuring the stiffness of single skinned rabbit psoas fibers at 5°C and μ = 170 mM. The stiffness was measured by applying rapid length changes to one end of the fibers. Using laser diffraction, resulting movements on the sarcomere level were detected near the force transducer to exclude end compliances and to reduce transmission time artifacts (Brenner *et al.*, PNAS, 1982). The stiffness measured during motion was found to change linearly with relative load (P/P_o with P_o = isometric force), reaching a minimum of about 20% of the isometric value when P/P_o approached zero. Varying the speed of the rapid length changes between ~ 10^3 and ~ 10^5 nm/half-sarcomere/sec, both isometric and isotonic stiffness increased only slightly but in parallel. As stiffness measurements could be affected by changes in stiffness per bridge during motion or very rapid crossbridge turnover, equatorial X-ray diffraction patterns, not sensitive to these factors, were measured. For P/P_o = 0.05-0.10 the isotonic pattern was shifted from the isometric pattern far toward a relaxed pattern. Thus, both stiffness and X-ray diffraction indicate that at 5°C and μ =170 mM during motion, the decrease in force is paralleled by a substantial (~ 80%) decrease in number of attached bridges. In addition, stiffness being only slightly sensitive to speed of rapid stretches indicates that at μ = 170 mM no large number of non-force producing bridges of the type seen in relaxed muscle at μ = 20 mM (Brenner *et al.*, PNAS, 1982) is attached in either isometric or isotonic state.

M-AM-H7 HOW ARE MUSCLE STIFFNESS AND FORCE RELATED? by R.B. Stein & T. Gordon. (Intro. by J. Steele.) Depts. of Physiology and Pharmacology, Univ. of Alberta, Edmonton, Alta., Canada T6G 2H7.

Muscle stiffness resides primarily in the cross-bridges between actin and myosin filaments which generate force. The relationship between stiffness and force is still unclear although stiffness is believed to vary with the number of cross-bridges formed. We have recorded stiffness and force by imposing small amplitude (0.1% of muscle length), high frequency (500-2000Hz) sinusoidal length changes on isolated fast and slow twitch muscles in mice and frogs. A computer program was developed to measure force amplitude (dF) and length (dL) oscillations, cycle by cycle, as well as the mean levels. Thus, stiffness was recorded directly and simultaneously with force during isometric contractions, in response to single and repetitive stimulation of the motor nerve.

Stiffness increased more rapidly than force on the rising phase of contraction and declined more slowly than force during relaxation. This relative time course was found in all muscles and was not altered by change in temperature between 10 and 37°C for mouse muscles and 0 and 24°C for frog muscles. The relative time course was also similar over a range of muscle lengths. When stiffness was plotted as a function of force, it became evident that stiffness is a non-linear function of force which is largely independent of time except for a slight difference between the rising and falling phases of contraction (i.e. the plots showed some hysteresis). These results are compatable with a simple muscle model consisting of elastic elements, whose elasticity varies with force. Lag of stiffness after force during relaxation may be explained by cycling of bonds from a force producing state to a rigor state in which the bonds contribute to muscle stiffness but do not generate force. Supported by MDAC (RBS) and AHFMR (TG).

M-AM-H8 IS THE INSTANTANEOUS ELASTICITY OF CONTRACTING SKELETAL MUSCLE NON-LINEAR? Bernard H. Bressler & Lauren A. Dusik, Department of Anatomy, University of British Columbia, Vancouver.

Rapid length steps of isometrically contracting single muscle fibers or whole muscle provide a measure of the elastic properties of a structure believed to be an integral part of the myosin cross-bridge. The experiments to be described were designed to compare the characteristics of the instantaneous elasticity when measured with small amplitude (3-6 nm/hs) stretches versus releases given at various times throughout the isometric twitch and tetanus. All our experiments were carried out at < 1°C using small bundles (3-5 fibers) from frog semitendinosus muscle. The length steps were complete in 500μsec. Throughout the time course of the isometric twitch a positive correlation was seen between stiffness and force. During the initial development of tension in an isometric tetanus the stiffness was always seen to be rising faster than the force. In all instances, when stiffness values at a given force and measured with a rapid release were compared to those obtained with stretch, rapid lengthening produced consistently higher stiffness than a shortening step. A significant slowing of the initial recovery phase to the T_2 tension level following a step change of length was achieved by placing the fibers in hypertonic Ringer (1.5 x NR). The higher stiffness values obtained with a rapid lengthening step were still seen under these conditions. This appears to rule out the possibility that the observed difference in stiffness was due to a significant truncation of the T_1 phase of the tension transient. Our results would suggest that the instantaneous elasticity exhibits non-linear behaviour when contracting muscle fibers are rapidly stretched.
(Supported by M.R.C. and M.D.A.C., Canada).

M-AM-H9 **CROSS-BRIDGE KINETICS IN RABBIT'S FAST AND SLOW MUSCLE FIBERS CORRELATED WITH MYOSIN LIGHT CHAIN COMPLEMENT.** **M.Kawai, F.H.Schachat*, & A.Isaacson**. Neurology Dept., Columbia Univ., New York, N.Y. 10032. (*Anatomy, Duke Univ., N.C.; **Biology, William Paterson Coll. of N.J.)**

Single fibers from chemically skinned 1) psoas, 2) EDL, 3) soleus, 4) semitendinosus, and 5) diaphram were activated by solutions containing Ca (pCa 5) and MgATP (0-20mM) at 20°C, then subjected to sinusoidal length oscillations. The resulting amplitude and phase shift in tension are plotted in terms of Nyquist plots (Figures); the protein distribution of each fiber is analyzed by SDS polyacrylamide-gel electrophoresis. Fast fibers (1,2) show 3 characteristic fast light chains and have a typical Nyquist plot with 3 well-defined exponential processes (a,b,c). Fibers from slow muscles (3,4) have 3 characteristic slow light chains. Nyquist plots of slow fibers are very different from those of fast fibers: process c is well defined, process d (faster than c) is identifiable, while processes a,b are poorly defined. 5) is a mixed muscle, and we identified 3 kinds of fibers by both physiological and biochemical criteria. Apparently some intrinsic rate constants of the two fiber types differ, and this difference correlates with the distribution of myosin light chains. FREQUENCIES IN FIGURES (counter-clockwise in Hz): 250, 167, 133, 100, 80, 50, 33, 25, 17, 10, 7, 5, 3.1, 2, 1, 1/2, 1/4, 1/8, 1/16.

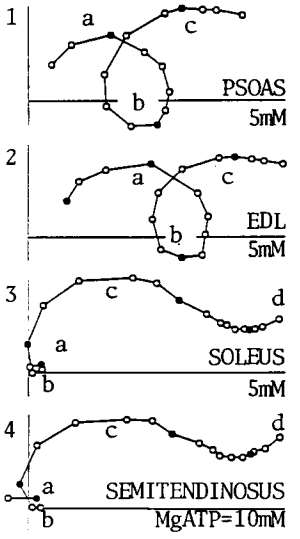

M-AM-H10 CROSS-BRIDGE PROPERTIES AT VARIED DEGREES OF ACTIVATION (β) OF ISOLATED FIBERS AND THE MECHANISM OF CONTRACTION WITH TEMP STEP. Jagdish Gulati and Aravind Babu.
Cardiovascular Research Center, Albert Einstein College of Medicine, Bronx, N.Y. 10461

It is generally agreed that Ca acts as an activating switch for the x-bridge attachment in vertebrate skeletal muscle. But the issue of whether the nature of the switch, under physiological conditions, is simple (i.e., "on-off") or modulatory (i.e., x-bridge kinetics are affected in conjunction with the number of attachments) remains unsettled. This is because the major studies on this issue have so far used skinned fibers, and the contraction kinetics of these are very sensitive to the external factors. We have now utilized isolated intact fibers (from tibialis muscles of the frog) to examine the action of Ca under in vivo conditions directly. The speed of unloaded shortening V_{max} was measured by the method of slack-test, as a function of the degree of activation under steady state conditions. The fibers were activated by a temp step technique (Science: 215, 1109, 1982) with .3-3 mM caffeine. The degree of activation (β) ranged from .16 to 1. β=1 was taken for activation with electrical tetanic stimulation. Maximal β for temp step was .76. In the slack tests at various β, slack times for 5 to 10% L_o releases were determined from the force traces by computer. The slack time for a given release was practically independent of β. Similarly, V_{max} at various β values were constant within 20% experimental uncertainty. The results indicate that the x-bridge turnover kinetics underlying V_{max} are quite independent of the degree of activation. Therefore, Ca appears to be a simple switch under the physiological conditions in intact fibers. Attention should be drawn to the observed fact that maximal β with temp step is .76, suggesting that Ca released is less than with electrical stimulation. Therefore, the mechanisms of Ca-release from the SR may be different in the two types of activations. (NIH-AM26632 and MDA)

M-AM-H11 CONNECTING FILAMENTS IN VERTEBRATE MUSCLE. Alan Magid, Department of Anatomy, Duke University Medical Center, Durham, NC 27710

The high resting stiffness of insect flight muscle is very likely due to elastic connections from the thick filament to the Z-lines. Known as connecting (or C-) filaments, they are thought to be specially-evolved structures peculiar to these muscles (Pringle, Proc.R.Soc.Lond.B. 201:107, 1978). Here I show that, on the contrary, frog skeletal muscle, among others, is also organized this way, and propose that the C-filament is a general feature of striated muscle. Semitendinosus fibers were mechanically- and Triton-skinned so that any tension appearing on stretch must arise in the myofibrils. Sarcomere length was monitored by HeNe laser diffraction, force with a silicon gage. When stretched progressively, isolated myofibrils showed exponentially-increasing passive tension which did not disappear when filament overlap was exceeded but continued to rise. A phasic component($> 3\times10^5$ N/m^2 at long lengths) followed by slow stress relaxation to a steady level characterized the responses. Six to eight diffraction orders were commonly seen in non-overlap fibers, indicating good long-range order. Electron microscopy of non-overlap fibers (by thin-sectioning and freeze-etch) showed, as expected from the laser patterns, orderly fibril structure. In the gap between clearly separated A- and I-segments could be seen filaments, 40 to 50 Å in diameter, extending from the thick filament ends. Their path through the actin filaments to the Z-line could be followed in rare views. Unlike actin, they did not "decorate" with myosin S-1. Functional implications of the C-filament will be discussed. Supported by MDA grants and NIH grant AM27763.

M-AM-I1 KINETICS OF K^+ CHANNEL ACTIVATION: I_K AND GATING CURRENT STUDIES. M.M.White, F.Bezanilla, and R.E.Taylor. Dept. of Physiology, UCLA, CA 90024 and Lab. of Biophysics, NINCDS, NIH, Bethesda, MD 20205.

We have used data obtained from measurements of K^+ channel ionic and gating currents to decipher the process of K^+ channel activation. Gating currents can provide information concerning transitions among closed states of the channel that cannot be obtained from ionic current measurements. K^+ channel gating currents as we study them do not contain information about the last transition in the activation sequence(Nature 296:657-659), so macroscopic currents are our only source of information about the actual opening of the channel.

Experiments were performed at 20°C using perfused squid giant axons. Na^+ channels were blocked by TTX and ~ 80% of the Na^+ channel gating currents were inhibited by a combination of 0.25 mM dibucaine and total replacement of Cl^- by NO_3^- in the external solution. These agents had no effect on K^+ channels. A triple pulse paradigm that isolates the last step in the activation process showed that the last step is not rate-limiting. Ionic currents cannot tell us where this rate-limiting step is, but gating currents can. K^+ channel gating currents show a pronounced rising phase, an indication that the 1st step is rate-limiting. This is consistent with the large Cole-Moore shift seen for K^+ channels.

Supported by NIH grants GM30376,NS07101, and a Grass Fellowship to M.M.W.

M-AM-I2 A TIME-INHOMOGENEOUS MARKOV MODEL OF A TWO-STATE VOLTAGE CONTROLLED POTASSIUM CHANNEL.

E. Levitan, Rappaport Family Institute for Medical Research; Department of Physiology and Biophysics, Faculty of Medicine, Technion-Israel Institute of Technology, Haifa, Israel.

The single-channel ionic current is regarded as a time-inhomogeneous Markov process with two possible states. Thus, following a voltage step the rate constants for the opening and closing of a channel are time dependent. Eventually they reach their new final values. In this case the first power of the probability of the channel to be in an "open" state is proportional to the macroscopic conductance of the membrane for a given ionic species. To evaluate the time dependence of the rate constants a fitting procedure was used. The sigmoidal and exponential potassium current responses to a potential step as well as the Cole-Moore effect were considered. To check the hypothesis of time-inhomogeneosity and to evaluate the time dependent rate constants experimentally, a statistical procedure on an ensemble of single-channel records was proposed.

This is essentially an estimation of a certain dwell-time distribution. The time dependent rate constants obtained formerly in the fitting procedure were used to calculate the expected dwell-time distributions in the time-inhomogeneous case.

M-AM-I3 INCORPORATION OF POTASSIUM CHANNELS FROM RAT BRAIN SYNAPTOSOMES IN PLANAR BILAYERS. Mark T. Nelson and Roland Reinhardt. Fakultät für Biologie, Universität Konstanz, Konstanz, F.R.G.

Due to their small size, direct measurements of ionic conductances in nerve terminals from the vertebrate central nervous system has not yet been possible, Indirect measurements using fluorescent dyes have shown that synaptosomes (isolated presynaptic nerve terminals) have a large resting K^+ conductance (Blaustein & Goldring, J.Physiol.,247,589). We have been able to incorporate K^+ channels from synaptosomes into 'painted' bilayers (PE:DPG or PE:PS, dia. 0.5mm) and into 'folded' bilayers (dia. 0.05 mm). Incorporation of a few channels to many channels was possible with both 'painted' and 'folded' membranes (Fig.1). With the 'folded' membranes, we could resolve about 0.1 pA at 300 Hz (Fig. 1). The single channel currents and macroscopic (multi-channel) currents were completely selective for K^+ over Cl^- (Fig. 1). We normally observed four unit conductances (10-40 pS in 300 mM KCl). The macroscopic current exhibited a nonlinear I-V relationship in asymmetric K^+ solutions that can be described by the Goldman-Hodgkin-Katz equation. These channels may be responsible for the resting conductance of synaptosomes. Supported by the Alexander von Humboldt Stiftung and the DFG (SFB 138).

Fig.1

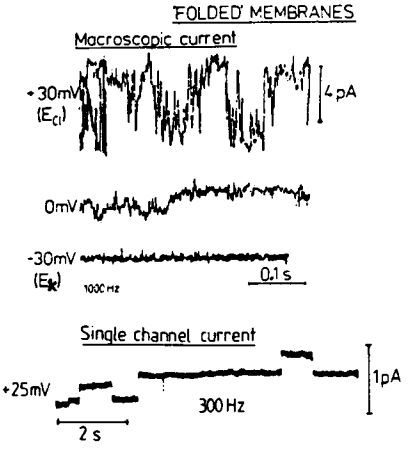

M-AM-I4 VOLTAGE-DEPENDENT POTASSIUM CONDUCTANCES IN MYXICOLA GIANT AXONS: EXACT KINETICS AND MODIFICATION BY D_2O AND MONOVALENT CATIONS. M. A. Chuman* and C. L. Schauf. (Intr. by K. J. Smith). Department of Physiology, Rush University, Chicago, Illinois 60612.

The exact time course of the K+ conductance(s) in most excitable membranes is obscured by K+ accumulation. In order to avoid this problem, experiments are often done in high external [K+]. However, reports that external monovalent cations can alter K+ channel gating suggest this procedure is not ideal. In Myxicola the exact time course of the g(K) in each axon was derived by first accurately measuring E_K as a function of time for a complete range of voltages, and then calculating g(K) from the measured I(K). External [K+]'s from 0 - 430 mM were used, and the kinetics compared, in an effort to separate effects due to K+ from those present intrinsically. In general K+ activation was biphasic, with an initial rapid phase obeying classical kinetics, followed by a much slower exponential activation. The slow phase was insensitive to 4-AP, but was eliminated by internal Cs+, and was greatly reduced by perfusion with EGTA. Either the K+ channels have more than one conducting state, or two different channel populations are involved. As in squid axons (Swenson and Armstrong, Nature 291: 427, 1981) external Cs+ and Rb+ stabilize the open state of the K+ channel, but in Myxicola the effect is greatly exaggerated so that in the presence of these ions the K+ channel becomes conducting at the normal resting potential (K_d for Rb+ and Cs+ = 30 mM). Heavy water (D_2O) substitution for H_2O slows K^+ activation, however the Cole-Moore shift in the K+ conductance produced by conditioning hyperpolarizations is unaffected by D_2O, suggesting that the early stages of K+ channel activation involves solvent-independent conformational changes. (Supported by USPHS grants NS15741 and HL07320 and by NMSS grant 1313A2).

M-AM-I5 EFFECT OF VOLTAGE DEPENDENT K^+ CONDUCTANCES UPON INITIAL GENERATOR RESPONSE IN B-PHOTORECEPTOR OF H. CRASSICORNIS. J. J. Shoukimas and D. L. Alkon. Sect. Neural Systems, Lab. of Biophysics, NINCDS, Woods Hole, MA

The type-B photoreceptor soma of Hermissenda crassicornis has both voltage and light dependent K^+-conductances. Two voltage dependent K^+-conductances, a transient A conductance and a delayed, sustained K^+ conductance, have been characterized with voltage clamp techniques. We have also characterized a light dependent sodium conductance which is primarily responsible for the early part of the light dependent generator response. A Hodgkin-Huxley model which incorporates a quantitative description of these three conductances has been used to simulate the effect of different resting potentials and altered conductance parameters upon the early peak of the generator response.

Resting potentials more depolarized than -60 mV lead to a decrease in the amplitude of the generator response, but do not change the kinetics of this response. Both K^+ currents are found to follow the waveform of the Na^+ current.

A 30% reduction in the magnitude of the A conductance, which simulates experimental observations on days following associative conditioning (Alkon, Lederhendler and Shoukimas, Science, 215: 693, 1982), has little effect upon the initial generator response of the model, but does change the slope of the I versus V relation for current injection, results consistent with experimental observations (West, Barnes and Alkon, J. Neurophysiol., 48: 1243, 1982).

M-AM-I6 MEASUREMENTS OF POTASSIUM CHANNEL ACTIVATION KINETICS IN SQUID AXONS IN THE ABSENCE OF ION ACCUMULATION. John R. Clay, Lab. of Biophysics, NINCDS, MBL, Woods Hole, MA 02543.

Potassium channel kinetics in squid axons are usually obscured by ion accumulation in the periaxonal space under normal ionic conditions. One method of circumventing this problem, which has been suggested at various places in the literature, consists of measuring the instantaneous change in current following a jump in membrane potential from a depolarized level to holding potential. This method is appropriate provided that the instantaneous IV is linear and that its slope is independent of K_o, and provided that gating kinetics are independent of ion accumulation. The first two assumptions are incorrect, in general. The latter assumption appears to be appropriate, because the relative effect of K_o on the IV, measured after a brief depolarizing pulse, is independent of the prepulse potential. Moreover, tail current kinetics appear to be independent of ion accumulation for depolarizing pulses up to 100 ms in duration. The change of kinetics with K_o reported by Swensen and Armstrong (1981. Nature. 291:427) is apparent for $V \lesssim -50$ mV and it appears to require a change either in bulk K_o or in local K_o lasting significantly longer than $\sim$ 50 ms. One consequence of the effect of K_o on the IV is that the jump procedure will, in general, provide a misleading view of gating kinetics. For example, jump kinetics (T=7°C) with K_i = 300 mM, K_o = 50 mM, V_{step} = 0 mV, V_{hold} = -80 mV reveal sigmoidal activation of $\sim$ 75% of the conductance at V = 0 mV for $0 \leq t_{step} \leq 10$ ms followed by a relatively slow increase to the final conductance level between 10 and 30 ms. Results of the same procedure with K_o = 300 mM reach the final conductance level between 10 and 15 ms. The latter results are consistent with Hodgkin and Huxley n^4 kinetics.

M-AM-I7 BURSTING ACTIVITY OF POTASSIUM CHANNELS IN THE CUT-OPEN AXON. I. Llano and F. Bezanilla. Department of Physiology, School of Medicine, UCLA, Los Angeles, CA.

Patch pipettes were used to record current fluctuations due to potassium channels in voltage-clamped cut-open squid axons under ionic conditions similar to those used by Conti and Neher (Nature,285:140-143,1980). The sheet of axonal membrane, perfused with high external potassium, was maintained at a holding potential of -90 mV and the potential of the patch under the pipette was stepped to values ranging from -70 to -50 mV for one-minute periods. Within this voltage range, unitary events were recorded with a mean amplitude of 2.56±0.28 pA , corresponding to a single channel conductance of 16.0 pS. The values for open times of the unitary events were distributed exponentially, with a mean open time of 6.3 ms at -70 mV. Current fluctuations due to the simultaneous activation of several channels were also observed at these potentials. This activity ocurred in bursts separated by long quiescent periods. Histograms of amplitudes of the maximun current during a burst showed peaks corresponding to multiples of the amplitude of the unitary event. The maximum current at any time ranged from 7.5 to 12.5 pA, setting a lower limit of five for the number of active channels in the patch. The burst duration varied widely, ranging from 20 to 500 ms. Each burst was composed of both, unitary and multiple events separated by short interruptions to the baseline current level. At -70 mV the duration of these events ranged from 3.5 to 12.5 ms while the intervals between events had durations ranging from 8 to 27 ms. With larger membrane depolarization (to -50 mV) the frequency and duration of bursts, as well as the mean current level and average duration of the events composing a burst increased.

Supported by USPHS grant GM 30376.

M-AM-J1 ACTIVITY OF ANALOGUES AS PRIMARY AND SECONDARY QUINONES IN PHOTO SYNTHETIC REACTION CENTERS by J.C. McComb and C.A. Wraight, U. of Illinois,Urbana, IL 61801

The electron acceptor complex of reaction centers (RC) from Rp. Sphaeroides contains two ubiquinones as primary (Q_A) and secondary (Q_B) acceptors. Both quinones are redily extractable from isolated RC's. We have studied the reconstitution of activity by various analogues including UQ prenylogues (Q10-Q0). Activity was restored with high binding affinity (pKd = 7 in 0.3% LDAO) for all prenylogues except QØ (pKd = 4). pKd's increased with T for Q 7, 9, 10 but decreased for lower prenylogues, indicating that binding is entirely entropic for the more hydrophobic quinones but partially enthalpic for shorter chain ones.

Q_n	K_d (Molar)	ΔG (kJ mole^{-1})	ΔH (kJ mole^{-1})	ΔS (J mole^{-1}°K^{-1})
10	1.6×10^{-7}	-38.8	+13.6	+176
9	1.7×10^{-7}	-38.6	+ 9.3	+161
7	2.0×10^{-7}	-38.2	+ 6.5	+150
6	2.2×10^{-7}	-37.9	- 7.4	+102
5	2.5×10^{-7}	-37.6	-12.0	+ 86
4	2.7×10^{-7}	-37.4	-12.0	+ 85
3	2.7×10^{-7}	-37.4	-12.3	+ 84
2	2.0×10^{-7}	-38.5	-12.5	+ 86
1	4.9×10^{-7}	-36.0	-18.5	+59

Secondary quinone activity, as measured by oscillations in the appearance of a semiquinone spectra (Q_B^-) or cyt c oxidation, was seen in all prenylogues even though a marked slowing of the back reaction by Q_B was absent in the short chain ubiquinones. Turnover in RC's reconstituted with lower prenylogues was less sensitive to o-phenanthroline, which competitvely displaces Q_B but not Q_B^-. We interpret this as due to less effective binding of the short chain ubisemiquinones allowing some leakage of the electron out of the RC and through the o-phen block. Low molecular weight quinones (methylbenzoquinones) show a similar leak even from the primary quinone site. Supported by NSF PCM 80-12032.

M-AM-J2 WHAT ULTRASTRUCTURE INFORMATION CAN SELECTIVE LIGHT SCATTERING PROVIDE ABOUT CHLOROPHYLL IN VIVO? Paul Latimer, Department of Physics, Auburn University, AL 36849

The phenomenon of selective light scattering, the occurrence of scattering peaks and valleys near absorption maxima, has been of interest for some time (P. Latimer & E.I. Rabinowitch, Arch. Biochem. Biophys. 84,428 (1959)). This anomalous dispersion phenomenon promises information about the packing and arrangement of light absorbing molecules in vivo since it imbues scattering spectroscopy with the chemical specificity of absorbance spectroscopy. Information about ultrastructure will have to be obtained by interpreting experimental findings in terms of light scattering and dispersion theories. Thus far, studies of the effect in terms of theory have sought to describe its character rather than to obtain useful information from it.

Recently, Gy. I. Garab, G. Paillotin, & P. Joliot (Biochim. Biophys. Acta. 545, 445 1979) produced microsecond changes in selective scattering by carotenoids with light flashes. A.P. Brown (Photochem. Photobiol. 34,207, 1981) has added reagents to chloroplast preparations and changed selective scattering by chlorophyll a with little change in absorption. This partial experimental uncoupling of absorption and selective scattering means that the scattered light must indeed contain different information than that from absorption measurements. In this study, we are using the tools of scattering and anomalous dispersion theories which have recently become available to learn what factors are involved in producing selective scattering. This should tell what the changes in selective scattering mean in terms of cell ultrastructure.

M-AM-J3 A POSSIBLE MECHANISM OF ADRY DESTABILIZATION OF PS II OXIDIZING EQUIVALENTS. C.T. Yerkes and A.R. Crofts, Dept. of Physiology and Biophysics, University of Illinois, Urbana, IL 61801.

Recent work examining the effect of ADRY reagents on the decay kinetics of EPR Signal IIf (Ghanotakis, Yerkes and Babcock (1982)BBA,682,21-31) has led to a model for the mechanism of the ADRY effect. It is proposed that ADRY reagents act as high potential electron donors to PS II, reducing the Z^+ radical directly in Tris-inhibited systems. In the past, a catalytic role has been assumed for the ADRYs because of the low (μM) concentrations required and the fact that no photo-depletion of the ADRY pool was observed after prolonged illumination. The new redox model must provide an additional mechanism for the re-reduction of oxidized ADRY. This occurs at the expense of reduced membrane components, among them cyt b-559, carotenoids and chlorophyll. We would predict, therefore, that the rate of these oxidation reactions should corresponds to the Signal IIf decay rate in the EPR experiments. Initial experiments did not appear to bear this out. At 20 μM CCCP and 3mg/ml chlorophyll, typical EPR conditions, the decay half time of Signal IIf is 20ms. At 20μm CCCP and 50ug/ml chlorophyll, typical optical conditions, the oxidation half time of b-559 is under 10μs. However, when optical and EPR experiments are carried out at similar ADRY/reaction center mole ratios, the kinetics are in good agreement. With this model, it should be possible to replace the functional definition of ADRY reagents, that of lipid soluble anions, with a physico-chemical definition. This, in turn, should lead to a better understanding of the chemical nature of the intermediates in the water oxidation reaction.

M-AM-J4 PRIMARY AND SECONDARY ELECTRON ACCEPTORS IN Rp. VIRIDIS

R. J. Shopes and C. A. Wraight, U. of Illinois, Urbana, IL 61801

Reaction centers (RC) from the bacterium Rp. viridis contain both menaquinone (MK) and ubiquinone (UQ). In a series of flashes, oscillations in the formation and disappearance of a stable semiquinone are seen, as is well established for Rp. sphaeroides:

first flash: $Q_AQ_B \xrightarrow{h\nu} Q_A^-Q_B \rightarrow Q_AQ_B^-$ (stable)

second flash: $Q_AQ_B^- \xrightarrow{h\nu} Q_A^-Q_B^- \xrightarrow{2H^+} Q_AQ_BH_2 \xrightarrow{2H} Q_AQ_B$

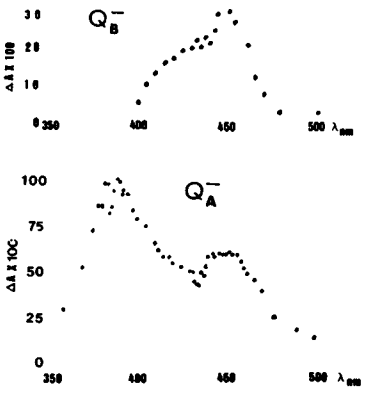

We find that the spectrum of the oscillating semiquinone in Rp. viridis RCs is consistent with the exclusive involvement of UQ as Q_B, peaking at 450nm ($\Delta\epsilon$ = 6 mM^{-1} after correction for double hits) with a shoulder at 430nm. The spectrum of Q_A^-, obtained by inhibiting electron transfer to Q_B, peaks at 390nm with $\Delta\epsilon$ = 10 mM^{-1}. It is characteristic of MK but also has a pronounced minor peak at 450 nm possibly indicating some involvement of UQ. However, extraction of all the UQ does not diminish the 450mn component of the Q_A^- spectrum, showing this to be a true attribute of MK in situ. When Q_A in RCs from Rp. sphaeroides (normally (UQ) is replaced by MK, the spectrum of Q_A^- resembles that from Rp. viridis. We conclude that in Rp. viridis the primary quinone is MK only. NSF support

M-AM-J5 REACTION CENTER TRIPLET STATE IN PHOTOSYSTEM II

A.W. Rutherford, K. Satoh* and P. Mathis (Intr. by J. Coursaget) DB-SBPH, CEN Saclay, 91191 Gif-sur-Yvette cédex, France, *Dept Biol. Okayama University, Japan

The PS II reaction centre triplet is thought to be formed by the following photochemistry at low temperature : $P_{680}PhQ^- \xrightarrow{h\nu} P_{680}^+Ph^-Q^- \rightarrow {}^3P_{680}PhQ^- \rightarrow P_{680}PhQ^-$. The formation of the triplet is dependent upon the redox state Q, the primary quinone acceptor, and Ph, the pheophytin acceptor. The decay kinetics of the triplet have been measured in a purified PS II preparation by epr following flash excitation. Approximate t½ for the triplet sublevels were as follows x peak : 0.7 ms, y peak : 1.0 ms, z peak : 4.2 ms. Under similar conditions changes have been observed by flash absorption spectroscopy. Time resolved spectra in the red and near infrared show a negative peak at 680 nm and a positive peak at 760 nm. This change is characteristic of a Chl triplet and may be due, at least in part, to the P_{680} triplet state. The t½ for this absorbance change is multiphasic with an average value of approx. 0.9 ms. Assuming the extinction coefficient of the triplet is similar to that of P_{680}^+ at 820 nm the amount of centres exhibiting the triplet state after a flash has been estimated to be approx 5 %. However preliminary epr studies indicate that the yield of triplet can vary greatly depending upon the conditions used to prepare the PS II centres. Possible explanations include a) a detergent-induced change in the route of decay of $P_{680}^+Ph^-$ from a fluorescence or heat generating pathway to a triplet route and b) a detergent induced dislocation of a carotenoid which normallly quenches all the triplet chlorophyll soon after it is formed.

M-AM-J6 THE INITIAL STAGES OF ATP SYNTHESIS ASSOCIATED WITH PHOTOSYSTEM I AND PHOTOSYSTEM II PARTIAL REACTIONS. Susan Flores and Donald R. Ort, Department of Botany, University of Illinois, Urbana, IL 61801.

In spinach lamellar membranes, ATP synthesis associated with electron transport from H_2O to methylviologen or to ferricyanide is fully efficient after only a small number of saturating single turnover flashes. 20 flashes given at 10 Hz gave an ATP/$2e^-$ of approximately 0.8 - 1.1, a value comparable to the steady state efficiency. However, when electron transport was blocked by DBMIB the ATP/$2e^-$ associated with reduction of PS II acceptors such as DAD_{ox} or dimethylquinone was 0.2 - 0.3, much less than would be expected given the yield for the overall chain. However PS I, assayed as durohydroquinone→MV, supported phosphorylation efficiencies greater than 0.5.

The unexpectedly low efficiency of PS II driven phosphorylation was investigated futher, and appears to be due to an inability to build up a sufficiently energetic protonmotive force. If phosphorylating electron transport through PS II was preceded by 20 turnovers of the whole chain, the subsequent system II ATP/$2e^-$ was about 0.5. The efficiency of PS II could also be improved by adding a ΔpH which was in itself insufficient to make ATP. Initial results suggest that the additional ΔpH was not required to activate coupling factors not normally activated by PS II, since inactivation of part of the coupling factor pool by DCCD was less inhibitory of PS II phosphorylation than of phosphorylation associated with the whole chain. At present, we cannot explain why PS II is less tightly coupled, although distance from the coupling factor may be important. Alternatively, the H^+/e^- ratio for PS II may be less than one.

M-AM-J7 A BINUCLEAR Mn PROTEIN ISOLATED FROM SPINACH THYLAKOIDS. Daniel A. Abramowicz and G. Charles Dismukes, Chemistry Department, Princeton University, Princeton, NJ 08544.

A binuclear Mn protein, implicated as the O_2 evolving enzyme, was isolated from spinach thylakoids by lysing. The purified Mn protein has an apparent MW=67-59 kM_r on SDS-PAGE and low, variable Mn content. When chemical oxidants were included in the isolation medium to preclude reduction of high valent Mn to the labile Mn^{+2} state, the yield of Mn bound to the protein increased to a maximum of 2.0 ± 0.25 atoms. The protein also contained 0.8 ± 0.5 atoms Fe. The protein has an optical absorption peak at 420 nm with ε = 25-50,000 $cm^{-1}M^{-1}$. The EPR spectrum of the isolated protein (9.4 Ghz, 4.2 K) is given. Five prominent transitions are seen between 0 and 1 Telsa. A resolved hyperfine splitting of 55G (inset) on the two central fine structure peaks is strong evidence that this signal arises from at least two Mn ions in an $S \geq 1$ spin state. We have observed these same EPR spectral features in spinach thylakoids and whole cells of the green alga Scenedesmus obliquus when poised in the S_2 = 1 Kok state. The EPR spectral features can be modeled by two exchange coupled Mn(III) ions. This oxidation state of the enzyme appears to be one equivalent less oxidized than the (III,IV) state produced in spinach chloroplasts by single flash photooxidation (Dismukes and Siderer, 1981, PNAS 78, 274-278). Supported by USDA-CRGO and the Searle Scholars Fund.

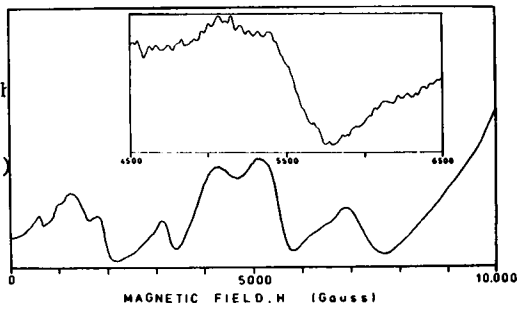

M-AM-J8 THE FUNCTION OF THE QUINONE POOL IN PHOTOSYNTHETIC ELECTRON TRANSPORT
M.S.Snozzi and A.R.Crofts,Department of Physiology and Biophysics, University of Illinois, Urbana

Chromatophores from Rps. sphaeroides contain about 30 ubiquinone molecules per RC. Previous models of photosynthetic electron transport involved only a small number of bound quinones. A new model (1) explains the kinetic behavior of the system, but also suggests that the whole quinone pool is involved in photosynthetic electron transport. The model postulates that, in the presence of antimycin A, reduction of cyt b_{561} can occur only through reaction of QH_2 at a quinol oxidase site catalysing the reaction: $QH_2 + \{FeS^+ b_{566} b_{561}\} \longrightarrow Q + \{FeS\ b_{566}\ b_{561}^-\} + 2H^+$. The rate of reduction of cyt b_{561} is determined by the rate of oxidation of QH_2, which depends on $[QH_2]$. The speed up of b_{561} reduction as E_h is lowered from 200 to 100 mV is due to the change in $[QH_2]$ on reduction of the pool, rather than the reduction of a bound Q_z as previously postulated. To test the model, reduction kinetics of b_{561} at different E_h have been analyzed. Plots of $\ln QH_2/b_{561}^{ox}$ vs. time gave a straight line, as expected by the model. Values of k_2 derived from those plots were around $2.5 \cdot 10^5$ M^{-1} s^{-1} for the E_h range of 250 - 140 mV. Below 130 mV the measured k_2 values changed drastically, indicating that below this potential the second order reaction was no longer the only rate limiting process. The model is supported by the fact that above 200 mV, where the quinone pool is almost completely oxidized, the rate of cyt b_{561} reduction was doubled by producing two QH_2 per b-c-complex using two flashes <1 ms apart. The rate increase after two flashes versus one flash diminished with lower E_h; at 110 mV, where about 10 chemically reduced quinols are present before the flash, no increase of the reduction rate with two flashes was observed.

1) Crofts,A.R., Meinhardt,S.W., Snozzi,M., Jones,K.R. (1982) 2nd EBEC Short Reports, pp 327-328

M-AM-J9 QUINOL OXIDATION IN SPINACH CHLOROPLASTS. M.A. Selak and J. Whitmarsh, Department of Botany, USDA/ARS, University of Illinois, Urbana, Illinois 61801.

The function of the cytochrome b/f-Rieske complex in chloroplasts has been investigated by spectroscopic measurements of the electrochromic shift at 515nm and cytochrome b6 and f redox changes. Duroquinol in the presence of DCMU was used to support the PSI driven reaction using single-turnover flashes. Under these conditions the rise of the electrochromic shift is composed of both a fast and a slow kinetic phase with each component representing approximately one-half of the total absorbance change at 515nm. The fast phase arises from the primary charge separation in PSI and the slow phase is believed to arise from a second electrogenic step mediated by the cyt b/f-FeS complex. DBMIB completely abolishes the 515-slow phase, cytochrome b6 turnover, and blocks cytochrome f rereduction by preventing plastoquinol oxidation. In the presence of HQNO the slow phase of the electrochromic shift is completely abolished while the reduction of cytochrome b6 remains rapid and the extent is enhanced three-fold. These results demonstrate that the electrogenic step associated with quinol oxidation is subsequent to the reduction of at least one cyt b_6. The enhanced reducibility of cyt b upon illumination in chloroplasts in the presence of HQNO is analagous to the so-called "oxidant-induced reduction" of mitochondrial cytochrome b. A comparison of the rate of reduction of cytochrome b6 with that of cytochrome f in the presence of HQNO indicates that quinol oxidation may proceed in a stepwise manner with the first electron going to cytochrome b6 and the second going to cytochrome f via the Rieske FeS center. These data indicate that under the above conditions an electrogenic Q cycle is functional in the main electron transfer pathway in chloroplasts.

M-AM-J10 MEASUREMENT OF THE STATE OF REDUCTION OF THE PRIMARY UBIQUINONE ACCEPTOR IN BACTERIAL PHOTOSYNTHESIS M. C. Woodle, P. L. Bustamante, A. Anderson and P. A. Loach, Dept. Biochemistry, Molecular Biology and Cell Biology, Northwestern University, Evanston Illinois, 60201, USA.

The formation of ubisemiquinone anion has been observed in isolated reaction center systems and is thought that it can result from the reduction of the primary ubiquinone acceptor under appropriate conditions. As a result of these studies, it is usually assumed that in the in vivo system the primary ubiquinone also undergoes reduction to the semiquinone anion. However, from evidence in our laboratory we have suggested an alternative scheme of two-electron reduction of the primary ubiquinone (1). If ubiquinone is normally reduced by one electron to its anion radical, it should be possible to directly measure absorbance changes in the ultaviolet and visible regions of the spectrum attributable to this species. To investigate this question, we have developed instrumentation for the quantitative measurement of light-induced absorbance changes from 250 nm to 950 nm at liquid nitrogen temperatures. Measurements were made on chromatophores and benzene-extracted chromatophores from R. rubrum, chromatophores and reaction centers from the G-9 mutant of R. rubrum, and R. sphaeroides R-26 reaction centers. These were compared to room and low temperature difference spectra of ubiquinone and its reduced states in several solvent systems. In addition, low temperature absorbance spectra of bacteriochlorophyll and bacteriopheophytin were measured. From these comparisons, we have assigned each part of the complex set of absorbance changes to individual components of the reaction center. As a result of this evaluation, no evidence for formation of a stable ubisemiquinone anion in vivo was obtained with either continuous or flash illumination.

1. Loach, P.A. (1976) In "Progress in Bioorganic Chemistry", Kaiser and Kedzy Ed., Vol IV, p89-192.

M-AM-K1 AN ACCESSIBLE CHYMOTRYPTIC SITE IN THE NUCLEOSOME CORE, Nancy Rosenberg and Randolph Rill, M. D. Anderson Hospital and Tumor Institute, University of Texas System Cancer Center, Physics Department, Houston, Texas 77030, and The Institute of Molecular Biophysics, FSU, Tallahassee, Fl. 32306.

α-chymotrypsin was used to probe the non-basic accessible surface of the nucleosome core. Electrophoresis of histones from partially proteolyzed cores on 18% polyacrylamide gels containing SDS showed that H3 was rapidly converted to partial histone, CP1, 112 residues long, by the enzyme. Comparative electrophoresis performed on gels containing 8m Urea, 5% acetic acid, and 6 mM triton X-100 established that other core histones were essentially resistant to digestion until the majority of H3 was degraded. HPLC peptide analyses confirmed that the major chymotryptic product, CP1, was derived from H3 and had an intact carboxy terminus. HPLC analyses of dansyl amino acids derived from CP1 made it possible to assign leucine 20 as the preferential chymotryptic cleavage site in H3. Second dimension electrophoresis further confirmed this site to be the only accessible chymotryptic site in native cores. The effects of perturbation at this site were studied by a variety of physical biochemical techniques.

M-AM-K2 SALT-INDUCED DISSOCIATION OF NUCLEOSOMES. T. D. Yager and K. E. van Holde, Department of Biochemistry and Biophysics, Oregon State University, Corvallis, OR 97331

We have prepared chicken erythrocyte nucleosomes lacking proteins other than inner histones, and containing long DNA. The distribution of DNA lengths is approximately Gaussian, with $\bar{x} \pm \sigma = 190 \pm 15$ bp. No DNA < 155 bp is present. The stability of these nucleosomes in high salt was studied by ultracentrifugation and nucleoprotein gel electrophoresis. We find (i) centrifugation of concentrated nucleosomes through a sucrose gradient in 50 mM NaCl, followed by incubation at a nucleosome concentration (C_n) of 730 nM yields in subsequent analytical centrifugation a 10.5 S nucleosome boundary (90%) and a 5.5 S boundary (10%). Free DNA sediments at 5.5 S. On nucleoprotein gels, the minor component moves and silver-stains as free DNA. (ii) In 0.5 M NaCl, the homogeneous 5.5 S boundary increases from 10% to 30% as C_n decreases from 190 nM to 60 nM. (iii) In higher salt, the slow boundary is inhomogeneous, ranging from 5.5 S to 7.5 S (0.75 M NaCl) or to 9 S (1 M NaCl) suggesting non-specific association of histones with DNA. As C_n is lowered from 130 nM to 60 nM in 0.75 M NaCl, the slow boundary increases from 50% to 60%. In 1 M NaCl, only the slow boundary is seen at all C_n. (iv) The fast boundary has a relatively constant S from 0 to 0.75 M NaCl; at most a decrease of 15% is seen. (v) In high salt sucrose gradients, two bands are seen. The faster contains DNA and inner histones, the slower only DNA. We conclude that salt causes nucleosome dissociation rather than unfolding.

M-AM-K3 CHARACTERIZATION OF THE 10 TO 30 nm TRANSITION IN CHROMATIN USING FLOW BIREFRINGENCE AND VISCOSITY **Rodney E. Harrington, Department of Biochemistry, University of Nevada, Reno.** **Work supported by NSF research grant PCM 7905609.**

We have studied the cation induced transition in chicken erythrocyte chromatin ∿30 to ∿50 nucleosomes in length from the 10 nm filament to the 30 nm solenoid over the range (Mg^{++}) 0 to 0.1 mM using flow birefringence and viscosity measurements conducted at very low velocity gradient and concentration conditions. The sign of the birefringence was found to be negative over this (Mg^{++}) range, and its numerical magnitude decreased with solenoid formation. The transition appeared complete at (Mg^{++}) <∿ 0.6 mM. No temperature dependence of these results was observed over the range 4° to 22°C. The significance of these results and their relation to other published studies will be discussed.

M-AM-K4 EXPERIMENTAL VERIFICATION OF A PREDICTIVE MODEL OF CHROMOSOME CONDENSATION. John P. Langmore (Intr. by Robert Zand) Biophysics Research Division, The University of Michigan, Ann Arbor MI 48109.

There is a well known correlation between chromosome condensation and transcriptional inactivity. Studies of nuclei in vitro have revealed a divalent ion-dependent reversible phase transition between the decondensed and condensed states of chromosome fibers. Although several investigators have noted the similarities between these condensation phenomena in vitro and those apparently involved with gene regulation in vivo a theoretical basis for the condensation has never been proposed. We suggest that the counterion condensation theory of Manning can be used to describe and predict the ionic dependence of the phase transitions. The transitions can be quantitatively measured by using a) low angle x-ray scattering and b) Percoll pycnometry. These two techniques provide independent measures of the average distance between chromosome fibers. The quantitative agreement between the theoretical predictions and the experimental results is very good for a variety of monovalent and divalent cations. This result indicates that non-specific polyelectrolyte effects dominate the transition in vitro, and that the physical state of the chromosomes fibers in vivo is close to the midpoint of the observed transition. Deviations from the normal polyelectrolyte behavior of chromosome fibers are being investigated as a method to determine the roles that changes in chromosomal protein composition or modification play in the physical state of chromosomes.

M-AM-K5 DNA, PROTEIN, LIPID AND WATER CONTENT OF CHROMOSOMES AND CHROMATIN AT VARIOUS LEVELS OF DISSOCIATION. Arthur Cole, Douglas Vizard, Ruthann Langley* and Margaret Hall*. The University of Texas System Cancer Center, Houston, Texas 77030.

Chromosomes and chromatin from labeled synchronized CHO cells were isolated to determine the amount and type of proteins and lipids which co-sedimented with DNA following various purification and dissociation protocols. Four major classes of proteins were defined: loosely bound proteins, salt-dissociable proteins, protease digestable proteins and residue proteins. The residue proteins consisted of 2% of the cell proteins and remained associated with both mitotic and interphase DNA "unit" structures after extensive salt, protease and detergent treatments. In addition about 2% of the choline labeled cell lipids were found associated with unit structures. In sucrose density gradients unit structures exhibited $S_{20,w}$ values of about 300 S and buoyant density values of 1.11 g/cm^3. This surprisingly low density suggested that a relatively large amount of water of hydration was associated with the unit structures. The various classes of chromosomal proteins are being characterized by gel electrophoresis and the lipids characterized by using different lipid labels. Supported in part by DOE contract DE-AS05-76EV0-2832.

M-AM-K6 STRUCTURE OF TOBACCO MOSAIC VIRUS AND STRAINS BY FIBER DIFFRACTION. Keiichi Namba and Gerald Stubbs, Rosenstiel Center, Brandeis University, Waltham, MA 02254.

The structure of tobacco mosaic virus (TMV) has been studied by X-ray fiber diffraction methods. The TMV particle is a long rod, 3000 Å x 180 Å, with 2100 protein subunits in a helical array and a single RNA molecule following the basic helix. The self-assembly process of TMV has been investigated by many groups, and a complicated pathway has been described. However, the method of recognition of a specific RNA sequence to initiate assembly is not yet understood, nor is it known how RNA binding switches the disk precursor to the virus into the helical state. More detailed knowledge of the molecular structure should answer these questions.

The structure of the *vulgare* strain of TMV was determined at 4 Å resolution some years ago. We are using newly developed methods of data processing and phase determination to improve and extend this structure, and to study other strains such as aucuba and U2. U2 is of particular interest because of major differences in the nature of its RNA binding site. Modification of Makowski's angular deconvolution method allows us to measure small deviations from linearity in the layer lines (splitting), and more reliable intensities. The deviations provide additional phase information, independent of that from the intensities, reducing the number of derivatives needed to reach a given resolution. A solvent flattening method is used to further refine the electron density maps. These procedures yield maps of higher quality and resolution than have been available previously, and therefore allow more reliable interpretations to be made.

M-AM-K7 PREPARATION AND PROPERTIES OF PARTIALLY ASSEMBLED TOBACCO MOSAIC VIRUS. Mary L. Adams and Todd M. Schuster, Biological Sciences Group, Biochemistry & Biophysics Section, University of Connecticut, Storrs, CT 06268.

Self-assembly of Tobacco Mosaic Virus (TMV), especially during the later stages, has sometimes been investigated using partially assembled rods (PARs) of various lengths as starting material. We have undertaken a study of the PARs themselves, without the addition of extra protein, in order to characterize them and further investigate the self-assembly process. PARs were formed at 20°C in 0.1μ KPO_4, 1mM azide pH 7.0 with final concentrations of 0.4 mg/ml RNA and 0.08 to 4.0 mg/ml coat protein. TMV protein (TMVP) was added to the RNA in the form of "20S" (~85%) and 4S (~15%) equilibrium mixture and the rate of formation of the PARs was monitored by light scattering changes. Electron microscopy revealed rod lengths of 40 to 260 nm (depending on TMVP concentration). Sedimentation velocity measurements showed a fairly sharp boundary in each case with $S^{\circ}_{20,w}$ values from ~60S to ~175S. In all cases where less than stoichiometric amounts of TMVP were used (i.e. 20:1 ratio) a boundary sedimenting at ~25S was observed, corresponding to free RNA. All the PARs formed appeared stable for at least several hours at 20° or when cooled to 4° and rewarmed to 20° later. The significance of these findings in relation to TMV assembly studies using PARs will be discussed.

Supported by NIH grant AI-11573.

M-AM-K8 BIOPHYSICS OF BACTERIOPHAGE P22 ASSEMBLY IN VITRO. S. Rajalakshmi and Philip Serwer, Dept. of Biochemistry, The University of Texas Health Science Center, San Antonio, TX 78284.

All studied DNA bacteriophages package DNA "in vivo" in a preformed, DNA-free procapsid. Bacteriophage P22 procapsids have been isolated by electrophoresis and have been used for the packaging of DNA "in vitro". As previously found for a bacteriophage T7 procapsid, the P22 procapsid had a negative zeta potential which: (1) was higher in magnitude than the negative zeta potential of the mature bacteriophage capsid, (2) had a microheterogeneity. The efficiency of "in vitro" DNA packaging was an increasing function of the magnitude of the procapsid zeta potential. It was also shown that the efficiency of P22 "in vitro" DNA packaging was an increasing function of the concentration of sucrose present. Dextrans 10, 40 and 500 were, at any percentage, more efficient than sucrose in stimulating packaging. However, glucose, sorbitol and smaller polyols did not stimulate packaging; these latter compounds did not inhibit packaging stimulated by dextrans. The above observations suggest that non-penetration of some particle, possibly a capsid, is required for the stimulatory effect of the above compounds on packaging. DNA packaging has been made efficient enough so that it was observed by: (1) DNA staining of capsid-migrating particles after agarose gel electrophoresis, (2) high resolution agarose gel electrophoresis of DNAase-resistant DNA after release from capsids. It was found that particles with completely packaged, mature-length DNA appeared 1.5 min after the initiation of packaging at 35°C; infective particles appeared 0.5 min later. Thus far no evidence of partially-packaged DNA has been obtained, suggesting that entry of DNA into the capsid takes even less than 1.5 min.

Supported by NIH (Grant GM24365) and the Robert A. Welch Foundation (Grant AQ-764).

M-AM-K9 ANALYSIS OF THE SALT DEPENDENT KINETICS OF OPEN-COMPLEX FORMATION BY *E. coli* RNA POLYMERASE AT THE lacUV5 PROMOTER.

Martin E. Mulligan and William R. McClure; Dept. of Biological Sciences, Carnegie-Mellon University, 4400 Fifth Ave., Pittsburgh, PA 15213.

We have studied the kinetics of open-complex formation on the lacUV5 promoter, as a function of salt concentration, in order to define, more precisely, the reaction intermediates on the pathway to open-complex formation. Measurement and comparison of the values of the forward and the reverse rate constants, in the range 0.04-0.2M KCl, suggests that the functional two-step mechanism is inadequate in describing the physically relevant pathway. Rather, a three-step mechanism is more appropriate:

$$R + P \overset{K_B}{\rightleftharpoons} C_1 \underset{k_{-2}}{\overset{k_2}{\rightleftharpoons}} C_2 \underset{k_{-3}}{\overset{k_3}{\rightleftharpoons}} RP_o$$

In this scheme, the enzyme binds rapidly to the promoter (under all salt conditions) to form an initial complex (C_1), with the release of 4-5 counterions. The isomerisation of C_1 to C_2 was found to have negligible salt dependence, whereas the isomerisation of C_2 to the open-complex (RP_o) involves 10 ion-pairs. Thus, under different salt conditions, either or both of the isomerisation steps may be rate limiting.

These results are consistent with sequential binding, recognition and DNA melting steps in the pathway to the formation of active open-complexes at promoters.

M-AM-K10 NUCLEASE MAPPING OF ESCHERICHIA COLI INITIATION FACTOR 3 INTERACTIONS WITH THE 49-NUCLEOTIDE 3' TERMINAL CLOACIN FRAGMENT OF 16S RNA. Eric Wickstrom, Department of Chemistry, University of South Florida, Tampa, Florida 33620

The 3' end of 16S RNA is the site of basepairing with the Shine-Dalgarno sequences of procaryotic mRNAs, and is also part of the 30S ribosomal binding domain of initiation factor 3 (IF3) and ribosomal protein S1, which both greatly stimulate mRNA binding to 30S ribosomal subunits. Analysis of the interactions of IF3 with the 3' terminal 49-nucleotide fragment of 16S RNA produced by cloacin DF13 treatment of 70S ribosomes was therefore of interest.

The cloacin fragment was prepared from 70S ribosomes (the kind gift of Dr. A.J. Wahba) cleaved with cloacin DF13 (the kind gift of Dr. F.K. de Graaf), and 5'-^{32}P labeled. The fragment was incubated 5 min. at 37° in 40 mM Tris-HOAc, pH 7.4, 100 mM NaCl, 1 mM $Mg(OAc)_2$, 1 mM $ZnSO_4$, with or without IF3 or ribosomal protein S1 (the kind gift of Dr. A.J. Wahba), then reacted a further 5 min with nuclease S1, RNase T1, or RNase A. Reaction mixtures were analyzed on denaturing polyacrylamide gels and autoradiographed. IF3 appears to protect some residues near the 5' end of the fragment (U2, A6, A9, and A10) from nuclease S1, and potentiates S1 attack on others (G1, G4, C8, G11, G12, U13, G24, G36, G37, and C40). A series of equimolar reactions at increasing dilution imply a binding constant of about 2×10^7 M^{-1}. The interactions are only moderately reduced by increasing ionic strength, up to 0.4 M NaCl, suggesting that the interactions are not primarily ionic. Surprisingly, no such binding by ribosomal S1 could be detected, with up to a 50-fold excess of ribosomal S1 over RNA.

M-AM-K11 DNA JUNCTION SITE SEQUENCES OF A TRANSPOSON-LIKE MITOCHONDRIAL PLASMID. Donald J. Cummings and Richard M. Wright. University of Colorado Health Sciences Center, Denver, CO 80262

During cellular senescence, specific regions of mitochondrial DNA from the filamentous fungus Podospora anserina are excised and amplified. The most frequently occurring of these autonomously replicating plasmids, termed α-sen DNA is 2600 bp in its monomer form and contains most of the oxi3 gene. During senescence this plasmid has been found integrated into the nuclear genome. We have cloned this plasmid and have sequenced the excision site junction sequences and compared them directly with the young mitochondrial genome (Hae 23 and Hae 14).

```
Hae23 3'      CCGGTTCCACAAGTTATATAACGTC  CACGCGGCAAATTGCACGCAAAATTCAGG  5' Msp

                                        J1

α Hinf  <--ATATATCTGATTCCTGACCGACGAATAGGATG  CACGCGGCAAATTGCACGCAAAATTCAGG  5' Msp
                                        J2

Hinf  <--ATATATCTGATTCCTGACCGACGAATAGGATG  TATTGGTTAATATATTATCGTAGTAAGTC-->  5'Hael4
```

The pertinent features of these sequences will be discussed.

M-AM-Pos1 BROWNIAN DYNAMIC ANALYSIS OF ION MOVEMENT IN MEMBRANES. Kim Cooper, Eric Jakobsson, and Peter Wolynes, Department of Physiology and Biophysics, Program in Bioengineering, and Department of Chemistry, University of Illinois, Urbana, Illinois 61801.

It has been known since the work of Einstein in 1905-8 that the microscopic basis of all processes involving thermal motion of dissolved or suspended particles is Brownian motion. The widespread availability of digital computers has made it practical to apply Brownian dynamics to many-particle problems, such as ion permeation in membranes. This method treats the system in more detail and with fewer approximations than either bulk diffusion theory or absolute rate theory. We have used Brownian dynamics to consider the problem of single-file ion movement through membrane channels. We find that constant-field electrodiffusion results are reproduced to good accuracy when the electrostatic repulsion term between ions is turned off (obviously impossible experimentally). When the electrostatic repulsion term is turned on, we find the results to be different from the corresponding electrodiffusion calculation (simultaneous solution of the Nernst-Planck and Poisson equations). The apparent reason for this discrepancy is that electrodiffusion theory treats the charges as "smeared-out" spatial distributions with each element of the distribution repelling each other element. In the Brownian dynamic theory with reasonable parameters, there is only one ion in the channel a large fraction of the time. Since this ion does not repel itself, its behavior as it moves about in the channel does not correspond to that of the distributed charge described in electrodiffusion theory.

Support was received from the Bioengineering Program and the Research Board of the University of Illinois at Urbana-Champaign.

M-AM-Pos2 WATER AND IONS IN PORES. Hladky,S.B., Dept. of Pharmacology, Cambridge, ENGLAND CB2 2QD

Ions pass through gramicidin pores by 1st ion entry,transfer, and exit or by 2nd ion entry, 1st ion exit, and transfer (Urban,Hladky&Haydon, BBA 602,331,1980). Ions and water cannot pass inside the pore, thus water must also move, n_s or n_d molecules/ion respectively. With a gradient of an impermeant, Δc_s , the water transferred per charge may depend on direction in the 2ion mode, thus n_d' and n_d'' must be specified with $n_d=(n_d'+n_d'')/2$. The number measured by electroosmosis or streaming potential measurements is $n=(n_sB+n_dDa)/(B+Da)$ where D and B are the rate constants for 2nd ion entry and 1st ion exit. The open circuit water flux is (in molecules/sec)

$$\phi_w^{o,c}=\mathcal{A}P_o X_{oo}\Delta c_s+\frac{ADa^2}{B+Da}X_{oo}\frac{(n_s-n_d)^2}{2}\bar{V}_w\Delta c_s+\frac{ADa^2}{2B}X_{oo}(n_d'-n_d'')$$

where P_o is the no-ion water permeability of a pore, X_{oo} the probability pores contain no ions, A the rate constant for 1st ion entry, and $\mathcal{A}$ is Avagadro's No. The short circuit current (scc) equals the streaming potential times the conductance. The short circuit water flux exceeds the open circuit flux by n(scc)/e. Application of the theory to the data of Dani&Levitt (Biophys.J. 35,485,1981) yields first binding constants close to those reported, but shows the data to be consistent with 2nd ion binding. In doubly occupied pores, the ions repeatedly exchange with the solutions at each end, thus the water may do the same, which may explain the high tracer flux of water reported by Finkelstein&Andersen (J.Memb.Biol. 59,155,1981) using 2M NaCl.

The theory is based on the linear superposition of osmotic and electrical gradients and is thus restricted to the same range of validity as the expressions from irreversible thermodynamics.

M-AM-Pos3 OPTIMUM DETECTION OF SINGLE-CHANNEL CURRENTS
F.J. Sigworth, Max-Planck-Inst. Biophys. Chemie, Göttingen, F.R.G.

High-resolution analysis of single-channel current recordings is limited by the background noise. For example, sufficiently brief channel-current pulses are indistinguishable from random noise fluctuations. I have analyzed the performance of event-detection and characterization schemes based on linear signal processing. Some results to be presented are:

1. Comparison of the commonly-used Bessel filter with optimum (matched) filters. (The Bessel filter performs quite well.)
2. The probability of detecting "false events" due to noise fluctuations.
3. Calculation of filter and threshold settings yielding the maximum probability of event detection.
4. Distortion of event-duration histograms due to noise effects.
5. Limitations on the simultaneous determination of amplitude and duration of events.
6. Post-filtering of data using a digital Gaussion filter.

M-AM-Pos4 STEADY-STATE CURRENT NOISE FROM THE INTRINSIC GATING OF INWARD RECTIFIER CHANNELS IN NEANTHES OOCYTES. R. Gunning and S. Ciani. Dept. of Physiology, UCLA, Los Angeles, Calif. 90024. USPHS GM 27042-06 and Muscular Dystrophy Assn.

Steady-state inward rectifier current noise from the eggs of the marine polychaete Neanthes arenaceodentata was recorded under voltage-clamp conditions. Lorentzian-shaped power spectra with corner frequencies near 1Hz and zero-frequency asymptotes of $1\text{-}5\times10^{-23}A^2/Hz$ were obtained for test potentials 15-45mV positive to E_K in solutions containing 10-40mM Ko. The source of this noise is identified with the gating of the inward rectifier channels based on 1) the corner frequencies match well with the time-constants of inward rectifier current relaxation under similar experimental conditions, 2) power spectra in the form of Lorentzians are not seen when $V=E_K$ or when the inward rectifier open-channel probability is zero. The spectra are compatible with the predictions of a three-state kinetic model for inward rectification in which the single-channel rectification is independent of voltage and the apparent instantaneous rectification is due to a fast kinetic process. The single-channel conductances derived from this interpretation were proportional to the .6 power of the external potassium concentration, as are the macroscopic steady-state conductances. The single-channel conductance obtained when $Ko \lesssim 40mM$ was 8pS, in good agreement with the values obtained in experiments where gating is provided by blocking ions (Ohmori, 1980, Journal of Membrane Biology, 53:143; Ohmori, Yoshida & Hagiwara, 1981, PNAS, 78:4960).

M-AM-Pos5 SIMULTANEOUS ALTERATION OF ION SELECTIVITY AND VOLTAGE DEPENDENCE BY REACTING THE CHANNEL FORMER, VDAC, WITH SUCCINIC ANHYDRIDE. Charles Doring and Marco Colombini, Department of Zoology, University of Maryland, College Park, MD 20742

The possibility that the same structure in a voltage-dependent channel may serve both as a selectivity filter and a voltage sensor was tested by using the amino group reagent succinic anhydride. VADC (the voltage dependent anion-selective channel in mitochondria) was incorporated into planar phospholipid membranes from a Triton X100 solution in the presence of 1 MKCl 5mM $CaCl_2$. Succinic anhydride dissolved in dimethylsulfoxide was added to the aqueous solution bathing the membrane together with sufficient $NaHCO_3$ to control the pH. A rapid non-reversible loss of voltage-dependent-conductance-decrease occured which was dependent on the dose of succinic anhydride. At least 70 percent of the voltage-dependence could be eliminated. In the presence of a salt gradient (1 MKCL vs 0.1 MKCl) the selectivity of the channel shifted from $U_{Cl}/U_K = 1.6$ (Nernst-Planck) $P_{Cl}/P_K = 1.9$ (Goldman-Hodgkin-Katz) to $U_K/U_{Cl} = 3.4$ and $P_K/P_{Cl} = 4.8$ upon addition of the anhydride. This degree of selectivity change was also dose dependent. Considering the large size of the channel (40 Å in diameter), it is reasonable to conclude that amino groups within the channel are responsible for the preference for anions and the conversion of some of these to carboxyl groups by the anhydride results in the selectivity reversal. These same amino groups may also be involved in sensing the voltage thus inducing voltage dependence. Supported by NIH grant GM28450.

M-AM-Pos6 SPERM ACTIVATED CHANNELS IN ASCIDIAN OOCYTES, Louis J. De Felice, Brian Dale, Dept. of Anatomy, Emory University, Atlanta, Georgia, and Stazione Zoologica, Naples, Italy.

One of the first events of activation in the sea urchin oocyte is a decrease in resistance of the plasma membrane accompanied by an increase in voltage noise [(Dale, B., DeFelice, L.J. and Taglietti,V., Nature 275, 217-219 (1978); DeFelice, L. J. and Dale, B., Dev. Biol. 72, 327-341, (1979)]. By analogy with similar events in other membranes, these changes were interpreted as representing the activation of non-specific ionic channels. The purpose of the present report was to see if a comparable change occurs during the activation of ascidian oocyte and, if so, to study the properties of these hypothesized channels directly. All experiments were carried out at room temperature and in natural sea water using gametes of the ascidian Ciona intestinalis collected in the Bay of Naples. The gametes were obtained by dissection. To expose the plasma membrane the chorion was removed using fine steel needles. Nude oocytes are about 100 μm in diameter and usually stick to the bottom of the glass recording chamber. Fire polished electrodes filled with natural sea water having a resistance of 2-5MΩ and a tip diameter less than 1 μm were used for recording channel currents. Gigaohm seals were obtained by standard techniques. Fertilization channels in the ascidian oocyte have a single channel conductance of 400pS, a reversal potential of 0 mV and a mean open time of 2 to 30 msec, depending upon membrane potential. The open channel probability is 0.1 near 0 mV and increases as the membrane is depolarized. These channels are among the largest ever observed in a biological membrane. We raise the possibility that the activation of non-specific channels may be a universal event in oocyte stimulation.

M-AM-Pos7 STRUCTURE ACTIVITY RELATIONSHIP OF SAXITOXIN ANALOGS FROM PROTOGONYAULAX. A. Michael Frace, Sherwood Hall*, D. C. Eaton, and M. S. Brodwick. Dept. of Physiology and Biophysics, University of Texas Medical Branch, Galveston, TX 77550; *Institute of Marine Science, Seward Marine Station, Seward, AK 99664.

The structure-activity relationships of a new series of saxitoxin analogs isolated from dinoflagellates (genus Protogonyaulax) were studied using voltage clamped squid axon. The previously described toxins, gonyautoxins II and III (GTX II and GTX III) and saxitoxin (STX), which are closely related structurally to the new toxins, were also studied. All of the toxins examined selectively blocked I_{Na} without effecting I_K. The new toxins are carbamoyl-N-sulfo-11-α-hydroxysaxitoxin sulfate, the 11-β-epimer, and carbamoyl-N-sulfo-hydroxysaxitoxin, designated as C_1, C_2, and B_1, respectively. Potencies, relative to STX at pH7.7 are: B_1 (0.39), C_1 (0.023), C_2 (0.35), GTX II (0.17), and GTX III (0.49). Both 11-carbon-OSO_3^--β-epimers failed to show complete reversal despite long, sustained wash-off. The addition of (SO_3^-) to the carbamyl arm of STX (B_1) produces only a small decrease in potency suggesting a minor contribution to binding at the 21-nitrogen atom site. Similarly, addition of (OSO_3^-) to the 11-carbon shows only a minor drop in potency explainable by removal of an 11-carbon hydrophobic interaction or by interference with the 12-carbon geminal diol. The second possibility seems more likely, since α-epimers with closer proximity to the diol display less potency than β-epimers. To test the role of the charged 8-carbon guanidinium group, STX was used to block guanidinium currents at constant ionic strength and a 50 mM Ca^{++} concentration. Reduction in K_d was to 21% of control with a K_i for guanidinium of 116 mM. (Supported by NIH grant NS 11963)

M-AM-Pos8 On the origin of the voltage-dependence of monazomycin-induced conductance. J.-L. Mazet, R.U. Muller and O.S. Andersen. Departments of Physiology, Cornell Univ. Med. Center and Downstate Med. Center (SUNY).

Monazomycin (Mon), a polyene-like antibiotic (MW = 1352), induces conductance in lipid bilayers by forming oligomeric channels that are quite selective for univalent cations. The steady-state conductance (G_{ss}) depends strongly on the aqueous Mon concentration ($G_{ss} \propto [Mon]^6$) and is a steep exponential function of the membrane potential (V; G_{ss} changes e-fold for 4-5 mV changes of V). It has been suggested that the voltage-dependence arises from trans-membrane movements of Mon's positively charged amino group (pKa $\gtrsim$ 9.5) through the applied V gradient. We report here that 1) An uncharged Mon derivative, N-acetyl Monazomycin (NAM), is also able to induce conductance changes. 2) The dependence of G_{ss} on V is dramatically reduced for NAM; G_{ss} changes e-fold for $\sim$ 50 mV changes of V, averaged over the range $-75 \lesssim V \lesssim 75$ mV. 3) Preliminary measures of the variation of G_{ss} with [NAM] indicate that it is very similar to that for Mon. 4) NAM has nearly the same "potency" in uncharged films as Mon in that equal concentrations give rise to very similar values of G_{ss} near V=0. We conclude that the dependence of G_{ss} on V for Mon is indeed due to the existence of the charged amino group. We thank Dr. Noburu Otake University of Tokyo) for making this research possible by synthesizing the N-acetyl monazomycin. This work was supported in part by funds for J.-L.M. from CNRS (France) and NSF (USA) and by Grant GM-21342 to O.A.S.

M-AM-Pos9 GATING KINETICS OF BATRACHOTOXIN-MODIFIED SODIUM CHANNELS IN NEUROBLASTOMA CELLS DETERMINED FROM SINGLE-CHANNEL MEASUREMENTS. Li-Yen Mae Huang*+, Nava Moran+, and Gerald Ehrenstein+, +NINCDS, NIH, Bethesda, MD 20205 and *Marine Biomedical Institute, University of Texas Medical Branch, Galveston, TX 77550.

The gating mechanism of batrachotoxin (BTX)-modified sodium channels was studied in neuroblastoma cells NG108-15 using the patch-clamp method. The single-channel conductance is 10 pS. The histogram of the open-state dwell time could be fit by a single exponential at all membrane potentials. The histogram of the closed-state dwell time could be fit by a single exponential only at membrane potentials more hyperpolarized than -60 mV. These results are consistent with our macroscopic voltage clamp measurements that show first order activation kinetics at hyperpolarized membrane potentials. By contrast, two exponentials were needed to fit the closed-state dwell times at membrane potentials more depolarized than -60 mV. The experimental data can be fit by a model with a single open state, but more than one closed state. The data are not adequate to uniquely determine the closed states, but the data do determine the voltage dependence of the opening and closing transition rates between the open state and the closed state to which it immediately returns. As membrane potential increases, the opening rate increases exponentially and the closing rate decreases exponentially.

M-AM-Pos10 PHARMACOLOGICAL ACTIONS OF A DINOFLAGELLATE TOXIN (T17) ON CRAYFISH SODIUM CHANNELS. James M.C. Huang and Chau H. Wu, Department of Pharmacology, Northwestern University Medical and Dental Schools, 303 E. Chicago Avenue, Chicago, Illinois, 60611.

Experiments using conventional intracellular microelectrodes on crayfish giant axons show that T17 toxin (isolated from the red-tide dinoflagellate Ptychodiscus brevis) causes a 30-mV depolarization. This depolarization was reversed by tetrodotoxin and low sodium, suggesting that the T17 toxin affects primarily sodium channels. Voltage clamp experiments on internally perfused crayfish giant axons confirmed that T17 toxin affects only the sodium channels. Held at a membrane potential of -90 mV, the axon exhibited an increase in inward sodium current upon T17 toxin application. T17 toxin caused the threshold for sodium current activation to shift from -80 mV to -110 mV. The current-voltage (I-V) curve exhibited a W-shape, corresponding to modified and unmodified populations of sodium channels. The toxin depressed the current of the unmodified population. In addition, the reversal potential for the sodium current was shifted by 30 mV in the hyperpolarizing direction. The instantaneous I-V curve also showed a similar shift in the reversal potential. The development of a W-shaped I-V curve followed a similar time course as that of the membrane depolarization of unclamped axons. Neither the falling phase kinetics of the peak current nor the kinetics of the tail current was affected by T17 toxin even at high doses. These results indicate that T17 toxin induces a sodium conductance at the resting potential, thereby causing a depolarization; in addition, the toxin modifies the ion permeability of sodium channels.
(Supported by a grant from Muscular Dystrophy Association).

M-AM-Pos11 CATION SELECTIVITY OF THE PURIFIED RECONSTITUTED SODIUM CHANNEL FROM SKELETAL MUSCLE SARCOLEMMA. J.C. Tanaka*, J.F. Eccleston+ and R.L. Barchi*+. Departments of Neurology* and Biochemistry and Biophysics+, Univ. of Pennsylvania, Philadelphia, PA.

The voltage-dependent sodium channel from rat skeletal muscle was purified and reconstituted into unilamellar PC vesicles. The flux of various labelled cations into vesicles was measured using a quenched flow apparatus following activation of the channel by batrachotoxin (BTX) or veratridine (VER) in the absence of a voltage gradient. Uptake rates for ^{42}K, ^{86}Rb and ^{137}Cs were measured directly in BTX activated vesicles and halftimes for equilibration were determined to be 350 ms, 2.5 s and 10 s respectively. ^{22}Na equilibration occurred within the minimum quenching time of the system (90 ms); an upper limit of 50 ms could be assigned to its halftime. Apparent cation selectivity ratios in BTX activated vesicles were Na (1): K (0.14): Rb (0.02): Cs (0.005). Toxin stimulated influx was blocked by saxitoxin with a K_i of 5×10^{-9} M at 22° C. Rates of cation movement through VER activated channels were much slower with halftimes of 1.0, 1.2, 2.0 and 2.6 min at 36° C for ^{22}Na, ^{42}K, ^{86}Rb and ^{137}Cs respectively giving apparent selectivity ratios of Na (1): K (0.83): Rb (0.50) and Cs (0.38).

The temperature dependence of BTX and VER stimulated cation influx were markedly different. Activation energies for ^{86}Rb and ^{137}Cs influx into BTX activated vesicles were 7.6 and 6.1 Kcal/mol respectively while comparable measurements for these cations in VER activated vesicles were 31 Kcal/mol. Measurements of cation exchange with BTX activated channels may reflect characteristics of an open channel whereas the process of channel opening may be rate limiting when VER is used for activation.

M-AM-Pos12 CURRENT-VOLTAGE RELATIONSHIPS OF SINGLE SODIUM CHANNELS IN NEUROBLASTOMA CELLS. Daisuke Yamamoto, Jay Z. Yeh and Toshio Narahashi (Intr. by Martin Frank). Dept. Pharmacol., Northwestern Univ. Med. Sch., Chicago, IL. 60611.

Instantaneous current-voltage (I-V) relationships for single sodium channels of neuroblastoma cells (N1E-115) have been studied by means of gigaohm sealing, patch clamp technique. Most of the experiments were carried out in the presence of the sodium channel modulator, tetramethrin, which drastically prolongs the open time of single sodium channels (Yamamoto, Quandt and Narahashi, Abstr. Soc. Neurosci., Vol. 8, p. 251, 1982). The prolonged opening allowed us to change the membrane potential to various levels while the channel was kept open. The shape of the instantaneous I-V curve changed depending on the external Ca concentration. At 1.8 mM Ca, the inward current through the single sodium channels increased linearly with hyperpolarization from 0 to -40 mV, but decreased with further hyperpolarization. Thus the I-V curve bended between -40 and -50 mV showing rectification. When the Ca concentration was reduced to 0.18 mM, the I-V curve became linear between 0 and -100 mV, and bended towards the potential axis with further hyperpolarization. A similar change in the I-V curve was also observed by increasing the external Na concentration while keeping the external Ca concentration at 1.8 mM. These findings can be explained by a model in which a Ca ion binds to a site in the sodium channel thereby reducing the inflow of Na ions through the channel. Binding of Ca ions to the Na channel site is strongly voltage dependent. The present result on the single channel conductance accounts for the rectification of the I-V curve observed for macroscopic sodium currents. Supported by NIH grants NS 14144 and NS 14143.

M-AM-Pos13 CURRENT-VOLTAGE RELATIONS OF NORMAL AND FENVALERATE-MODIFIED SODIUM CHANNELS IN CRAYFISH AXONS. Vincent L. Salgado and Toshio Narahashi. Dept. Pharmacol., Northwestern Univ. Med. Sch., 303 E. Chicago Ave., Chicago, IL 60611.

The pyrethroid insecticides drastically modify gating kinetics of sodium channels. Fenvalerate is especially potent, causing the channels to open at the resting potential without inactivation. We have studied the instantaneous current-voltage (I-V) relationships of both normal and fenvalerate-modified sodium channels over a wide range of membrane potentials between -200 and +140 mV in internally perfused, voltage-clamped crayfish giant axons. The instantaneous current in normal sodium channels increased with hyperpolarization reaching a maximum at -50 mV, but decreased with further hyperpolarization, and was completely blocked at -200 mV. When the external calcium concentration was increased from 10 mM to 93 mM, complete block of sodium channels occurred at -100 mV, suggesting a voltage-dependent calcium block of open channels. The fenvalerate-modified channels also showed rectification, but the voltage-dependent block saturated at 80% at membrane potentials more negative than -120 mV. The time constant for the normal channel closure decreased with hyperpolarization, but reached a minimum of 40 μsec at membrane potentials more negative than -100 mV. The closing rate appears to be limited by a voltage-independent process. It is suggested that the observed voltage-dependent block of normal and fenvalerate-modified sodium channels is caused at least in part by calcium ions. Supported by NIH grant NS 14143.

M-AM-Pos14 EFFECTS OF pH AND CALCIUM ON SODIUM CHANNELS IN RABBIT MUSCLE MEMBRANE. G.E. Kirsch, Dept. of Biol. Sci., Rutgers University, New Brunswick, NJ 08854

Recently, denervation of rat skeletal muscle was observed to cause a -10 mV shift in the voltage dependence of sodium channel gating (Pappone, 1980). The present study attempted to extend and corroborate this observation by measuring the effects of external pH and calcium ion concentration on sodium currents in normal and denervated rabbit muscle. In Tyrode's solution, the midpoint of the relationship between peak sodium permeability (PNa) and membrane potential (Em) was (mean, mV, no. of fibers): -51.2, n=10 innervated fibers; and -53.0, n=6 denervated fibers. Thus, negligible shift of the activation curve was observed. The effects of pH and calcium on PNa-Em curves were the same in both denervated and innervated fibers, as well. When analyzed in terms of a voltage-dependent block and a shift of the voltage-dependence of gating (Woodhull, 1973), the pH effect could be described by: voltage dependence of block, δ = 0.26 and pKa (0 mV) = 5.7, n=5. The mean voltage shift required to fit the data ranged from +6.2 to -6.0 mV for pH 5.5 to 10.0, respectively. The calcium effect could be described by δ = 0.30 and Kd (0 mV) = 58.5 mM, n=8. For calcium levels of 50 to 0.1 mM, the mean voltage shift ranged from +14.0 to -16.4 mV. In conclusion, denervation of rabbit muscle does not appear to alter the voltage dependence of sodium channel activation or the response of the channels to altered pH or calcium levels. Furthermore, protons appear to exert a strong, voltage dependent block and to cause small changes in surface potential which can account for the pH-induced changes in the shape of the PNa-Em curve. Calcium ions exert a less potent block; voltage shifts of gating appear to be the predominant effect of calcium. Supported by MDA and NIH NS17799.

M-AM-Pos15 EVIDENCE FOR VOLTAGE SENSITIVE Na CHANNELS IN HUMAN RED BLOOD CELLS. R. B. Gunn and B. E. Scanley, Dept. of Physiology, Emory Univ., Atlanta, GA 30322 and Dept. of Pharm. and Physiol. Sci. Univ. of Chicago, Chicago, IL 60637

Fresh washed red cells were treated for 15 min. at 0°C with 0.1 mM lysolecithin (lyso-PC), then washed thrice in the same medium (140 mM KCl, 10 mM NaCl, 50 mM sucrose, 27 mM glycylglycine pH 7.4) without lyso-PC (Vm≈0 mV). In this medium these treated cells have a high Na self-exchange rate. When placed in 150 mM NaCl at 37°C, the treated cells initially take up NaCl (20-60 mmoles/(kg hemoglobin x min) = 900 times untreated cells). After 1-2 minutes they return to the Na permeability of untreated cells. Increased Na permeability of red cells after treatment with phospholipid vesicles and lysophospholipids has been reported (Huestis JBC 252, 6764, 1977; Bierbaum et al. BBA 555, 102, 1979), but the inactivation of the permeability has not been reported. The cell Na concentration is still far smaller than Na_o when the induced high Na flux is inactivated. Valinomycin (10μM) added to the 150 mM NaCl causes the treated cells to lose 90% of their K over 15 min, increases both the initial net Na influx and the final cell Na content and delays, but does not prevent, the inactivation of the high Na permeability. The net Na influx of treated cells can be prematurely inactivated by increasing K_o when valinomycin is present. The temperature change, incubation time in low Na medium, initial cell volume, 10^{-8}M TTX, 10^{-3} dinitrodisulfonic stilbene or 10^{-4} ouabain do not alter the Na flux. These results suggest that Na^+ is entering as an ion through a voltage sensitive channel that is inactivated by depolarization of the cell membrane. (Supported in part by NIH grant GM 30754)

M-AM-Pos16 LONGITUDINAL STRETCH OF SQUID GIANT AXON. David E. Goldman and Jay B. Wells. Laboratory of Biophysics, NINCDS, NIH at MBL, Woods Hole, MA 02543.

Squid giant axons were mounted in a chamber similar to those used for voltage clamping but modified to permit application of rapid longitudinal stretches to one end, of up to ten percent of axon length in 0.5 msec or more. The stretches were then maintained for varying lengths of time. The other end was fixed to a force transducer which also supported an axial wire and internal electrode. Under such conditions the axon behaved like a mechanical transmission line having a propagation velocity of about 50 m/sec. The measured force increased to a peak value after a delay corresponding to the axon length and then fell to a small steady value for the duration of the holding phase of the stretch. The time constant of the falling phase was two to three msec. The electrical response of the axon was a depolarization which followed closely the rising phase of the stretch. It then manifested further depolarization of subthreshold responses or action potentials analogous to responses evoked by electrical stimulation. Finally, the subthreshold depolarization response decayed to a temporary small hyperpolarization. The application of TTX or the replacement of external Na^+ by choline abolished the active response but had little or no effect on the initial rise or the hyperpolarization. Reduction in stretch rate resulted in reduced depolarization. Very slow stretches were completely ineffective. A simple inference from these observations is that stretching the membrane increases some ion permeabilities. An elementary model of the system mimics the experimental results fairly well.

M-AM-Pos17 STOCHASTIC GATING OF IONIC CHANNELS: THE ROLE OF Ca++ IN INCREASING SENSITIVITY. F.F. Offner, Northwestern University, Evanston, IL 60201

The maximum change in conductance ratio resulting from a voltage change ΔV acting on a gate carrying a charge e is $exp(e\Delta V/kT)$. ΔV is classically assumed to be limited to the change in the voltage across the membrane. I have previously shown that if the stochastic cycling of the gates is rapid as compared to the relaxation of the electric field in the channel, the sensitivity may in fact be much higher (J. Phys. Chem. 84, 2652 (1980)). However, single channel experiments indicate that conformational gating rate is probably of the same order as field relaxation, or even slower, which would reduce sensitivity to the classical value. External Ca++ (or other divalent cations) reduces channel conductance by voltage-dependent adsorption having a very short mean cycle time, probably $<10^{-7}$sec; it may thus have a high voltage sensitivity. The interaction of such adsorbed ions with the electric field in the channel is shown to catalyze the conformational gating, restoring increased voltage sensitivity. Using parameters based on available data, activation curves conforming to Hodgkin-Huxley parameters are readily obtained. While the theory gives no information as to a specific gating mechanism, the much larger energy available to the gates makes a wide variety of mechanisms energetically possible. Supported by NIH Contract NS08137.

M-AM-Pos18 A FUNDAMENTALLY DIFFERENT ACTION POTENTIAL AND Na CHANNEL. L. C. Schlichter, Botany Dep't., Univ. of Toronto, Ontario, Canada M5S 1A1.

Action potentials (AP's) of most excitable cells are produced by Na^+ or Ca^{2+} influx followed by K^+ efflux. Na channels in all excitable cells studied exhibit the same selectivity and kinetics of activation and inactivation, but channels in different cell types vary in their voltage dependence and TTX sensitivity. I report here the existence of an AP with an unusual ionic basis and in which the Na channel differs fundamentally from Na channels of other excitable cells.

AP's in maturing oocytes of the frog, Rana pipiens, were studied using intracellular-recording and voltage-clamping techniques. These oocytes are apparently unique among egg cells in their ability to generate trains of AP's spontaneously. The AP's are fundamentally different from those of other excitable cells. (1) Young oocytes have voltage-gated Na, K, and Cl channels. However, as the oocyte matures, the K^+ current disappears and Cl^- current repolarizes the membrane. (2) The activation kinetics of the Na^+, K^+, and Cl^- currents are extremely slow, with time constants of the order of seconds. (3) The Na channel does not inactivate. (4) The Na^+ current (I_{Na}) is not blocked by TTX, but the channel is partially blocked by Ca^{2+}. Co^{2+} eliminates the inward current. (5) The conductance versus voltage relation for the Na channel is typically S-shaped, but it is displaced to unusually positive potentials (threshold -10 to 0 mV). (6) I_{Cl} is blocked by SITS. The Cl channel behaves as a delayed rectifier. (7) I_K appears to be a Ca-stimulated K^+ current.

M-AM-Pos19 NOISE PERFORMANCE OF A GIANT AXON VOLTAGE CLAMP. R. A. Levis and F. Bezanilla. Dept. of Physiol., Rush Medical College, Chicago, Ill. 60612 and Dept. of Physiol. UCLA, Los Angeles, California 90024.

Theoretical aspects of the noise performance of a giant axon voltage clamp are discussed. Dominant noise sources are identified and methods for minimizing each are presented; effects of compensation of series resistance, R_s, are also considered. A wideband ultra-low noise voltage clamp, suitable for both fluctuation measurements and measurements of mean ionic and gating currents, is described, and practical designs for low-noise wideband amplifiers are presented.

Because current through the membrane capacitance, C_m, is the derivative of transmembrane voltage, noise in the measured current at frequencies above a few tens to hundreds of Hz can be dominated by the noise involved in the measurement of membrane potential (input voltage noise, e_n, of the differential amplifier, DA, and the thermal voltage noise of the potential electrodes, plus the thermal voltage noise of R_s). Several versions of DA have been constructed with $e_n < 500$ pV/$\sqrt{Hz}$ and bandwidths >1MHz at gains of 20-100. Moreover, a new voltage electrode formed by the combination of a DC electrode (pipette) connected directly to an input of DA and an extended (~4 mm) length of Pt-Ag-AgCl wire connected to the input through a large (10-100 μF) capacitor, when used in conjunction with these amplifiers, can reduce the noise in the measured current to near the theoretical limit imposed by R_s and C_m. Preliminary measurements on squid axon with components of the improved voltage clamp showed dramatic reduction of noise in the measurement of Na^+ gating currents and demonstrated that the new electrode was fast, extremely low noise, and free from drift.

M-AM-Pos20 PREPULSES SHIFT SODIUM CHANNEL GATING CURRENT AND SODIUM CURRENT IN FROG SKELETAL MUSCLE. Ning-Leung Sizto, Department of Physiology, University of Rochester, School of Medicine & Dentistry, Rochester, NY 14642.

Using the double vaseline gap voltage clamp technique, sodium channel gating current I_g and sodium current I_{Na} were studied in the same cut frog muscle fiber detubulated by hypertonic glycerol treatment (Sizto, Biophy. J. 37, 69a, 1982). Holding potential of -150 mV was used. The overlap between the steady-state activation and inactivation curves for the sodium current was very small. A prepulse to -60 mV for 50 ms, which by itself did not give detectable I_{Na}, could inactivate 95% of the sodium channels. Short prepulses (1-2 ms) to -80 and -60 mV reduced the size of I_{Na} and the amount of gating charge moved during the test pulse immediately after the prepulse by 5-30%. After normalization according to peak I_{Na} to correct for such effect of inactivation, the kinetics of I_{Na} with and without prepulse were similar except that the prepulse decreased the time delay by 30-60 μs. A similar shift was also observed in the kinetics for I_g after normalization using the same scaling factor as was used for I_{Na}. The normalized I_g after prepulse was still smaller than I_g without prepulse. Longer prepulses (10 ms) at more negative potentials (further away from the voltage for detectable I_{Na}) produced a smaller reduction in the time lags for I_g and I_{Na}. These reductions in time lag were too large to be accounted for by the effect of the prepulse on the time to attain the final voltage during the voltage step. This suggests that part of the charge moved during the prepulse is involved in the early transitions for the activation process.

M-AM-Pos21 THIONIN-SIMULATED "INACTIVATION" PERSISTS AFTER THIONIN WASHOUT IN PRONASE-TREATED CRAYFISH GIANT AXONS. S.T. Heggeness and J.G. Starkus. University of Hawaii, Dept. of Physiology, Honolulu, HI 96822.

Internal perfusion of crayfish giant axons with low concentrations of thionin (10μM and 100μM) produces an apparent acceleration of sodium current inactivation. This suppression of I_{Na} does not demonstrate any frequency dependence at interpulse intervals of 1 sec or greater. Sodium tail currents appear severely suppressed during perfusion with 500μM thionin, and do not demonstrate the "hooking" that is observed with methylene blue and other inactivation simulators. Gating currents do not appear suppressed by these concentrations of thionin in the absence of TTX, but are reduced severely if 100μM TTX is added to the external solution.

Following the removal of normal inactivation by pronase, 100μM thionin demonstrates two components of I_{Na} block: tonic block and time dependent block. The time constant for time dependent block by 100μM thionin at OmV is approximately 3 fold faster than the time constant observed for block by 100μM methylene blue. Following a 45 minute washout of thionin, a voltage sensitive decay of I_{Na} persists. Interestingly, this "reconstituted inactivation" can subsequently be removed by a 5 minute treatment with pronase. Reapplication of thionin restores simulated inactivation which again persists after thionin washout but which is also pronase-sensitive. (Supported in part by NIH Grant No. GM29263-03, and U.H. Research and Training Grant)

M-AM-Pos22 A THREE-PARTICLE, EIGHT-STATE MODEL FOR CONTROL OF SODIUM CONDUCTANCE IN CRAYFISH GIANT AXONS. B.D. Fellmeth and M.D. Rayner. University of Hawaii, Dept. of Physiology, Honolulu, HI 96822.

A simple three-particle, eight-state model for the gating mechanism regulating ionic conductance in sodium pores is described; the responses of this model are compared with data obtained from internally-perfused, voltage-clamped crayfish giant axons.

Three non-identical interactive but separately-mobile, charged, particles are hypothesized. Each particle moves (in accordance with first order reaction kinetics) between depolarization-favored and hyperpolarization-favored energy wells. Two of these particles effect gating of the ion permeation channel (and are equivalent to the "M"- and "h"-gates of standard terminology). The additional particle takes no direct part in channel gating but affects, by its position, the kinetics of the other particles. All particles may contribute to gating current but with differing effective valencies (i.e. "z.f.", where z is time particle valence and f is the fraction of the applied transmembrane field which appears between that particle's energy wells). The model requires an eight-state reaction scheme, in which the differing interactive states can be represented diagrammatically as the corners of a cube.

In our formulation the variable parameters governing the behaviour of each particle are: the energy levels of the two wells and the intervening barrier height (all in kT units), together with the effective particle valence. Although this formulation necessarily obeys microscopic reversibility, additional restraints can also be imposed to ensure a reasonable symmetry in the proposed interactive effects of one particle on another.

M-AM-Pos23 THE EFFECT OF HYDROSTATIC PRESSURE ON Na GATING CURRENTS OF SQUID GIANT AXONS. W. Stühmer F. Conti, I. Inoue. Istituto di Cibernetica e Biofisica, CNR, 16032 Camogli, Italy.

Sodium gating currents have been measured in squid giant axons at hydrostatic pressures ranging from 1 to 600 atm, at 10°C. The axons were perfused intracellularly with a K-free solution containing 300 mM-CsF, 45 mM-TEACl and 20 mM-Na phosphate buffer at pH 7.2. The extracellular medium contained 460 mM-TrisCl, 50 mM-$CaCl_2$ and 1 M-TTX, pH 7.8. Intra- and extracellular perfusion were stopped before transferring the axons to a pressure bomb as described by Conti, Fioravanti, Segal & Stühmer (1982) (J. Membrane Biol. 69, 23). The voltage clamp circuit allowed at least 50% compensation of the series resistance, to speed up the rise-time. Gating currents were measured according to the P/4 protocol with a holding potential of -70 mV and using a control level of -140 mV. Following the onset of step depolarizations up to +26 mV the major part of asymmetrical displacement current was fairly well fitted by a single exponential. Other components could not be resolved quantitatively enough to be studied also at high pressures. Increasing pressure slowed the kinetics of gating currents in a reversible way. At 600 atm the time constant was increased by a factor of 2 to 3, depending on voltage, whereas the amplitude was decreased by about the same factor, so that the total charge displaced was roughly independent of pressure. The factoral change of the time constant of displacement currents was of the same order of that describing the slowing of Na currents in intact axons. This confirms the hypothesis that both effects arise from the fact that a gating isomerization of the Na channel involves a transient volume increase of 40 to 60 $Å^3$.

I. Inoue is recipient of a joint fellowship from JSPS and CNR. W. Stühmer is a recipient of a short-term fellowship from EMBO.

M-AM-Pos24 DIVALENT CATIONS CAUSE IDENTICAL SIMPLE SHIFTS IN THE KINETICS OF SODIUM AND GATING CURRENTS. Richard Hahin & Donald T. Campbell, Dept. Physiol. & Biophys., U. of Iowa, Iowa City, IA.

The effect of elevated divalent cation concentration on the kinetics of sodium ionic and gating currents was studied in voltage clamped frog muscle. When measured from a holding potential of -150 mV, raising external Ca from 2 to 40 mM causes nearly identical 30 mV shifts in the time courses of activation, inactivation, tail current decay and ON- and OFF-gating currents; in the steady state levels of inactivation and charge immobilization; and in the charge vs. voltage relationship. These results support the hypothesis that Ca acts by altering surface potential. A prediction of this hypothesis is that biasing the holding and test potentials by the hypothesized change in surface potential will exactly compensate for the effect of elevated Ca on gating current kinetics. The result of such an experiment is illustrated in the figure which shows ON- and OFF-gating currents recorded in 2 mM Ca (lines) for two different steps in potential from a holding potential of -90 mV. Superimposed are currents recorded in 40 mM Ca (dots) when both the holding and test potentials were shifted by +30 mV. At these and all other test potentials the control and test records coincide over the entire time-course of ON- and OFF-gating current. Adding 38 mM Mg to 2 mM Ca produced a smaller 20 mV shift in gating current kinetics, lending additional support to the surface charge hypothesis and suggesting that Ca and Mg bind to fixed surface charges with different affinities, in addition to possible screening. Supported by MDA and NIH (NS-15400).

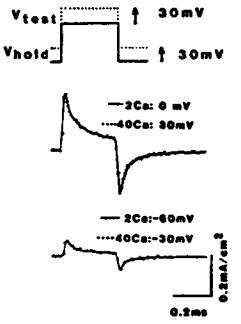

M-AM-Pos25 ACCUMULATION AND DEPLETION OF Na IONS IN THE PERIAXONAL SPACE OF THE SQUID GIANT AXION. V. Scruggs and T. Narahashi. Dept. Pharmacol., Northwestern Univ. Med. Sch., Chicago, IL 60611.

To determine the extent of Na accumulation and depletion in the periaxonal space, we have investigated changes in the amplitude of a test Na current (INa,t) as a function of [Na]o, conditioning pulse (Vc) potential, and the interval between Vc and test pulse. Internally perfused axons were voltage clamped to a holding potential of -100 mV at 11.6°C in K-free media with 50 mM Na inside. A 20 ms Vc was followed 100 ms later by a test pulse to -20 mV. As Vc was stepped to various levels from -50 to +60 mV, INa,t progressively decreased to a minimum at Vc = -20 mV which occurred at maximum inward INa during Vc. Thereafter INa,t increased as Vc was made more positive. In 50//50 Na ([Na]o// [Na]i in mM), INa in the absence of a Vc (INa,c) was -273 μA/cm2. The ratio INa,t/INa,c was 0.93 for Vc = -20 mV, and 1.42 for Vc = +60 mV. In 450//50 Na, these values were -1910 μA/cm2, 0.97 and 1.004 respectively. In all cases, INa,t ≅ INa,c when Vc was at VNa. In 100//50 Na, the ∫INa dt of Vc for potentials where Na flux was predominantly inward (-30 and -20 mV) or outward (+50 and +60 mV), was -40.9, -49.1, +81.5 and +113 pmoles/cm2 respectively. For the same potentials ΔI =(INa,t - INa,c) was -36, -45, 45, and +66 μA/cm2. Recovery of INa,t occurred exponentially with a time constant of 225 ms. Na flux direction and magnitude during a conditioning pulse have appreciable effects on INa,t amplitude in low external Na with 50 mM Na internally but are negligible in normal external Na. The apparent space thickness was 4.17 X 10^{-6} cm and the permeability for the diffusion barrier was 1.85 X 10^{-5} cm/sec. Supported by NIH grant NS 14144.

M-AM-Pos26 GATING KINETICS OF A Ca-ACTIVATED K-CHANNEL IN PLANAR LIPID BILAYERS: EVIDENCE FOR TWO VOLTAGE DEPENDENT Ca BINDING REACTIONS. Edward G. Moczydlowski and Ramon Latorre, Department of Physiology and Biophysics, Harvard Medical School, Boston, MA 02115.

The Ca and voltage dependent gating kinetics of a Ca-activated K-channel from rat muscle plasma membrane were investigated by stochastic analysis of single-channel current fluctuations. Channel activity was recorded at 1-4 kHz resolution after incorporation of membrane vesicles into pure PE bilayers cast from decane (pH 7, 0.2 M KCl). The following scheme is consistent with the observed Ca and voltage dependence of the open and closed dwell time probability distributions of the primary gating mode:

$$\text{Closed} \overset{K_1(V)}{\rightleftharpoons} \text{Ca.Closed} \underset{\alpha}{\overset{\beta}{\rightleftharpoons}} \text{Ca.Open} \overset{K_2(V)}{\rightleftharpoons} \text{Ca}_2\text{.Open}$$

As this scheme predicts, we find that the mean open, $\bar{\tau}_o$, and mean closed, $\bar{\tau}_c$, times are well described by the relations: $\bar{\tau}_o = \alpha^{-1}\,(1 + [Ca]/K_2)$; $\bar{\tau}_c = \beta^{-1}\,(1 + K_1\,[Ca])$. We also find that α and β are voltage independent, while the two Ca binding dissociation constants follow the relations: $K_{1,2} = K_{1,2}(0)\exp(-z\delta FV/RT)$. These expressions and the following set of kinetic constants accurately predict the steady state opening probability over the complete range of Ca and voltage that we have examined (1 μM to 10 mM; +60 to -60 mV): $\beta = 480\ \text{sec}^{-1}$, $\alpha = 280\ \text{sec}^{-1}$, $K_1(0) = 370$ μM, $\delta_1 = 0.67$, $K_2(0) = 14$ μM, $\delta_2 = 0.91$. Our interpretation is that the closed channel has a low affinity Ca site that must be occupied in order to lower the activation energy for opening. In the open conformation, Ca binding to a second high affinity site further stabilizes this conformation. (Supported by NIH grants GM-25277 and GM-28992.)

M-AM-Pos27 FORMATION OF LIPID BILAYER MEMBRANES ON PATCH-CLAMP PIPETTES: A RECONSTITUTION TECHNIQUE FOR IONIC CHANNELS. Roberto Coronado and Ramon Latorre, Department of Physiology and Biophysics, Harvard Medical School, Boston, MA 02115.

Phospholipid bilayers have been formed on the tip of standard patch-clamp pipettes (tip diammeter less than 4 microns). Bilayers are formed by raising and lowering the pipette through a solution which sustains a phospholipid monolayer at the air/water interface (see Figure). The glass pipette does not require any pretreatment nor fire-polishing. Bilayer resistance varies with phospholipid composition of the monolayer and ionic strength of the solution. The resistance for phosphatidylethanolamine-phosphatidylserine bilayers in 0.1 M KCl is typically 3-10 giga-ohms. Channels present in isolated membrane vesicles can be recorded in this type of bilayers if the monolayer is formed from mixtures of native vesicles and an excess of liposomes. This general procedure has been used to record potassium channels from lobster axons and potassium and chloride channels from cardiac sarcolemma. The technique permits the study of reconstituted channels on a time-scale and noise levels comparable to cellular patch-clamp standards. Supported by NIH grants GM-25277 and GM-28992 and by a Postdoctoral Fellowship from Muscular Dystrophy Association.

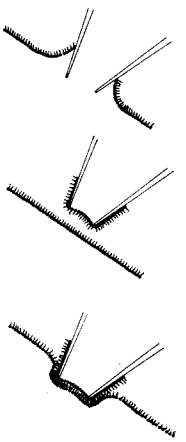

M-AM-Pos28 IDENTIFICATION AND CHARACTERIZATION OF A Ca^{++}-ACTIVATED K^+ CHANNEL IN FRESHLY DISSOCIATED, VERTEBRATE SMOOTH MUSCLE CELLS USING THE PATCH-CLAMP TECHNIQUE. John V. Walsh, Jr. and Joshua J. Singer, Dept. of Physiol., U. Mass. Med. Sch., Worcester, MA 01605

Single channel currents were recorded with the patch-clamp technique from single vertebrate smooth muscle cells enzymatically dissociated from the stomach muscularis of Bufo marinus (J. Gen. Physiol. 80: 23a (1982). Of a variety of single channel currents observed, one displayed a large nearly linear conductance of 180 pS in the cell-attached state (when the patch pipette contained 160 mM K^+). Unless the cell was somewhat contracted, indicating elevated $[Ca^{++}]_i$, this channel opened only at large, positive patch potentials. Excising an inside-out patch containing this channel permitted a direct demonstration that it is Ca^{++}-activated and K^+-selective. The channel did not open when the intracellular surface of the excised patch was exposed to solutions with negligible free Ca^{++} (1 mM EGTA). Upon perfusion with Ca^{++}-containing solutions from a small glass pipette, the channel opened, spending more time in the open state at more positive membrane potentials. When the K^+ concentration in the perfusing solution was changed from 120 mM to 40 mM (NaCl replacing KCl), the zero-current, or reversal, potential shifted 27 mV, as expected for a channel highly selective for K^+. Although the conductance was approximately linear in symmetric K^+ solutions, it rectified in asymmetric K^+ solutions, the lower conductance occurring when current was carried away from the region of lower $[K^+]$. The density of channels in the membrane could be estimated from the macroscopic $I_{K(Ca)}$ recorded in these cells using a two microelectrode voltage clamp (Pflugers Arch. 390: 207 (1981)). A minimum density of two channels per 10^2 was calculated which is in accord with our experience of finding at least one such channel in almost every patch. (Supported by NSF PCM-7904938 and PCM-8208015)

M-AM-Pos29 CALCIUM-DEPENDENCE OF OPEN AND SHUT INTERVAL DISTRIBUTIONS OF CALCIUM-ACTIVATED POTASSIUM CHANNELS IN CULTURED RAT MUSCLE. B. S. Pallotta and K. L. Magleby, Dept. of Physiology and Biophysics, University of Miami School of Medicine, Miami, Florida 33101.

The patch clamp technique was used to study the stochastic properties of single Ca-activated K channels in excised patches of surface membrane from cultured rat muscle cells. The distribution of all open intervals was described by the sum of two exponential distributions. Increasing the concentration of Ca at the inner membrane surface, $[Ca]_i$, had little effect on the mean duration of the short open distribution but increased the mean duration of the long open distribution. The frequency of openings to each distribution increased with $[Ca]_i$. The rate of increase was a less steep function of $[Ca]_i$ for openings in the short open distribution than for openings in the long open distribution. The distribution of all shut intervals was described by the sum of three exponential distributions with mean durations (0.5 uM Ca_i, +30 mV) of: 44 msec (long shut distribution), 1.9 msec (intermediate shut), and 0.21 msec (short shut distribution). In addition, a few longer shut intervals not accounted for by the above distributions suggested that there was an additional infrequently occurring closed channel state. These results indicate that the Ca-activated K channel has a minimum of two open channel states of similar conductance and four closed channel states, and kinetic modeling suggests that there may be additional open and closed channel states. Openings are Ca-dependent, with openings to the long open distribution typically requiring the binding of more Ca ions than openings to the short open distribution. Supported by NIH grants NS 10277, NS 12207, and the Muscular Dystrophy Association.

M-AM-Pos30 CONDUCTANCE, SELECTIVITY AND BLOCKADE PROPERTIES OF A Ca^{++} ACTIVATED K^+ CHANNEL FROM RABBIT SKELETAL MUSCLE MEMBRANES. Cecilia Vergara and Ramon Latorre, Department of Physiology and Biophysics, Harvard Medical School, Boston, MA 02115.

The conductance, selectivity and blockade properties of a Ca^{++} activated K^+ channel incorporated in planar lipid bilayers were studied. Membranes were formed from a mixture of phosphatidylethanolamine and phosphatidylserine in decane. The single channel conductance follows a single site saturation curve with K^+ concentration having a maximal conductance of 480 pS and a dissociation constant (K_d) of 0.1 M. The channel is perfectly Nernst selective for K^+ over Cl^-. P_{K^+}/P_{Rb^+} is $\sim$10, Na^+ and Li^+ block the channel. Addition of Tetraethylammonium ions (TEA) to either side of the membrane causes a decrease in single channel conductance. Blockade by TEA added to the same side as the vesicles (cis side) is voltage dependent and has a K_d of 45 mM at zero volt. This site feels 34% of the total membrane electric field. Trans TEA block is voltage independent and has a K_d of 0.29 mM. These results indicate that the cis and trans TEA binding sites are different. Ba^{++} ions added to the cis side cause the appearance of periods of time when the channel remains silent (blocked periods). The block caused by Ba^{++} is voltage dependent, competitive with K^+ and can be described by a single site blocking model with a zero volt K_d of 3.3×10^{-5} M. Ba^{++} at the blocking site feels 90% of the total membrane electric field. The kinetics of TEA and Ba^{++} block differ widely with respect to the gating reaction, TEA block being much faster and Ba^{++} block much slower than the gating. From these results we picture the channel as having two wide mouths at each side of the membrane connected by a conduction pathway that cannot accommodate more than one ion at a time. (Supported by NIH grants GM-25277 and GM-28992.)

M-AM-Pos31 POTASSIUM CURRENT IN CARDIAC MEMBRANE BY SINGLE CHANNEL ANALYSIS. D.E. Clapham and L.J. DeFelice, Brigham and Women's Hospital, Boston, MA and Dept. of Anatomy, Emory University, Atlanta, GA. DEC's present address is Max-Planck-Inst. fur Biophys. Chemie, Gottingen, W. Germany.

We are studying the development of cardiac membrane excitability by measuring voltage dependent currents with the single channel recording technique. Here we report the characteristics of K current in 10 day chick ventricle. All experiments were done at 27°C in 4 mM external K and 1.8 mM external Ca. Under these conditions, there is a stable resting potential of -49.6 ± 3.3mV. The channel reported on has a constant conductance of 62 pS between -70 and 0 mV absolute membrane potential. This extrapolates to a reversal potential of -87.5 mV. The channel rectifies inwardly above 0 mV. The steady-state probability of being open increases monotonically between 0.02 at -70 mV and 0.92 at 20 mV. The half-way point occurs near -20 mV, illustrated at left. At this potential the open channel current is 4.05 ± 0.44 pA, the average open time is 4.11 ± 4.76 msec and the average closed time is 4.73 ± 8.83 msec. An analysis of channel kinetics and the role of this current in cardiac excitability will be presented. This work was supported by the Mass. Heart Assoc. and NIH Grant PO1 HL27385.

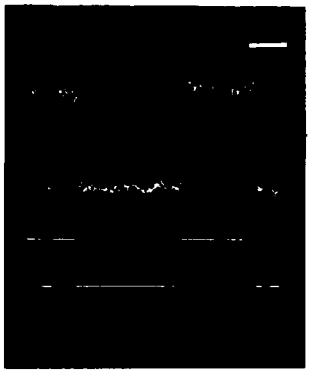

K channel current from 10-day ventricle at V = -20 mV. Top trace is actual data, bottom trace is a computer-generated idealization. Bar signifies 10 msec.

M-AM-Pos32 A MINIMAL MODEL FOR MEMBRANE OSCILLATIONS IN THE PANCREATIC β-CELL, T.R. Chay* and J. Keizer**, *Department of Biological Sciences, University of Pittsburgh, Pittsburgh, PA 15260, **Department of Chemistry, University of California, Davis, CA 15260.

Following the experimental findings of Atwater et al., we have formulated a mathematical model for ionic and electrical events that take place in pancreatic β-cells. Our formulation incoporates a Hodgkin-Huxley type gating mechanism for Ca^{2+} and K^+ channels, in addition to Ca^{2+} gated K^+-channels. Consistent with the experimental observations, our model generates spikes and bursts in β-cell membrane potentials and gives the correct responses to additions of glucose, quinine, and tetraethylammonium ions. The response of the oscillations to ouabain and changing concentrations of external K^+ can be incorporated into the present model, although a more complete treatment could require inclusion of the Na^+/K^+ pump.

*T.R.C. was supported by NSF PCM79 22483.

**J.K. was partially supported by PHS Grant GM 30688-01.

M-AM-Pos33 OSCILLATING DEPOLARIZATIONS ARE ELICITED BY STIMULATING MYOEPITHELIAL CELLS. M. Anderson. Department of Biological Sciences, Smith College, Northampton, MA 01063

Long duration (5-50 sec) depolarizing current pulses of varying intensities (1-5 x 10^{-7} A) were applied with an intracellular electrode to single myoepithelial cells that make up the proventriculus of the marine polychaete worm Syllis spongiphila. A recording microelectrode was placed either in the same cell or in an adjacent strongly coupled cell. In calcium-free artificial sea water (ASW) solutions, depolarizing responses of low amplitude had smooth plateaus, but higher amplitude responses exhibited oscillations of depolarizations and repolarizations (period 2-4 sec, 14 preparations), which persisted as long as the applied current pulse. The amplitudes of the depolarizing peaks were constant for a given intensity of applied current pulse and increased as the pulse intensity was increased. Bathing preparations (n=3) for ≥6 hrs in Ca-free solutions containing 10 mM EGTA did not change the oscillations. Several treatments reversibly diminished or abolished repolarizations, and resulted in maintained plateaus: (a) high intensity current pulses; (b) the K-channel blockers tetraethylammonium (10 mM, n=2), 4 aminopyridine (1-10 mM, n=2) and CsCl (10 mM, n=2); (c) 10 mM Co (n=1); and (d) the antagonist of intracellular calcium ions, TMB-8 (8-diethylamino)octyl 3,4,5-trimethoxybenzoate hydrochloride, n=7). When Ca was present in the ASW (controls), applied pulses elicited repeating cycles of slow depolarizations (apparently composed of small subunits), fast spikes and rapid repolarizations; the period between spikes was 2-5 sec. A model that includes alternate activation and inactivation of K channels, at least some of which open only in the presence of free intracellular Ca ions, would explain these results.
Supported by NIH Grant NS12196.

M-AM-Pos34 ION CONDUCTANCE EFFECTS IN THE LOW FREQUENCY IMPEDANCE OF SNAIL NEURON.
S. Miyamoto & H.M. Fishman, Physiology & Biophysics, Univ. of Texas Med. Branch, Galveston.

The complex impedance of isolated subesophagal ganglion cells was determined in the frequency range 0.25 to 100 Hz by a previously described method (Fishman et al., The Biophysical Approach to Excitable Systems, Plenum, p. 65,1982). The impedance was measured 2 sec after step current clamps, applied by a modified suction pipet-technique (Brown et al., J. Neuro. Method, 2,51, 1980) in combination with an internal voltage-sensing micropipet. In normal external solution (containing K, Na, Ca, Mg) a voltage-dependent impedance resonance near 10 Hz was observed at depolarized potentials (10, 20 and 30 mV from rest) and the magnitude of impedance was reduced with increasing potentials. These results were unchanged in the absence of K ion in the external solution (5 mM Cs substituted for K). In buffered Ca (only) solution, the resonance became broader and the decrease in the impedance magnitude was smaller. Substitution of Co for Ca in the Ca solution abolished the resonance, whereas the voltage-dependent impedance change was almost the same as that in Ca solution. When the Ca channel blocker Cd (1.0 mM to 1.5 mM) was added to the normal solution, the resonance disappeared but the voltage-dependent impedance change was still observed. These results suggest that the voltagedependent impedance reflects the increase of the slow outward K current (time constant ≈ 15 msec). Only in Ba solution (Ca replaced by 10 mM Ba) did the impedance magnitude increase with increasing depolarization. At hyperpolarized potentials (30 to 50 mV from rest) no impedance change was observed in all the external solutions. This voltage-dependent impedance increase suggests that Ba ion enters the cell through Ca channels and blocks the slow outward K channel.
Supported by NIH grant NS13778.